Characterization of regulatory T cells in Autoimmune Polyendocrine Syndrome type I, a model disease for autoimmunity

Marte Heimli

This thesis is submitted in partial fulfillment of the requirements for the degree of Master of Science

Department of Biological Sciences
KG Jebsen Center for Autoimmune Diseases, Department of Clinical Science
University of Bergen

Autumn 2018

List of contents

Acknowledgements

First of all, I would like to thank Anette Susanne Bøe Wolff for being a highly interested and engaged supervisor. The effort she has put into my instruction, and the faith she has shown in me throughout the project, has been astonishing. She has allowed me to continuously challenge myself, and always been willing to discuss my own suggestions and ideas. I also want to thank co-supervisors Øyvind Bruserud and Bergithe Eikland Oftedal for their outstanding support. The insights they have supplied, and their involvement in everything from technical training to giving manuscript feedback, has proven to be nothing short of essential.

In addition to being a proficient group leader, professor Eystein Sverre Husebye has played a pivotal role in patient recruitment. Lab technician Hajirah Muneer has been a crucial asset, always there to patiently answer questions and provide practical assistance. PhD. candidate Amund Holte Berger has been invaluable for the RNA-seq data analysis. Head engineer and ROAS secretary Lars Ertesvåg Breivik has facilitated material orders. I highly appreciate the contributions of all members of the group in creating an inclusive work environment, and in making our lab a place where advice and encouragement is generously given.

Without the willingness of the APS-1 patients to participate, this project would not have been possible. The same is true for the blood donors and staff at the Haukeland University Hospital Blood Bank. The competence provided by Brith Bergum at the Flow Cytometry core facility, and by Rita Holdhus and Hans-Richard Brattbakk at the Genomics core facility, has been absolutely instrumental. I want to thank student councilor Lill Kristin Knudsen at the Department of Biological Sciences for her vital guidance. Funding for the project was provided by the University of Bergen, the Western Norway Health Authority and the Kristian Gerhard Jebsen foundation.

Marte Heimli
December 2018

UNIVERSITY OF BERGEN

HELSE BERGEN
Haukeland University Hospital

KRISTIAN GERHARD JEBSEN FOUNDATION

Abstract

The T and B lymphocytes of the adaptive immune system face the challenge of correctly recognizing antigens originating from a vast number of rapidly evolving pathogens, while ignoring those pertaining to the host itself. A failure to ensure such self-tolerance may lead to autoimmune responses, the cause of a wide range of adverse pathologies. One self-tolerance mechanism is the negative selection of developing T cell progenitors with self-reactive capabilities in the thymus, another is the peripheral tolerance inferred by regulatory T cells (T_{regs}). The Autoimmune Regulator (AIRE), which induces the ectopic expression of tissue-restricted antigens in the thymus, has been indicated to be of importance in both central and peripheral tolerance. Mutations in the *AIRE* gene is the cause of autoimmune polyendocrine syndrome type I (APS-1), an established model disease for autoimmunity.

In this project, we aimed to characterize expression patterns in T_{regs} in APS-1, both at the protein and RNA levels. By assessment of the expression of pre-selected candidate genes, a number of subtle trends could be observed. It was indicated that the thymic output of T_{regs} was lower in APS-1 patients compared to healthy controls, but that the patient's T_{regs} were capable of inducing expression of genes associated with an activated state. However, the observations failed to reach statistical significance, preventing reliable conclusions. The exception is a significant increase in the expression of mTOR, a downstream mediator of signaling though PKB/Akt. This is of interest as the inhibition of PKB/Akt by the PTEN phosphatase appear to be important for T_{reg} lineage identity.

When using RNA sequencing to perform a global search for gene expression perturbations, a number of genes were found to exhibit significant changes in expression levels in T_{regs} from APS-1 patients compared to the controls. Among the genes indicated to be significantly perturbed are *SKI* and *NOTCH-1*, potentially affecting TGF-β signaling. TGF-β has been suggested to have implications in T_{reg} suppressive function and in the induction of the regulatory T cell phenotype.

Further validation of these results, and elucidation of their functional implications, would be relevant for future work. Our hope is that continued work on T_{reg} biology, and identification of clinically relevant biomarkers, can contribute to the successful implementation of this cell population in diagnostics and treatment of patients with immune-mediated diseases.

1. Introduction

1.1 The adaptive immune system

The vertebrate immune system is divided into two main components, termed the innate and adaptive immune system. The innate immune system represent a first line of defense, and include physical barriers and phagocytic cells recognizing pathogen-associated molecular patterns (PAMPs) (Janeway, 1989). The innate immune system is also capable of alerting the adaptive immune system, by production of attracting molecules such as chemokines (Bennouna *et al.*, 2003). The responses of the adaptive immune system are slower to arise, but encompass an enormous capability for specificity and diversity. The ability of this system to adapt to encountered threats, and to retain information about such encounters, is invaluable in the arms race against pathogens and cancerous cells (Agrawal, Eastman and Schatz, 1998; Hedrick, 2004). However, the very same features of the adaptive immune system may also pose a risk to the host, as observed when autoimmune responses against self-tissues causes precarious disease states (Anderson *et al.*, 1957; Ota *et al.*, 1990).

Among the lymphocytes of the adaptive immune system are the B cells, developing in the bone marrow, and the T cells, which develop in the thymus (Cooper, Peterson and Good, 1965; Owen, Cooper and Raff, 1974). These populations, in turn, encompass multiple subpopulations. The conventional subpopulations of T cells include cytotoxic T cells (CTLs), directly involved in attacking virus-infected or cancerous cells (Cerottini, Nordin and Brunner, 1970; Zinkernagel and Doherty, 1973; Vose and Bonnard, 1982), and helper T (T_H) cells, which produce a wide range of cytokines required by the CTLs and by B cells for activation (Tada, Okumura and Tokuhisa, 1978; Keene and Forman, 1982). For activation to occur, a T cell must encounter its specific antigen, presented on the surface of antigen-presenting cells (APCs), such as macrophages, dendritic cells (DCs) and B cells, bound to a major histocompatibility complex (MHC) molecule (Rosenthal and Shevach, 1973; Lanzavecchia, 1985; Freudenthal and Steinman, 1990). This interaction is dependent on the T cell receptor (TCR), but must also be stabilized by co-receptors. On the CTLs, the co-receptor is CD8, which interacts with MHC class I molecules present on the surface of APCs. On the T_H cells, the co-receptor is CD4, which recognize surface-bound MHC class II molecules on the APCs (Kisielow *et al.*, 1975; Doyle and Strominger, 1987; Rosenstein *et al.*, 1989).

Structurally, the conventional TCR consists of an α and a β chain (Allison, Mcintyre and Bloch, 1982), although a δγ version also exist (Hayday *et al.*, 1985; Brenner *et al.*, 1986). The α and β chain each consist of a constant (C), variable (V), joining (J) and diversity (D) segment. Each segment is encoded by a separate genetic region, and the ability to use gene rearrangements to assemble different combinations of these segments allows for an astonishing diversity of TCRs being encoded by a relatively modest amount of genetic information. Finally, the complex also contains an invariant molecule termed CD3 (Garcia *et al.*, 1996; Call *et al.*, 2002) .

1.2 Immunological education in the thymus

In addition to its role in peripheral activation of T cells, signaling though the TCR plays a crucial role in T cell development in the thymus. The precursors are infiltrating hematopoietic stem cells from the circulation, originating from the bone marrow (Moore and Owen, 1967). The early lymphoid progenitors exhibit a double negative (DN) $CD4^-CD8^-$ phenotype (Kingston, Jenkinson and Owen, 1985). As maturation proceeds, thymocytes reach the double-positive (DP), $CD4^+CD8^+$ stage, a transition that is dependent on the successful recombination of the TCR β chain (Mallick *et al.*, 1993). Depending on their interactions with MHC molecules, DP thymocytes may subsequently progress to the single-positive (SP) stage, by committing to either the $CD4^+CD8^-$ or the $CD4^-CD8^+$ lineage (figure 1.1) (Teh *et al.*, 1988).

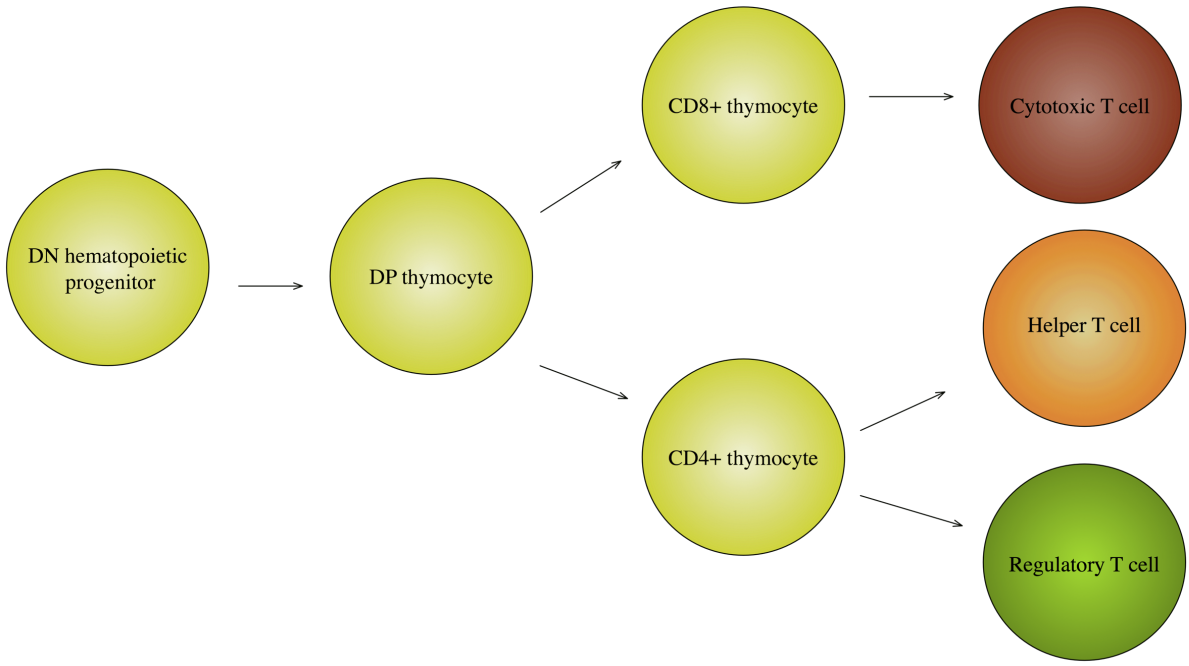

Figure 1.1: Development and differentiation of T cells. *Bone-marrow derived, double-negative progenitors enter the thymus from the circulation. Following recombination of the TCR β chain, the thymocyte reaches the double-positive stage. The expression of either CD8 or CD4 is retained, and the single-positive thymocyte differentiates into one of several T cell subpopulations.*

During the course of development, thymocytes undergo the process of immunological education. The enormous capacity for TCR diversity means that some immature thymocytes will express TCRs with no binding capacity for MCH-peptide complexes. Others may express TCRs with high affinity for peptides pertaining from the host itself, which could lead to a deleterious autoimmune response. To prevent this, the developing thymocytes are exposed to self-peptide-MHC complexes on APCs (Zinkernagel *et al.*, 1978; Brocker, Riedinger and Karjalainen, 1997). Only thymocytes with TCR affinity above a certain threshold receive the required signals for continued maturation, a feature termed positive selection (Kisielow *et al.*, 1988; Ashton-Rickardt *et al.*, 1994). Thymocytes exhibiting an excessively high affinity for self-peptide-MCH class II complexes undergo what is called negative selection, where induction of apoptosis ensures that development of potentially self-reactive thymocytes is discontinued (Ashton-Rickardt *et al.*, 1994; Baldwin *et al.*, 1999).

For the successful deletion of potentially self-reactive T cell progenitors, the thymocytes must be exposed to a complete set of self-antigens for TCR engagement within the thymic environment. A crucial role has been attributed to thymic medullary epithelial cells (mTECs), present in high numbers in structures of the thymic medulla termed Hassall's corpuscles. These cells exhibit promiscuous expression of genes normally restricted to specific peripheral tissues (Derbinski *et al.*, 2001; Watanabe *et al.*, 2005), a feature that has been linked to the transcription factor Autoimmune Regulator (AIRE) (figure 1.2) (Anderson *et al.*, 2002). The role of AIRE as a transcriptional regulator has gained support by its transactivating properties and its interaction with the transcriptional coactivator CREB-binding protein (CBP) (Pitkänen *et al.*, 2000). The highest expression of *AIRE* has been found in mTECS (Anderson *et al.*, 2002; Derbinski *et al.*, 2005), although lower levels also has been observed other cell types such as dendritic cells and thymic B cells (Poliani *et al.*, 2010; Gardner *et al.*, 2013; Yamano *et al.*, 2015). Mechanistically, the AIRE-induced expression of tissue-restricted antigens (TRAs) has been explained by binding to unmethylated H3K4 and subsequent induction of a chromatin structure in compliance with active transcription (Abramson *et al.*, 2010). However, not all TRAs appear to be dependent on AIRE, and some of these AIRE-independent TRAs have been indicated to be regulated by the transcription factor FezF2 (Takaba *et al.*, 2015).

At a given time, the expression of individual TRAs appear to be induced in only a small proportion (1-3%) of mTECs (Derbinski *et al.*, 2008; Pinto *et al.*, 2013; Meredith *et al.*, 2015). This has puzzled researchers, as it indicates that expression of any one TRA is highly limited

in both time and space. While mTECs have been reported to have an autonomous APC function (Hinterberger *et al.*, 2010), a possible mechanism to enhance the tempospatial expression of TRAs would be transfer from mTECs to hematopoietic APCs such as DCs (figure 1.2) (Koble and Kyewski, 2009; Hubert *et al.*, 2011; Taniguchi *et al.*, 2012).

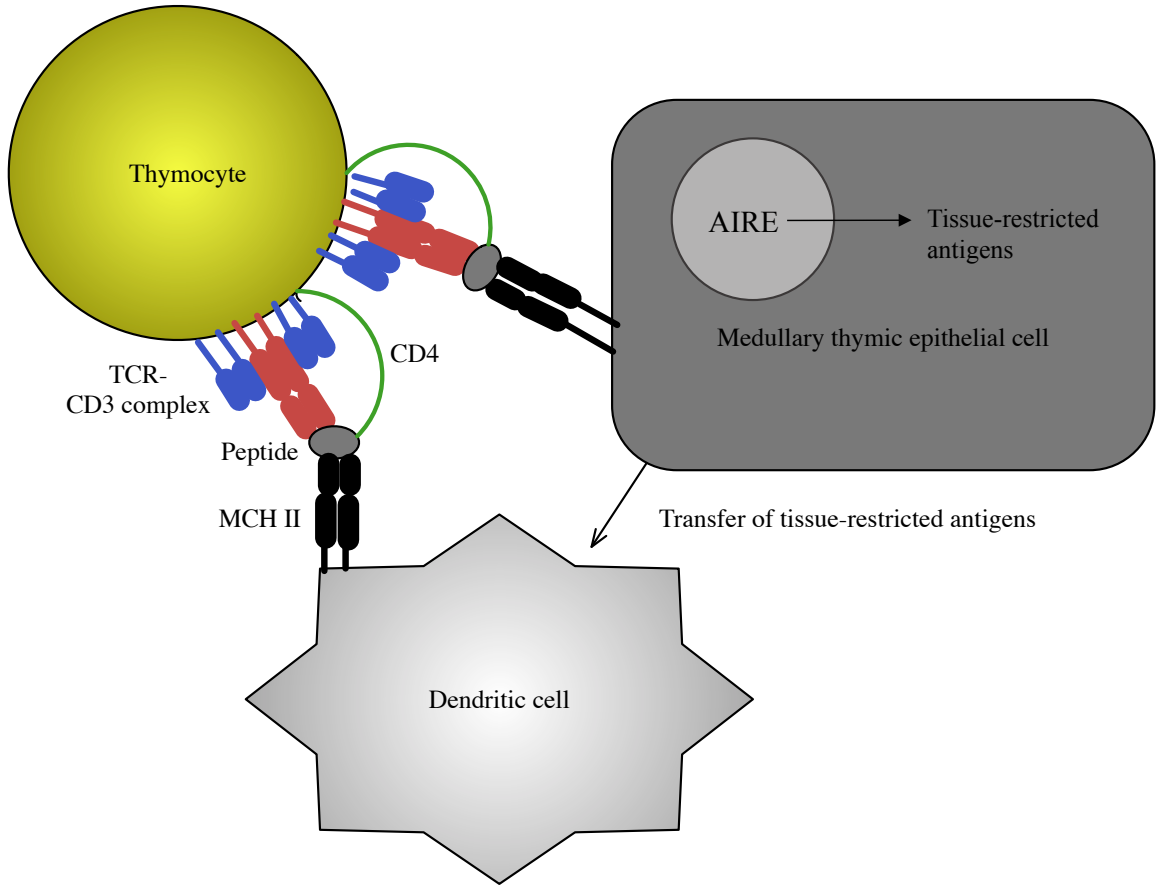

Figure 1.2: Presentation of self-antigens to a developing thymocyte. *Expression of a wide range of tissue-restricted antigens by medullary thymic epithelial cells (mTECs), induced by AIRE, ensures that the thymocyte encounters these self-peptides within the thymic environment. The peptides are presented directly by the mTECs, or transferred to other types of antigen-presenting cells such as dendritic cells.*

Roles of AIRE in mechanisms distinct from TRA expression is also increasingly being elucidated. For instance, it has been suggested that AIRE plays a role in the accumulation of dendritic cells in the thymic medulla. The elucidated molecular mechanism centers around a chemokine receptor, CXCR1, present on thymic DCs, and its ligand, CXL1, present on mTECs under regulation of AIRE (Lei *et al.*, 2011).

The process of ensuring the deletion of potential self-reactive T cell progenitors that takes place in the thymus is termed central tolerance (Gallegos and Bevan, 2004). However, an auxiliary tolerance mechanism in the periphery also exist. This leads us to the subpopulation of T cells termed regulatory T cells (T_{regs}).

1.3 Regulatory T cells

The presence of a $CD4^+CD8^-$ T lymphocyte subset with implications in the prevention of autoimmunity has long since been described (Sakaguchi, 1982). Should any self-reactive thymocytes manage to escape clonal deletion in the thymus and egress to the periphery, they would be prevented from raising a response towards their specific antigen by the action of these "suppressor cells". For years, studies into this cell population were hampered by the lack of specific molecular markers, casting doubt regarding its very existence (Möller, 1988). However, continued efforts by the scientific community proved this to be a solvable issue, and today, T_{regs} are not only generally accepted, but considered with a high degree of interest.

A molecule considered relatively early as a distinguishing hallmark of T_{regs} is the interleukin 2 (IL-2) receptor alpha-chain (CD25). CD25 has been found to be present in approximately 10% of $CD4^+$ T cells, although suppressive function in humans has been ascribed to a subset of approximately 1-2% of circulating $CD4^+$ T cells exhibiting especially high expression (Sakaguchi *et al.*, 1995; Baecher-Allan *et al.*, 2001). The critical role played by IL-2 for maintaining a functional T_{reg} population was established by the observations that injecting mice with anti-IL-2 antibodies resulted in reduced numbers of $CD4^+CD25^+$ T_{regs} and inhibition of their peripheral proliferation (Setoguchi *et al.*, 2005). A complicating factor for the use of CD25 as a T_{reg} marker is the notion that IL-2 also has effects as a growth factor on other T cell subpopulations. However, the presence of the IL-2 receptor is only transiently detected on other T cell subpopulations upon activation (Robb, Munck and Smith, 1981; Taniguchi *et al.*, 1983; Kuniyasu *et al.*, 2000).

Later on, Forkhead box P3 (FOXP3) was raised as a potential T_{reg} marker protein. Encoded by an X-linked gene, this transcription factor appear to have vital functions in immune regulation, as indicated by the immune dysregulation, polyendocrinopathy, enteropathy, X-linked syndrome (IPEX) that presents in males hemizygous for loss-of-function mutations in this gene (Bennett *et al.*, 2001). It has been suggested that lymphoid progenitors are dependent on FOXP3 as a master regulator for divergence into the T_{reg} lineage. There is a substantial upregulation of *FoxP3* in T_{regs}, and excision of *FoxP3* from murine models has been observed to lead to severe autoimmune manifestations (Fontenot, Gavin and Rudensky, 2003). $CD4^+$ T cells transduced with *FoxP3* attain regulatory function *in vitro* and inhibits autoimmune manifestations in mice deficient for *FoxP3* (severe combined immunodefiency (SCID) mice). FOXP3 has also been found to induce the expression of several T_{reg}-associated molecules (Hori,

Nomura and Sakaguchi, 2003). Intriguingly, data supports that stable expression of *FoxP3* is retained in mature T_{regs} by the ability of this transcription factor to induce its own expression. (Gavin *et al.*, 2007). As the expression of *FoxP3* has been indicated to not only be stable in, but also restricted to, T_{regs} (Hori, Nomura and Sakaguchi, 2003), it is considered a highly specific molecular marker for this T lymphocyte subpopulation.

Linking FOXP3 and IL-2 is the notion that signaling through CD25 induces binding of signal transducer and activator of transcription 5 (STAT5) to conserved noncoding sequence 2 (CNS2), a regulatory element in the *FoxP3* promotor region (figure 1.3). T_{regs} from CNS2-deficient mice have reduced *FoxP3* expression and suppressive function, an increased tendency to lose *FoxP3* expression during cell cycle progression, and a reduced ability to retain *FoxP3* expression upon challenge with pro-inflammatory cytokines or limiting IL-2. It is believed that in a wild type situation, a demethylated state of *CNS2* facilitates STAT5 binding, thus helping to retain *FoxP3* expression (Feng *et al.*, 2014; Li *et al.*, 2014).

Another downstream effect of IL-2 is signaling though phosphatidylinositol 3-kinase (PI3K). Interestingly, $CD4^+CD25^+$ $T_{regs,}$ but not $CD4^+CD25^-$ T cells, appear to negatively downregulate this signaling pathway by recruitment of the PTEN phosphatase (figure 1.3) (Bensinger *et al.*, 2004). This action of PTEN has been linked to T_{reg} lineage stability and expression levels of *CD25* (Huynh *et al.*, 2015; Shrestha *et al.*, 2015). Inhibition of PI3K and its downstream mediator PKB/Akt appear to be crucial in the regulation of *FOXP3* expression (Sauer *et al.*, 2008). This is due to signaling though PKB/Akt having an inhibitory effect on the transcription factors FOXO1 and FOXO3a, required for the expression of *FOXP3* (Merkenschlager and von Boehmer, 2010). In addition, an effector molecule downstream of PKB/Akt is mTOR, which is involved in modulating STAT signaling. High mTOR activity induce signaling through STAT4

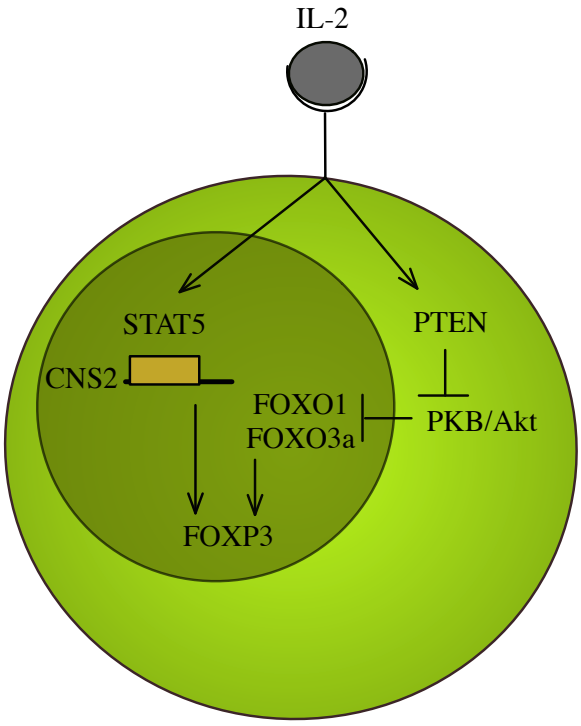

Figure 1.3: Effects of IL-2 signaling on T_{regs}. *IL-2 leads to STAT5-binding to the CNS2 promoter element. In addition, IL-2 signaling leads to recruitment of PTEN phosphatase and inhibition of the PKB/Akt pathway, so that inhibition of the transcription factors FOXO1 and FOXO3a is avoided. Both of these pathways are involved in ensuring FOXP3 expression.*

and STAT6, involved in divergence into T_H lineages. The activity of STAT5, by contrast, appear to be upregulated upon mTOR inhibition (figure 1.3) (Delgoffe *et al.*, 2009; Shan *et al.*, 2015).

1.4 Natural and induced regulatory T cells

Although some T_{regs} may obtain cellular identity during development in the thymus, the existence of an additional subset, which diverge into the T_{reg} lineage after emigration to the periphery, has also been indicated. These two subsets have been termed natural (n) and induced (i) T_{regs}, respectively (Chen *et al.*, 2003; Fantini *et al.*, 2004; Knoechel *et al.*, 2005; Jia *et al.*, 2018). It has also been concluded that, albeit the expression of some canonical T_{reg} genes are enhanced in iT_{regs}, among them *FOXP3*, this do apply to several other genes considered to be part of the T_{reg} signature transcriptome (Hill *et al.*, 2007). It has been indicated that signaling through the PI3K-Akt-mTOR pathway (Sauer *et al.*, 2008) and TGF-β plays major roles in this peripheral induction of T_{reg} lineage identity (Chen *et al.*, 2003; Fantini *et al.*, 2004; Jia *et al.*, 2018).

Several potential markers for differentiation between iT_{regs} and nT_{regs} have been suggested. One candidate, HELIOS, is encoded by the Ikaros zinc finger transcription factor family member 2 gene (*IKZF2*). It has been suggested that HELIOS is restricted to the thymic-derived subset of regulatory T cells (Thornton et al., 2010), In addition, it has been indicated that *HELIOS* expression correlates with suppressive capacity (Zabransky *et al.*, 2012). HELIOS has been found to bind to promoter regions of target genes essential for T_{reg} survival, and to induce signaling trough the CD25-STAT5 pathway (Kim *et al.*, 2015). Another gene, *Neuropilin-1*, has also been suggested to be expressed exclusively by nT_{regs} (Yadav *et al.*, 2012). It has been proposed that Neuropilin-1 functions as a receptor for Semaphorin 4a, which upon activation recruits PTEN phosphatase to the immunologic synapse (Delgoffe *et al.*, 2013).

1.5 Development of regulatory T cells

Similar to other T cell populations, T_{reg} progenitors are assessed for their affinity for self-peptides during thymic maturation. As for other T cell subsets, the transfer of tissue-restricted antigens from AIRE-expressing mTECs to hematopoietic APCs appears to play an important role in TCR avidity assessment, although some T_{reg} generation has been attributed to the

autonomous antigen-presenting activity of mTECs (Aschenbrenner *et al.*, 2007; Perry *et al.*, 2014; Mouri *et al.*, 2017).

It has been proposed, due to correlation between *FoxP3* expression and TCR signaling, that *FoxP3* expression is induced in thymocytes by interaction of their TCRs with peptide-MHC class II complexes with an intermediate avidity (fgure 1.4). Lower avidity would lead to positive selection and maturation into other T cell lineages, while higher avidity would lead to negative selection and clonal deletion (Fontenot, Gavin and Rudensky, 2003). It appears that the development of T_{regs} may be divided into two steps, where the first is dependent on TCR signaling. In the second, antigen-independent stage, cells are able to express *FOXP3* after exposure to IL-2, with no requirement for APCs (Lio and Hsieh, 2008).

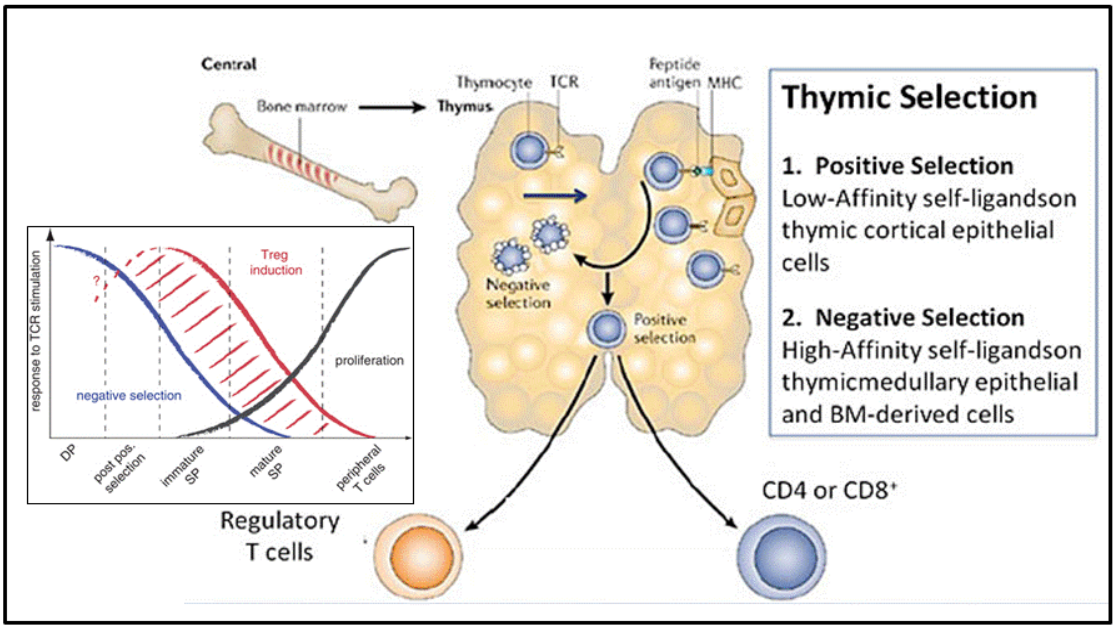

Figure 1.4: The TCR avidity model of T cell development. *During thymic maturation, the thymocytes are exposed to self-peptides bound to MHC class II molecules on antigen-presenting cells. For thymocytes exhibiting TCRs with excessively low or excessively high avidity for such self-peptide-MHC class II complexes, maturation is discontinued. Thymocytes exhibiting TCRs with moderate avidity survive and develop into mature T cells, such as $CD8^+$ cytotoxic T cells or $CD4^+$ helper T cells. Thymocytes with avidity for self-peptide-MHC class II sufficiently low for survival, but higher than the avidity leading to commitment to other T cell lineages, mature into regulatory T cells. Figure modified from Gregersen and Behrens, 2006.*

The TCR avidity model has been supported by the observation of diminished negative selection and increased T_{reg} emergence upon reduction of *Mhc-II* expression on a population of cells with APC activity in the murine thymus (Hinterberger *et al.*, 2010). Further, murine studies employing a panel of TCRs with a broad range of sensitivity for a specific antigen, found that the extent of T_{reg} generation correlates with efficiency of antigen recognition (Lee *et al.*, 2012). On the other hand, complicating the avidity model is the finding that both $CD4^+FOXPP3^+$ Tregs

and $CD4^+FOXP3^-$ non-Tregs could be selected for by identical TCRs, although this discovery has been debated (Wojciech *et al.*, 2014; Lin *et al.*, 2016).

An implication of the TCR avidity model is that it infers a strict requirement for T_{reg} lineage stability, as T_{regs} exhibit a certain level of affinity for self-peptide-MHC class II complexes. This means that loss of T_{reg} cellular identity could result in "ex-T_{regs}" with self-reactive capabilities (Zhou *et al.*, 2009; Bhela *et al.*, 2017).

1.6 Peripheral maintenance of regulatory T cells

In addition to its role during T_{reg} development, TCR engagement has been ascribed an important role in the maintenance of T_{reg} lineage identity and in the activation of T_{regs} after emigration to the periphery (Vahl *et al.*, 2014; Bluestone *et al.*, 2015; Liu *et al.*, 2015; Leventhal *et al.*, 2016). An intriguing suggestion is the existence of a peripheral "memory T_{reg}" pool, where T_{regs} resulting from earlier encounters with antigens remain in a resting state for an extended period of time. This is supported by studies using mouse models, where induction treatment with a specific antigen resulted in a persistent $FOXP3^+$ cell population, capable of activation and suppressive function upon re-exposure to antigen (Rosenblum *et al.*, 2011).

The presence of a peripheral pool of T_{regs} could be especially important upon aging. It has long since been known that a gradual involution of the thymus occurs after puberty (Simpson, Gray and Beck, 1975). Consistent with this, generation of T cells and TCR diversity appear to be reduced with increased age. This raises the question of whether T_{reg} generation is affected upon aging, and whether other mechanisms may be involved in maintaining a functional T_{reg} repertoire in adult individuals. Puzzlingly, it appears that the frequency of nT_{regs} is increased, not reduced, upon aging (Gregg *et al.*, 2005; Booth *et al.*, 2010; Hou *et al.*, 2017). An intriguing suggestion is that enhanced T_{reg} generation could be acting as a compensatory mechanism to alleviate the issue of reduced central tolerance induction (Oh *et al.*, 2017).

A complicating factor is the finding that mature T_{regs} may recirculate into the adult thymus (Thiault *et al.*, 2015; Cowan *et al.*, 2018). However, the functional relevance of this remains unknown. One suggestion is that recirculating T_{regs} negatively affect *de novo* T_{reg} generation due to increased competition for IL-2 (Thiault *et al.*, 2015). Interestingly, this recirculation of T_{regs} also appears to be influenced by AIRE (Cowan *et al.*, 2018).

1.7 Regulatory T cell function

The mature T_{regs} in the periphery are poised to react upon encounters with self-reactive lymphocytes. Several molecules have been described to be involved in the suppressive function of T_{regs}, among them IL-2, TGF-β, CTLA-4, GITR, CD39 and CD73 (figure 1.5).

IL-2

It has been suggested that due to the high expression of CD25, T_{regs} reduce the availability of the CD25 ligand, IL-2, of other T cells. $CD4^+FOXP3^+$ cells have also been reported to inhibit IL-2 production, and their suppression of $CD4^+FOXP3^-$ T cells could be overcome by addition of IL-2 (Fontenot *et al.*, 2005). Also, the main source of IL-2 for T_{regs} appear to be other T cells. This would constitute a negative feedback loop, where T cells activated during an immune response sustain the proliferation of T_{regs} by producing IL-2, and thus aid in their own suppression (Setoguchi *et al.*, 2005). A dire illustration of the importance of this negative feedback loop is provided by familial hemaphagocytic lymphohistiocytosis, where its dysregulation may yield fatal results (Humblet-Baron *et al.*, 2016).

TGF-β

In vitro studies have suggested that T_{reg} suppressive function is cell contact dependent, due to the observation that it is abolished if T_{regs} are separated from target cells by a semi-permeable membrane (Thornton and Shevach, 1998; Hori, Nomura and Sakaguchi, 2003). Whereas this does not negate the possibility of a contribution of contact-independent mechanisms, such as the IL-2 "sink" model, it infers a requirement for additional, contact-dependent mechanisms. One suggestion involves cell surface-bound TGF-β1 on T_{regs} (Nakamura, Kitani and Strober, 2001). However, others have found that T_{regs} can mediate suppressor function in the absence of TGF-β1 (Piccirillo *et al.*, 2002).

CTLA-4

Another molecule suggested to play a role in the suppressive function of T_{regs} is T lymphocyte-associated protein-4 (CTLA-4 or CD152). While *CTLA-4* normally is expressed exclusively upon activation in T cells (Salomon *et al.*, 2000), it is constitutively expressed in T_{regs} under the control of FOXP3 (Hori, Nomura and Sakaguchi, 2003). Mice with specific CTLA-4-deficiency in T_{regs} tend to develop severe autoimmune manifestations (Wing *et al.*, 2008). Imaging studies have reported that both naïve $CD4^+CD25^-$ T cells and $CD4^+CD25^+$ T_{regs}

aggregate around DCs, but that T_{regs} do so more readily. Following this initial, antigen-dependent aggregation, an antigen-independent down-regulation of B7-1 (CD80) and B7-2 (CD86) receptors were observed on DCs. This second step appears to be mediated by CTLA-4, and the final result is a failure of DCs to activate naïve T cells with reactivity towards specific antigens (Onishi *et al.*, 2008). In accordance with this, CTLA-4-lacking T_{regs} are reported to be incapable of preventing upregulation of B7-1 and B7-2 on DCs upon activation in culture (Wing *et al.*, 2008). In addition, CLTA-4 induces increased clustering, and thus increased avidity, of lymphocyte function-associated antigen-1 (LFA-1), an integrin associated with the previously discussed aggregation step (Schneider *et al.*, 2005).

CTLA-4 signaling through B7-1 and B7-2 receptors on DCs also leads to induction of the enzyme 2,3-dioxygenase (IDO), which catalyzes tryptophan metabolism. This can aid in T cell down-regulation by depleting the T cells of tryptophan and by yielding immunotoxic byproducts such as kynurenines (Mellor *et al.*, 2002; Orabona *et al.*, 2004; Fallarino *et al.*, 2006). Alternatively, binding of CTLA-4 to B7 receptors on activated T cells could directly mediate their suppression though pathway distinct from that activated in DCs. This suggestion is based on the observations that B7-deficient T_H cells were resistant to T_{reg}-mediated suppression *in vitro*, and that transfer of B7-deficient $CD4^+$ T cells into mice induced autoimmune disease which could not be inhibited by also transferring T_{regs} (Paust *et al.*, 2004).

GITR/TNFRSF18

Another protein involved in T_{reg} function is the glucocorticoid-induced tumor necrosis factor receptor family-related protein (Gitr), prevalent in $CD4^+$ $CD25^+$ T cells and in $CD4^+CD8^-$ $CD25^+$ thymocytes in naïve, wild-type mice. The observations that GITR stimulation abolishes T_{reg} mediated suppression indicates a role of GITR in abrogation of this self-tolerance mechanism. It has been suggested that GITR stimulation may antagonize the suppressive signals delivered through TCRs and CTLA-4 (Shimizu *et al.*, 2002).

CD39 and CD73

Finally, roles in suppressive function have been ascribed to ectonucleoside triphosphate diphosphohydrolase 1 (ENTPD-1/CD39) and 5' nucleotidase ecto (NT5E/CD73), ectoenzymes present on the surface of T_{regs}. CD39 functions in the hydrolysis of di- and triphosphates to their respective nucleosides, such as AMP. CD73, in turn, hydrolyzes AMP to adenosine and inorganic phosphate. The resulting alteration in adenosine levels in the environment

surrounding the T_{reg} is believed to mediate suppressive signaling though inhibitory A2A receptors on activated T cells (Deaglio *et al.*, 2007).

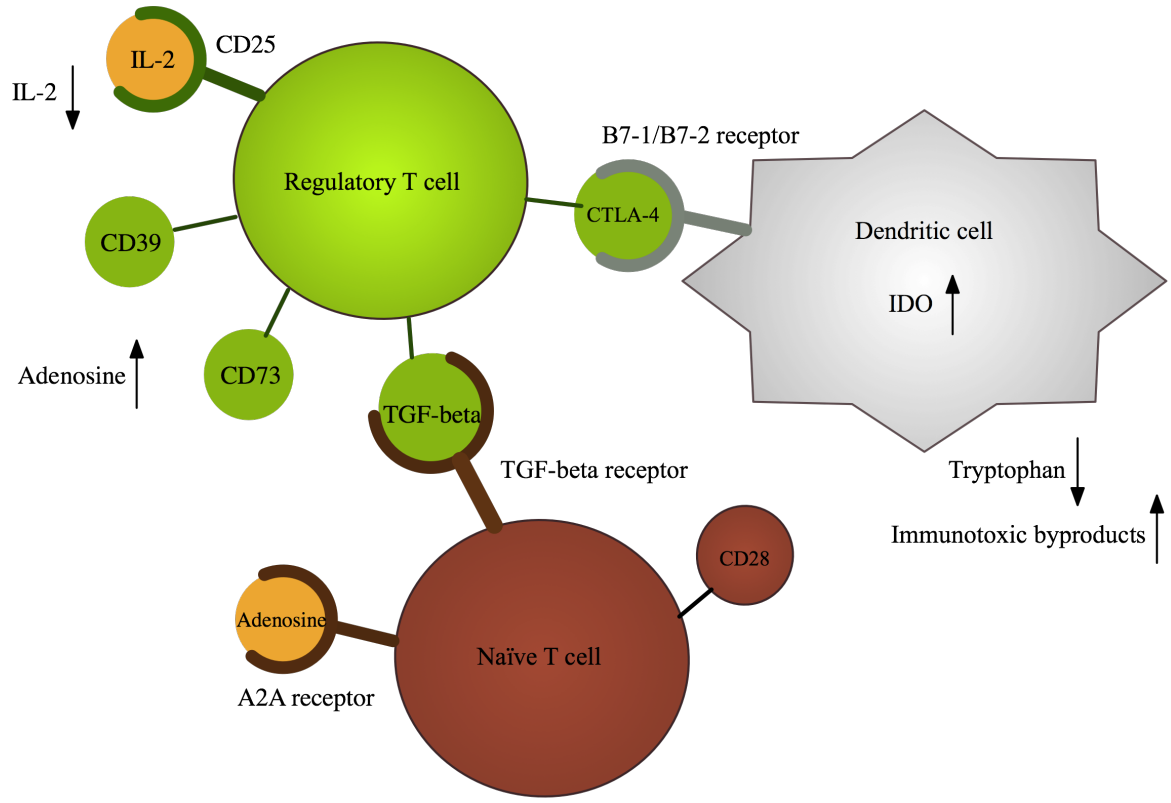

Figure 1.5: Proposed mechanisms of T_{reg} suppressive function. *By high expression of CD25, the receptor for IL-2, T_{regs} are suggested to function as "IL-2 sinks", reducing the availability of other T cells for IL-2. By expression of CD39 and CD73 on the cell surface, T_{regs} are suggested increase the concentration of adenosine, which has inhibitory effects by binding to A2A receptors on T cells. Signals from TGF-β on the cell surface of T_{regs} is suggested to negatively affect the activation of naïve T cells. CTLA-4 on the T_{reg} surface mediates downmodulation of B7-1/B7-2 receptors on dendritic cells, leaving fewer available receptors for binding of the alternative ligand, CD28, present on T cells. Binding of CTLA-4 to B7-1/B7-2 receptor also induces 2,3-dioxygenase (IDO) to metabolize tryptophan, yielding immunotoxic kyrunenines as byproducts.*

1.8 Autoimmune polyendocrine syndrome type I as a model disease for autoimmunity

Loss-of-function mutations *AIRE* has been established as the cause of autoimmune polyendocrine syndrome type 1 (APS-1) (Nagamine *et al.*, 1997; Aaltonen *et al.*, 1997), also referred to as autoimmune polyendocrinopathy-candidiasis-ectodermal dystrophy (APECED) (Perheentupa, 2006). The clinical hallmarks of APS-1 are chronic mucocutaneous candidiasis, hypoparathyroidism and adrenal insufficiency, although a number of other manifestations also occur frequently (figure 1.6). Diagnosis is set by the presence of at least two of this triad, but patients may exhibit pathologies long before this criterion is fulfilled. APS-1 is a rare condition, with an estimated prevalence in the Norwegian population of 1:90 000 (Wolff *et al.*, 2007; Husebye *et al.*, 2009).

1.9 Tolerance impairment in APS-1

It has been proposed that the AIRE deficiency in APS-1 patients leads to a reduction in expression of TRAs in mature mTECs, thus hampering the tolerogenic role played by these cells. In addition, AIRE deficiency has been linked to issues with mTEC development (Yano *et al.*, 2008). A resulting failure in TRA presentation by mTECs during education of T cell progenitors could be expected to lead to self-reactive T cells escaping thymic clonal deletion. These T cells may then attack self-tissues, ultimately resulting in overt autoimmune disease. Indeed, a failure in negative selection in APS-1 has been reported by several studies (Anderson *et al.*, 2002, 2005, Liston *et al.*, 2003, 2004).

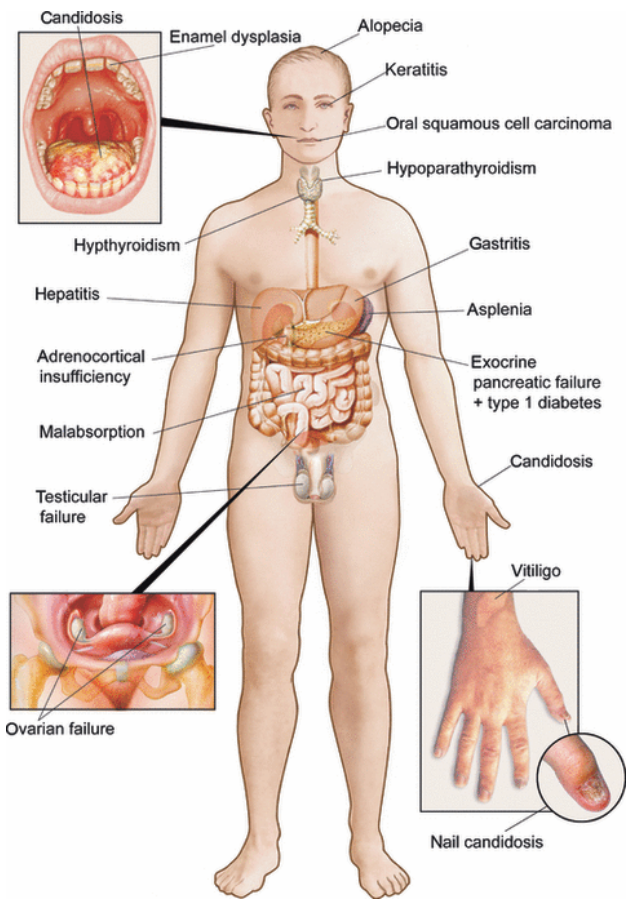

Figure 1.6: Clinical manifestations of APS-1. *The clinical picture is varied, with a large number of potential manifestations. Of special note is the classical triad of chronic mucocutaneous candidiosis, hypoparathyroidism and adrenal insufficiency. Figure from Husebye et al., 2009.*

In addition, a deficiency in T_{regs} could be argued to be a contributing cause of the autoimmune manifestations observed in APS-1 patients. A link between AIRE and the thymic development of certain specificities of T_{regs} has been indicated (Malchow *et al.*, 2013), and it appears that *Aire* expression in the newborn thymus is a prerequisite for correct T_{reg} development in mice (Guerau-de-Arellano *et al.*, 2009; Yang *et al.*, 2015). An interesting possibility that has been raised is that of an AIRE-mediated divergence of autoreactive T cells into the T_{reg} lineage. A comparative study of T cells from *Aire*$^{-/-}$ and *Aire*$^{+/+}$ mice indicated that TCR specificities found to be overrepresented among $CD4^+FOXP3^-$ T cells from the Aire-deficient mice, were found among the $CD4^+FOXP3^+$ T_{regs} in their Aire-sufficient counterparts (Malchow *et al.*, 2016).

One study reported that $CD4^+CD25^{hi}$ cells from APS-1 patients were unable to prevent a proliferative response of $CD25^-$ T cells upon general stimulation. When assessing for an antigen-specific response, by contrast, AIRE-deficient and –sufficient $CD4^+CD25^{hi}$ cells were

equal in suppressive capability. In addition, the TCR repertoire in patient $CD4^+CD25^{hi}$ cells appeared to be skewed toward the TCR repertoire of naïve T cells (Kekäläinen *et al.*, 2007). These findings could be interpreted as an indication of a generalized effect of AIRE-insufficiency, not only restricted to specific antigens. This could perhaps be attributed to effects of AIRE during T_{reg} development.

Quantitative effects on the T_{reg} population has also been reported in APS-1 (Ryan *et al.*, 2005; Wolff *et al.*, 2010). Flow cytometry studies of PBMC (peripheral blood mononuclear cells) from 19 APS-1 patients and age-and sex-matched healthy controls found that the frequency of $CD4^+CD25^+FoxP3^+$ T_{regs} was significantly reduced in the APS-1 patients (Wolff *et al.*, 2010).

1.10 Development and peripheral maintenance of regulatory T cells in APS-1

A T_{reg} deficiency in APS-1 could be due to issues both in the thymic development and the peripheral maintenance of T_{regs}. A study in favor of the former found no significant peripheral conversion into T_{regs} from other $CD4^+$ cells in healthy subjects, suggesting the thymus as the major source of T_{reg} impairment. In addition, the CDR3 length appeared to be increased in the T_{regs} of APS-1 patients compared to healthy subjects (Koivula *et al.*, 2017). This is interesting due to the notion that CDR3 length appears to be gradually shortened during the development of T cell progenitors in the thymus (Matsutani *et al.*, 2007, 2011; Niemi *et al.*, 2015). Thus, the increased length observed in the T_{regs} in APS-1 patients may be argued to be a result of issues with this central lymphoid developmental process.

Others favor the view that peripheral T_{reg} maintenance may be impaired in APS-1 and that this is a crucial cause of T_{reg} insufficiency. For instance, it was observed that a reduction in *FOXP3* expression in T_{regs} from APS-1 patients was less apparent in recent thymic emigrants. The possibility of a slowly dividing reservoir of naïve, peripheral T_{reg} cells in healthy individuals was raised, and that a failure in the maintenance of this reservoir afflict the ability of APS-1 patients to mount T_{reg} responses against self-reactive cells (Laakso *et al.*, 2010). This model corresponds well with the previously mentioned report of a T_{reg} "memory" pool (Rosenblum *et al.*, 2011).

In further support of peripheral effects, *Aire*-expressing cells in secondary lymphoid tissues and the spleen appear to induce the expression on a set of TRAs distinct from those expressed in mTECs (Gardner *et al.*, 2008). While expression levels are significantly lower compared to

mTECs, there is evidence for Aire also being present in peripheral DCs. These DCs have been indicated to express genes correlated with a tolerogenic phenotype, such as IDO (Poliani *et al.*, 2010). It is suggested that expression of *Aire* infers an immature status on DCs and reduces their prowess in T cell activation. Aire-deficiency in DCs has been found to inhibit the differentiation of naïve $CD4^+$ cells into the T_{reg} lineage, while promoting differentiation into other lineages such as T_H17 cells (Huo *et al.*, 2018).

1.11 Hypothesis and aims

Our hypothesis is that the AIRE deficiency in APS-1 patients have an impact on the development or differentiation of T_{regs}. To explore this, we aim to characterize gene expression patterns in T_{regs} from APS-1 patients, both at the RNA and protein level. The resulting knowledge could help us validate previous reports regarding impairment of T_{regs}-mediated tolerance in APS-1 patients, and enhance our understanding of the underlying mechanisms. This, in turn, could prove valuable for the overall goal of identifying molecular targets for implementation of T_{regs} in diagnostics and therapy, potentially with transfer value to other autoimmune diseases.

Aims:

1.) Method development
    a. Develop methodology for obtaining pure suspensions of Tregs
    b. Set up a flow cytometry panel for relevant target proteins
    c. Optimize a real-time qPCR protocol for use for assessment of RNA expression, both at bulk sample and single cell-level
    d. Optimize a low input protocol for whole RNA-sequencing

2.) Assessment of gene expression patterns in APS-1
    a. Assessment of the expression of selected candidate genes at the protein level by use of flow cytometry of PBMC samples from APS-1 patients and controls
    b. Assessment of the expression of selected candidate genes at the RNA level by use of real-time qPCR, conventional PCR and RNA sequencing, using T_{reg} samples from APS-1 patients and controls
    c. Perform a global search for gene expression perturbations in T_{regs} from APS-1 patients by use of total RNA-sequencing

2. Materials

Reagents and chemicals	Supplier	Ref. No.
Ficoll-Paque	Miltenyi Biotec	17-1440-03
Dulbecco's Phosphate Buffered Saline	Sigma Life Science	D8537
AB serum	Sigma Life Science	H4522
Dimethyl Sulphoxide (DMSO) Hybri-Max	Sigma Life Science	D2650
MACSxpress Treg Isolation Kit, human	Miltenyi Biotec	130-109-557
Rinsing buffer: Automacs Rinsing Solution 99.5%	Miltenyi Biotec	130-091-222
MACS BSA Stock solution 0.5%	Miltenyi Biotec	130-091-376
Flow cytometry buffer: Phosphate buffered saline 99.5%	Sigma Life Science	D8537
MACS BSA Stock solution 0.5%	Miltenyi Biotec	130-091-376
Tryphan Blue stain	Invitrogen	T10282
BD Pharm Lyse	BD Biosciences	555899
Anti-CD4 FITC, clone M-T466	Miltenyi Biotec	130-080-501
Anti-CD25 PE, clone 4E3	Miltenyi Biotec	130-091-024
Anti-CD127 APC, clone MB15-18C9	Miltenyi Biotec	130-098-121 130-113-969
Anti FoxP3-APC, clone 3G3	Miltenyi Biotec	130-098-121
Anti-human FoxP3 Staining Set	eBioscience	77-5774-40
BD CompBead Plus Anti-mouse Ig	BD	51-9006274
BD CompBeads Negative control	BD	51-9006227
UtraPure BSA, 50 mg/ml	Abion	AM2616
Absolutt Alkohol	Kemetyl Norge	200-578-6
β-mercaptoethanol	Aldrich chemistry	M6250
RNeasy Mini Kit	Quiagen	74106
Rneasy Plus Micro Kit	Quiagen	74034
Rnase Free DNAse set	Quiagen	79254
High capacity RNA-to-cDNA kit	Applied Bisosystems	4387406
SuperScript III first-stand cDNA synthesis kit	Invitrogen	18080-051
TaqMan Gene Expression Master Mix	Applied Biosystems	4369016
TaqMan gene expression assays:	Applied Biosystems	Hs99999907
B2M		Hs01085834
FOXP3		Hs00230829
AIRE		Hs00915979
IKKF2/HELIOS		Hs00175480
CTLA-4		Hs00969556
ENTPD-1		Hs00188346
GITR		Hs00826128
Neuropilin-1		
DEPC Treated Water	Ambion	AM9906
Nuclease Free Water	VWR chemicals	436912C
Betaine solution, 5M	Sigma Aldrich	B0300
AmpliTaq Gold DNA Polymerase with Gold Buffer and $MgCl_2$	Applied Biosystems	4311814
Custom PCR primers	Eurogentec	
(Details in supplementary information table S.3)		
B2M		
IKZF4		
PECAM-1		
CXCR3		
CD3δ		
mTOR		
TOLLIP		
CCR4		
	Invitrogen	A15629/A15630-
FOXO1		Hs00131544
CCR5		Hs00715153

Neuropilin-1		Hs00318297
TBE buffer	AccuGene	BE50843
Agarose NA	GE Healthcare	17-0554-02
PAGE GelRed Nucleic Acid Gel Stain	Biotium	41008
Amplisize molecular ruler, 50-2000 bp	BioRad	1708200
Gel Loading Dye blue	BioLabs	B70215
Illustra ExoStar	Life Sciences	US77720V
BigDye Terminator v1.1 Sequencing Kit	Applied Biosystems	4336774
RNA 6000 Pico Reagents	Agilent Technologies	5067-1513
High Sensitivity DNA reagents	Agilent Technologies	5067-4626
Smart-Seq v4 Ultra Low Input RNA Kit	Takara	634895
AMPure XP	Beckman Coulter	A63880
Nextera XT DNA Library Preparation Kit	Illumina	15032350
Nextera XT Index Kit	Illumina	15055293
Live/dead Fixable Yellow Dead Cell stain kit	Life technologies	L34959
Fc block	BD	564219
Anti-CD4 AF700, clone RPA-T4	BD	557922
Anti-CD8 PerCP-Cy5.5, clone SKI	BD	565310
Anti-CD25 PE-Cy7 clone 2A3	BD	335789
Anti-CD3 V500, clone UCHT1	BD	561416
Anti-CD45RA APC-H7, clone HI100	BD	560674
Anti-CD31 BV786, clone L133.1	BD	744757
Anti-CTLA4 BV421, clone BN13	Biolegend	369606
Anti-FOXP3 PE-CF594, clone 259D/C7	BD	563955
Anti-Nrp1 BV650, clone HIL-7R-M21	BD	743131
Anti-Ki67, clone 20Raj1	Invitrogen	11-5699-42
Anti-CD39 PE, clone ebioA1	Invitrogen	12-0399-42
Anti-Helios APC, clone 22F6	Biolegend	137222
OneComp eBeads	Invitrogen	01-1111-41

Equipment and consumables

ART Barrier reload insert pipette tips:		Molecular Bioproducts	2179-RI
	1000 µl		2069-RI
	200 µl		2065-RI
	100 µl		2139-RI
	10 µl		
Clip-Tip reload pipette tips 20 µl		Thermo Fischer	94420218
Finnpipette F1 pipettes		Thermo Fischer	
Fastpette		Labnet	
Pipette tips, 10 ml		Sterilin	475110
Disposable pipettes		VWR	1612-1613
Centrifuge tubes:	50 ml	VWR	21008-242
	15 ml		21008-216
Safe-lock tubes 1.5 ml		Eppendorf	0030 120.086
Round-bottom tubes, 5 ml		Corning Science	352063
Cryogenic vials 1.5 ml		Nalgene	5000-1020
BD Vacutainer, heparin 10 ml		BD	367526
Vacuette tube, K3E EDTA 9 ml		Greiner Bio-One	455036
Vortexer V1S000		IKA	
SB2 rotator		Stuart	
Countess cell counting chamber slides		Invitrogen	C10283
MacsExspress separator		Miltenyi Biotec	130-042-302
MidiMACS separator		Miltenyi Biotec	130-042-302
LS Columns		Miltenyi Biotec	130-042-401
MicroAmp Optical 96 well reaction plate		Applied Biosystems	N8010560
MicroAmp Optical Adhesive film		Applied Biosystems	201501347
5810R Centrifuge		Eppendorf	
Heraeus multifuge 3SR+		Thermo Fischer	

Kinetic energy 26 joules minicentrifuge	VWR	C1413V
Thermomixer	Eppendorf	
QuiaShredder Columns	Quiagen	79656
MicroAmp 8-tupe strip, 0.2 µl	Applied Biosystems	N8010580
MicroAmp 8-cap strip	Applied Biosystems	N8010535
GeneAmp 9700 PCR system	Applied Biosystems	
384 Well Multiply PCR Plate	Sarstedt	72.1984.202
Gel tray, comb, casting chamber	General supplier	
Hoefer HE33 electrophoresis unit	Pharmacia Biotech	80-6052-45
Electrophoresis power supply	Amercham Biosciences	
Chip Priming station	Agilent Technologies	5065-4401
RNA Pico Chips	Agilent Technologies	5067-1530
DNA High Sensitivity Chips	Agilent technologies	5067-4626
IKA vortex mixer	Agilent technologies	
SMARTer-Seq Magnetic Separator	Takara	635011

Instruments

Countess Automated cell counter	Thermo Fischer
Accuri C6 flow cytometer	BD
LSR Fortessa flow cytometer	BD
FACS Aria SORP	BD
NanoDrop ND-1000 Spectrophotometer	Saveen Werner
ABI Prism 7900HT sequence detection system	Thermo Fisher
GelDoc EZ gel documentation system	BioRad
ABI 3730 Sequencer	Applied Biosystems
Agilent 2100 Bioanalyzer	Agilent technologies
HiSeq4000 sequencing system	Illumina

Software

FlowJo 10.4	FlowJo, LLC
ND-1000 3.8	Thermo Fisher
SDS 2.3	Applied Biosystems
GelDoc EZ ImageLab 3	BioRad
CLC main workbench 8.0	Quiagen
2100 Expert	Agilent Technologies
GraphPad prism 8.0	GraphPhad Software

3. Methods

3.1 Experimental pipeline and choice of methods

The experimental pipeline is illustrated in figure 3.1. Blood samples were collected from APS-1 patients and controls, and isolated cells were distributed across the applied techniques.

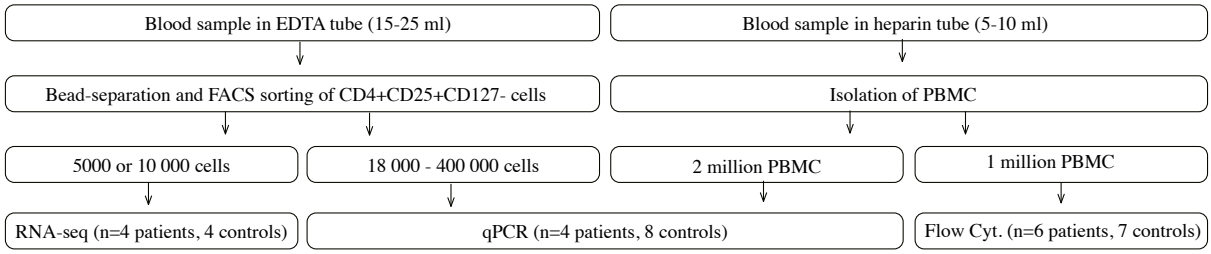

Figure 3.1: Overview of the experimental pipeline *$CD4^+CD25^+CD127^-$. T_{reg}, were isolated from peripheral blood by magnetic bead separation and FACS. Peripheral blood mononuclear cells (PBMC) were isolated from peripheral blood by density gradient centrifugation. RNA from both T_{regs} and PBMC were used for qPCR and conventional PCR. In addition, RNA-seq was performed for smaller T_{reg} samples. For assessment of the expression of T_{reg}-associated genes at the protein level, flow cytometry studies of PBMC were performed.*

One of the main techniques used in this project is flow cytometry, where cells are stained using flurochrome-conjugated antibodies specific for molecular targets of interest. The fluorescence resulting from antibody binding is then measured by the flow cytometer. The flurochromes are excited by lasers, and the emitted light is collected through filters allowing the passage of particular wavelengths. An additional feature is the ability to observe how light is scattered by the cells. Larger cells will result in a higher forward scatter compared to smaller cells, and more complex (granular) cells will result in higher side scatter compared to less complex cells. The same features are exploited when using fluorescence activated cell sorting (FACS).

To assess the expression level of selected genes at the RNA level, real-time quantitative qPCR is used. The selected approach is the TaqMan technology, as this is considered a highly sensitive method (Löseke *et al.*, 2003). The method is based on annealing of probe sequences containing a 3' fluorochome and a 5' quencher to the template. As the TaqMan polymerase has 5' exonuclease activity, amplification will release the fluorochrome from the quencher. This results in a fluorescent signal of a magnitude corresponding to the number of times a template has been amplified. This means that the more template sequences are present in the initial sample, the larger the signal will be. Output is given in the form of a C_T value, which reflects the number of amplification cycles that is required for the signal to reach a threshold value. To facilitate comparison across samples, the C_T values are normalized based on the results for a

reference gene, expected to be present at the same relative amount in all samples (Livak and Schmittgen, 2001).

The development of high-throughput sequencing methodologies has facilitated transcriptome analysis by RNA sequencing. First, RNA isolated from cell samples is reverse-transcribed into complementary DNA. By using poly-T sequences as primers for the reverse transcription, the resulting cDNA will pertain from mRNA sequences. If the RNA input for cDNA synthesis is low, it may be necessary to perform a pre-amplification of the cDNA, primed by random hexamer sequences. After cDNA synthesis, a library of cDNA fragments of suitable size for the selected sequencing platform must be created. To make the run on the sequencing platform more cost-effective, it may be desired to pool the libraries resulting from different samples and run them together on a single lane. This can be done by introducing unique, short index-sequences in each library (Kukurba and Motgomery, 2015).

3.2 Ethical aspects

The project was conducted in compliance with the Declaration of Helsinki, and approved by the Regional Ethical Committee of Western Norway (approval number 2009/2555 and 2018/1417). All patients had given written informed consent. Controls samples were obtained from the Haukeland University Hospital blood bank, and all blood donors had given written consent to samples being used in research.

3.3 Patients and controls

The APS-1 patients (4 Females, 2 males, range 40-64 years old, mean age 51 years old) all had mutations in the *AIRE* gene, and 5 fulfilled the criteria for clinical diagnosis (supplementary information table S.1). All patients were included in the protein profiling study, patients 1-4 were included in the RNA study. The control samples (1 female, 11 males, range 25-66 years old, mean age 43 years old) were obtained from healthy blood donors (supplementary information table S.2).

3.4 PBMC isolation by density gradient centrifugation

Fresh blood samples (5-10 ml) were collected in heparin tubes and diluted 1:1 in PBS. The samples were added on top of Ficoll-Paque (2:1) prior to centrifugation for 30 min at 500 xg at 20°C. The peripheral blood mononuclear cell (PBMC) layer was collected and washed by addition of 10 ml PBS and centrifugation for 15 min at 350xg at 4°C. Cell counting was

performed by use of a Countess automatic cell counter. Approximately $2x10^6$ cells, to be used for real-time quantitative PCR, were lysed in 600 µl RNeasy Lysis (RLT) buffer, and stored at -80°C. Batches of $1x10^6$ cells, to be used for flow cytometry, were resuspended in 500 µl AB serum 10% (v/v) DMSO and stored at -80°C for 24-72 hours, then at -150°C until use.

3.5 T_{reg} isolation by magnetic bead separation

Fresh blood samples (15-25 ml) were collected in EDTA tubes. T_{regs} were isolated using MacsExpress T_{reg} isolation kit according to the manufacturer's protocol. Briefly, peripheral blood, MacsExpress T_{reg} isolation buffer and Macsexpress T_{reg} isolation cocktail was mixed (20:10:1) prior to incubation in an overhead rotator for 10 min. The sample was then placed in a MacsExpress separator for 15 min, the supernatant was centrifuged for 10 min at 350xg 20°C, and the pellet was resuspended in 4 ml rinsing buffer (Automacs Rinsing solution with 0.5% BSA). This suspension was then passed through an LS column placed in a MidiMacs separator. After washing with 4 ml rinsing buffer, the column was removed from the MidiMacs separator and the cells were eluted by adding 2 ml rinsing buffer and using a plunger. The eluate was centrifuged for 10 min at 350xg 4°C and cells were resuspended in 300 µl rinsing buffer.

3.6 Fluorescence activated cell sorting (FACS)

Cells from the magnetic bead separation were stained with the antibodies α-CD4-FITC (dilution factor 1:20), α-CD25-PE (dilution factor 1:10) and α-CD127-APC (dilution factor 1:10 for Cat. No 130-098-121, 1:50 for Cat. No. 130-113-969). The dilution factors had been chosen based on initial experiments using two different dilution factors. After 30 min incubation in the dark at 4°C, the cells were washed by addition of 2 ml rinsing buffer and centrifugation for 10 min at 350xg at 4°C. The pellet was then resuspended in 500 µl rinsing buffer. The $CD4^+CD25^+CD127^{lo}$ cells were sorted into 300 µl PBS by use of a FACS Aria SORP (figure 3.2). Excitation was performed by 488 nm and 635 nm lasers, emitted light was collected though a 525/50 filter for FITC, a 575/25 filter for PE, and a 660/20 filter for APC. The yield varied from 18 000 to 400 000 cells. The cells were centrifuged for 10 min at 350xg 4°C and the pellet was lysed in 350 µl RLT plus buffer. The lysate was either immediately subjected to the RNA isolation protocol or stored at -80°C. In addition, samples of 5000 and 10 000 $CD4^+CD25^{hi}CD127^{lo}$ cells, meant for RNA sequencing, were sorted into 75 µl RLT plus buffer 10% v/v β-mercaptoethanol, and the lysate was stored at -80°C. For each sample, an unstained control was also prepared from 100 µl peripheral blood from the same individual.

Erythrocytes were lysed by addition of 2 ml 1X BD pharm lyse buffer and incubation for 10 min at room temperature. The cells were pelleted by centrifugation as before, and washed with 2 ml rinsing buffer. The pellet was resuspended in 350 µl rinsing buffer and run on the FACS Aria SORP as the stained sample.

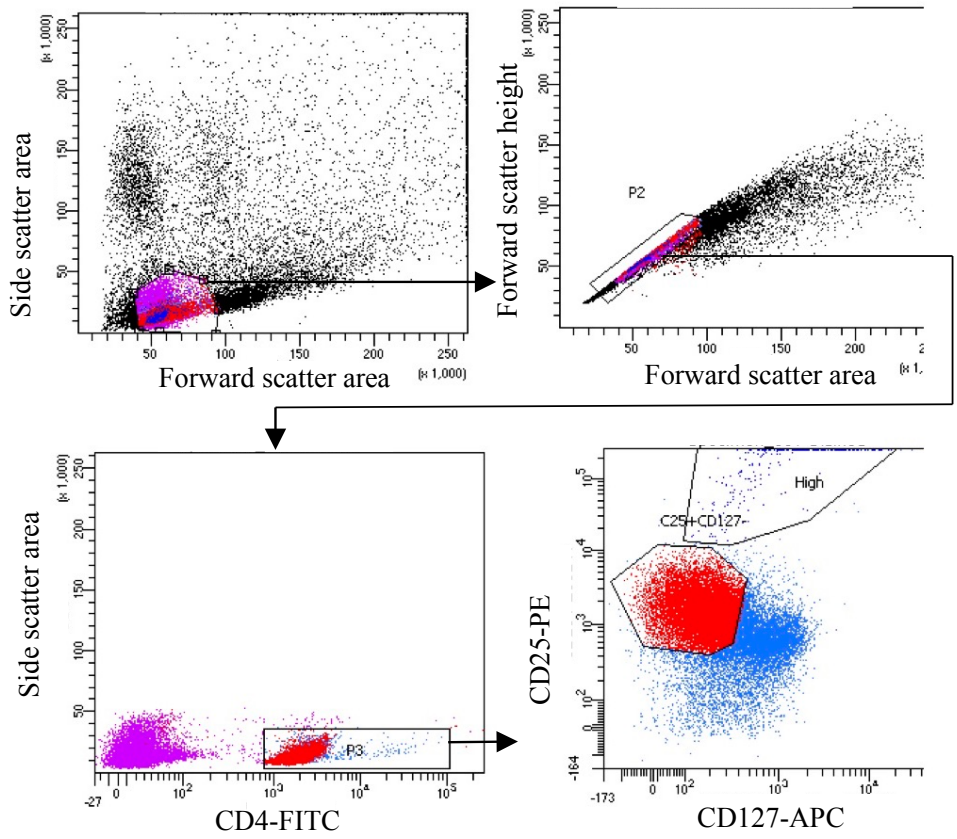

Figure 3.2: Gating strategy used during FACS sorting of $CD4^+CD25^+CD127^{lo}$ cells. *First, a gate was set for live cells, using a FSC area vs. SSC area plot, and cells having passed singly though the lasers were identified on a FSC area vs. FSC height plot. Then, FITC fluorescence vs. SSC-A was used to gate for the CD4-posotive cells. Finally, the $CD25^+CD127^{lo}$ cells were identified on a plot of APC vs. PE fluorescence.*

3.7 Validation of the T_{reg} isolation protocol using flow cytometry

The reasoning behind using the surface marker CD127 is that this marker has been reported to have a negative correlation with FOXP3 (Liu *et al.*, 2006). It should thus be possible to use this marker as a FOXP3 surrogate, avoiding the need for cell permeabilization. To determine whether this inverse correlation could be observed, and to validate the success of the magnetic bead separation protocol, flow cytometry of PBMC and bead separated cells was used. The frozen PBMC were thawed at 37°C, 200 µl AB serum was added, and the cells were washed by addition of 10 ml PBS and centrifugation at 350xg at 4°C for 10 min. The pellet was resuspended in 100 µl flow cytometry buffer (PBS with 0.5% BSA), and the surface markers (CD4, CD25 and CD127) were stained as previously. For FOXP3 staining, fixation and

permeabilization was performed by use of the anti-human FoxP3 staining set according to the manufacturer's protocol. Briefly, cells were spun down as before and resuspended in 1 ml fix/perm buffer. After incubation at 4°C for 45 min, 2 ml 1X permeabilization buffer was added, and the cells were centrifuged at 500xg 20°C for 5 min. The pellet was resuspended in 100 µl permeabilization buffer, and α-FOXP3-APC was added (dilution factor 1:10). After incubation for 30 min in the dark at 4°C, the cells were washed twice by adding 2 ml diluted permeabilization buffer and centrifugation as before. The pellet was then resuspended in 350 µl flow cytometry buffer. In addition to the stained cell samples, an unstained sample was included for each separate experiment. Compensation controls were prepared using BD compensation beads. For each antibody, 1 drop compensation beads and 1 drop negative control beads were stained as the cell samples. All samples were run on an Accuri c6 flow cytometer until 100 000 (PBMC) or 60 000 (bead separated cells) events had been collected. Excitation was performed by 488 nm and 640 nm lasers, and emitted light was collected though a 530/30 band pass filter for FITC, a 585/40 band pass filter for PE, and a 675/25 band pass filter for APC. The data analysis was performed using FlowJo software version 10.1.

One sample of bulk sorted cells was used for validation of the sorting procedure. After FACS sorting, the cells were stained with FOXP3-APC as described previously, the sample was run on the flow cytometer until 75 000 events had been collected.

3.8 T_{reg} protein profiling by flow cytometry

The T_{reg} flow cytometry panel (table 3.1) was inspired by a workshop regarding T_{regs} in clinical samples (Santegoets *et al.*, 2015). PBMC from the 6 patients and 7 controls (supplementary information tables S.1 and S.2) were thawed as before, and between $5x10^5$ and $1x10^6$ cells were resuspended in 100 µl flow cytometry buffer. The surface markers were stained using the chosen antibody concentrations, by the same protocol as previously explained. Staining of intracellular markers (FOXP3, Helios, and Ki-67) was subsequently performed using the eBioscience Anti-human FOXP3 Staining Set as previously explained, with some changes. The incubation in fixation/permeabilization buffer was increased from 45 min to overnight to ensure complete fixation of all cells. After the first wash step in permeabilization buffer, 2 µl Fc block was added to cells resuspended in the 100 µl permabilization buffer, in order to prevent non-specific antibody binding to Fc receptor on immune cells. The cells were then incubated for 15 min at 4°C in the dark prior to staining. Samples were run on a LSR Fortessa flow cytometer until 100 000-300 000 events had been collected in the lymphocyte gate. Excitation was

performed by use of 407 nm, 488 nm, 561 nm and 640 nm lasers, and emitted light was collected though the filters listed in table 3.1.

The dilution factors for all antibodies were chosen based on initial titration experiments applying five different antibody concentrations (representative experiments in figure 3.3). For abundant markers, PBMC from healthy controls were split into samples of 200 000 cells and stained using the relevant antibody. For the rare markers, PBMC were mixed 1:5 with bead-separated cells from the same healthy control, and cells were stained using the α-CD4-Alexa Fluor 700 antibody in addition to the antibody specific for the marker in question.

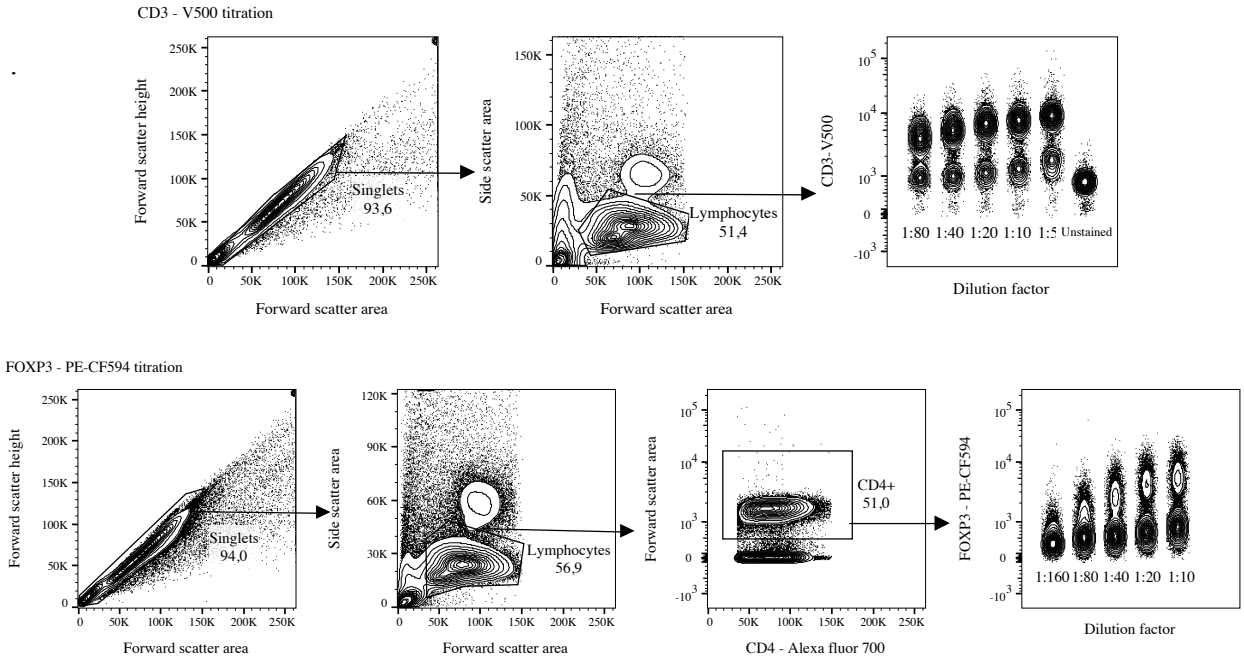

Figure 3.3: Titration of the α-CD3-V500 (top) and α-FOXP3-PE-CF594 (bottom) antibodies. *First, a plot of forward scatter area versus forward scatter height was used to gate for cells having passed singly by the lasers. Then, a plot of forward scatter area versus side scatter area was used to gate for lymphocytes. For the FOXP3 titration, an additional gate was set for $CD4^+$ cells based on a forward scatter area versus Alexa fluor 700 fluorescence plot. Then, for both antibodies, a concatenated plot showing the fluorescence pertaining from the respective antibody for five different samples, stained by the use of different dilution factors, was created. These concatenated plots formed the basis of the decisions regarding which dilution factors to use when staining the patient and control samples, based on the best possible separation of the negative and positive cell populations.*

For all antibodies except α-CD4, α-CD8 and α-CD3, fluorescence minus one (FMO) controls were performed. Compensation controls were prepared by staining of OneComp eBeads, for the Live/dead fixable yellow stain, single-stained PBMC were used as compensation control. The compensation controls were performed in order to account for "spillage" of emitted light, meaning that light from one fluochrome is detected by the channel designated for another fluorochrome.

Table 3.1: *Overview of the flow cytometry panel, with targets, fluorochomes, dilution factors and the wavelengths used for excitation and collection of emission.*

Target	Fluorochrome	Dilution factor	Excitation	Filter for emittance
CD3	V500	1:20	407 nm	670/30 band pass
CD4	Alexa Fluor 700	1:160	640 nm	730/45 band pass
CD8	PerCP-Cy5.5	1:20	488 nm	695/40 band pass
CD25/IL-2RA	PE-Cy7	1:40	561 nm	780/60 band pass
CD45RA	APC-H7	1:80	640 nm	780/60 band pass
CD152/CTLA-4	BV421	1:20	407 nm	450/50 band pass
CD39/ENTPD-1	PE	1:500	561 nm	582/15 band pass
CD31/PECAM-1	BV785	1:160	407 nm	780/60 band pass
CD304/Neuropilin-1	BV650	1:80	407 nm	670/30 band pass
FOXP3	PE-CF594	1:10	561 nm	610/20 band pass
Helios/IKZF2	APC	1:40	640 nm	670/14 band pass
Ki-67	FITC	1:10	488 nm	530/30 band pass
Dead cell stain	Q-dot585	1:1000	407 nm	585/42 band pass

3.9 RNA isolation

For cell numbers <5x10^5, RNA was isolated by using the RNeasy Micro Plus kit, while for samples of >5x10^5 cells, the RNeasy Mini kit was used. In both cases, the manufacturer's protocol was followed. The lysate was passed through a QuiaShredder column, and for the RNeasy Micro Plus Kit, genomic DNA was removed by passage through a gDNA eliminator column. One volume of 70% ethanol was added, and the samples were passed through an RNeasy MiniElute (for the micro kit) or Mini (for the mini kit) spin column. After washing with 350 µl buffer RW1, on-column DNase digestion was performed by using the RNase-Free DNase set. DNase I was diluted 1:8 in RDD buffer, and 80 µl was added to the column membrane prior to incubation for 15 min at room temperature. The column was washed with 350 µl buffer RW1, 500 µl buffer RPE and either 500 µl 80% ethanol (micro kit) or 500 µl RPE (mini kit). RNA was eluted in 14 µl (micro kit) or 30 µl (mini kit) RNAse free H_2O, which was passed twice though the column.

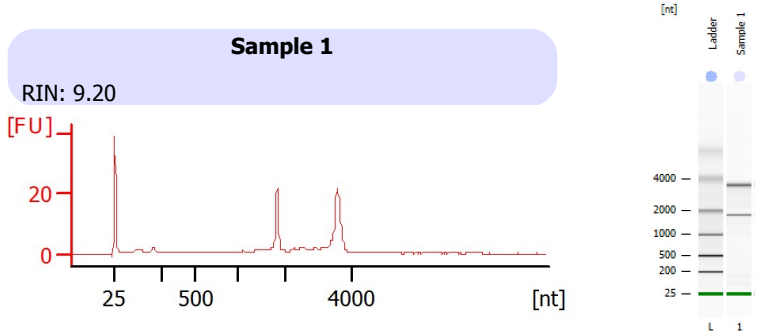

Figure 3.4: An example of Agilent Bioanalyzer output for a high quality RNA sample. *The sample is from control 1 T_{regs} and was used for RNA-seq. On the gel image, two clearly distinct bands, pertaining to 18S and 28S rRNA, are observed, and no smearing pertaining from degraded RNA fragments is present. On the fluorescence versus nucleotide number plot, the 18S and 28S rRNA are seen as two distinct peaks, and the baseline is otherwise stable. The RNA Integrity Number (RIN) of 9,2 also reflects high RNA quality.*

The RNA quality was assessed by the Agilent Bioanalyzer, using the Agilent 6000 Pico kit according to manufacturer's protocol (figure 3.4). The RNA concentration was determined by use of a NanoDrop ND-1000 Spectrophotometer, and the samples were stored at -80°C if not immediately used.

3.10 Real-time quantitative PCR of T_{reg} candidate genes in bulk samples

First-strand cDNA synthesis was performed using the high capacity RNA-to-cDNA kit, 45 ng RNA was mixed with 10X RT buffer (50% v/v) and RT enzyme (5% v/v) to a total volume of 20 µl and placed in a thermal cycler at 37°C for 60 min, then 95°C for 5 min. qPCR was performed using TaqMan gene expression assays. For each gene expression assay, cDNA (25% v/v), probe/primer mix (5% v/v) (supplementary information table S.4), TaqMan Gene Expression Master mix (48% v/v) and DEPC H_2O was mixed to a total volume of 30 µl. The reaction mixture was transferred in triplicates to a clear 384 well plate. A negative control was prepared for each gene expression assay on every separate run. The plate was placed in a ABI prism sequence detection system and run at the following program: 50°C 2 min, 95°C 10 min, then 45 cycles of 95°C 15s, 60°C 1 min.

3.11 Real-time quantitative PCR of single-cell samples

96-well plates were prepared with 5 µl buffer (Ultrapure BSA (2 mg/µl), DEPC H_2O) in each well. Single $CD4^+CD25^+CD127^-$ cells were sorted into separate wells using a FACS Aria SORP. cDNA synthesis was performed by use of the SuperScript III First-Stand synthesis kit. The sample in each well was mixed with random hexamers (5% v/v), oligo(dT)20 primer (5% v/v), dNTPs (0.5 mM) and DEPC H_2O (8% v/v) to a total volume of 6.5 µl. The plate was incubated at 65°C 5 min, and cDNA synthesis was set up by the addition of 10x RT buffer (5% v/v), $MgCl_2$ (1.25 mM), DTT (5 mM), RNase OUT (5% v/v), SuperScript III RT (2.5%) and DEPC-treated H_2O to a total volume of 10 µl. The plate was then run at the following program in a thermal cycler: 25°C 5 min, 50°C 60 min, 55°C 15 min, 70°C 15 min, 4°C storage. The plate was stored at -20°C until use. After thawing on ice, each sample was diluted 1:2 with DEPC-treated H_2O, and then used for real-time qPCR. The protocols were as for the bulk qPCR samples, with two exceptions: Triplicates were not achievable due to limited material, so only one reaction was run per well, and the cycle number was increased to 50.

3.12 Conventional PCR

A conventional PCR protocol was developed as a semi-quantitative approach in order to assess the expression of a larger number of candidate genes. The following reaction mix was set up to a final volume of 25 µl: PCR gold buffer 10x (10% v/v), $MgCl_2$ (1.5 µM), dNTP (0.8 µM), betaine (1.4 M), forward primer (0.4 µM), reverse primer (0.4 µM), enzyme (0.8% v/v), nuclease-free H_2O (35.2% v/v), cDNA (prepared as explained for bulk qPCR, 4% v/v). The reaction was run at the following thermal cycler program: 96°C 10 min, then 35 cycles of 95°C 20 s, 55°C 20 s, 72°C 1 min, followed by 72°C 7 min and 4°C storage. The PCR protocol was performed for PBMC and T_{regs} from control 1 (results not shown). Unfortunately, running the PCR on patient T_{reg} samples for comparison with control T_{reg} samples was not possible due to the limited amount of sample material available.

During initial testing, PCR products were sequenced to ensure that that they corresponded to the correct gene. First, 5 µl PCR product was rinsed by addition of 2 µl ExoStar and subjection to thermal cycler program 37°C 15 min, 80°C 15 min. For sequencing, the BigDye Terminator V.1.1 kit was used, reaction mixture with total volume 10 µl contained rinsed PCR product (35% v/v), BigDye v 1.1 (10% v/v), BigDye buffer (20% v/v), either fw or rv primer (0.2 mM), nuclease-free H_2O (25% v/v). The reaction was then run on the following thermal cycler program: 96°C 5 min, then 30 cycles of 96°C 15 s, 50°C 15 s, 60°C 2 min, 4°C storage. The samples were sequenced by the Medical Genetics Department at Haukeland University Hospital by use of a ABI 3730 sequencer, and data analysis was performed using CLC main workbench 8.0 software.

3.13 RNA sequencing

RNA-seq was performed using the SMART-Seq v4 Ultra Low Input RNA Kit according to the manufacturer's protocol. For 10 000 cell samples, the RNA was diluted 1:2, while RNA from 5000 cell samples was kept undiluted. Then, 1 µl 10x reaction buffer (10 X lysis buffer with RNase Inhibitor, 5% v/v) and 2 µl 3' SMART-Seq CDC Primer IIA (12 µM) was added to 9.5 µl sample, and tubes were incubated at 72°C for 3 min, then on ice for 2 min. First-Strand cDNA synthesis reaction mix was set up as follows to a total volume of 20 µl: 5x Ultra-Low First-Strand Buffer (20% v/v), SMART-Seq v4 oligonucleotide (5% v/v), RNase Inhibitor (2.5% v/v), SMARTScribe Reverse Transcriptase (10% v/v), and the prepared sample from the

previous step. The tubes were then run on the thermal cycler program 42°C 90 min, 70°C 10 min, 4°C storage.

Reaction mix for cDNA amplification was then set up to a total volume of 50 µl: 2x SeqAmp PCR Buffer (50% v/v), PCR Primer 11A (0.24 µM), SeqAmp DNA Polymerase (2% v/v), Nuclease-free H_2O (6% v/v), and the cDNA from the previous step. The tubes were subjected to the following thermal cycler program: 95°C 1 min, then 10 cycles of 98°C 10 s, 65°C 30 s, 68°C 3 min, then 72°C 10 min, 4 °C storage. The decision to use 10 cycles was based on the two initial experiments, where 7 and 10 PCR cycles was tested.

The amplified cDNA was purified by use of the Agencourt AMPure XP Kit. First, 1 µl 10 X lysis buffer from the SMART-Seq v4 Kit was added to each sample, prior to addition of 50 µl Agencourt AMPure XP beads and 8 min incubation at room temperature. Samples were then placed in a magnetic stand for 5 min. The supernatant was removed, and the beads were washed twice with 200 µl 80% ethanol while still in the magnet. The samples were spun briefly and placed back in the magnet for an additional 30s for removal of residual ethanol. After aspiration of ethanol, the pellet was allowed to dry for 5-10 min., and 17 µl elution buffer from the Smart-Seq v4 kit was added. The samples were removed from the magnet and allowed to rehydrate for 2 min. Then, samples were placed back in the magnet and incubated for at least 1 min, before supernatants containing cDNA were transferred to new tubes. The purified cDNA was assessed by an Agilent Bioanalyzer by use of the Agilent High Sensitivity DNA Kit (figure 3.5) according to the manufacturer's protocol. The samples were stored at -20°C.

Library preparation was performed using the Nextera XT DNA Library Preparation kit and the Nextera XT Index kit according to the manufacturer's protocol. The cDNA was diluted according to the results from the Agilent Bioanalyzer (1:10 for samples with peak at around 100 FU, 1:5 for samples with peak at around 50 FU), and 5 µl diluted sample was mixed with 10 µl Tagment DNA buffer. Next, 5 µl Amplicon Tagment Mix was added, and the samples were centrifuged at 280xg 20°C 1 min. The samples were then placed in a thermal cycler at 55°C for 5 min, with a subsequent temperature drop. As soon as the temperature reached 10°C, 5 µl neutralize tagment buffer was added to each well. Samples were centrifuged as before and incubated at room temperature for 5 min. Unique combinations of i5 (5 µl) and i7 (5 µl) index adapters were added to each respective sample. Then, 15 µl Nextera PCR Master Mix was

added, and the samples were centrifuged as before. The samples were subjected to the following thermal cycler program: 72°C 3 min, 95°C 30s, then 12 cycles of 95°C 10s, 55°C 30s, 72°C 30s, then 72°C 5 min and 10°C storage. The samples were purified using AMPPure XP beads as before, with the exception of shaking at 1800 rpm for 2 min. prior to the 8 min. incubation period, and elution in 52.5 µl resuspension buffer from the Nextera XT kit. The samples were then assessed by the Agilent high sensitivity DNA kit utilizing the Agilent Bioanalyzer (figure 3.5) according to manufacturer's protocol. Sequencing of the products was performed by the Bergen Genomics core facility, using a HiSeq4000 sequencer according to the Illumina TruSeq Stranded mRNA protocol. Sequencing depth was approximately 100 million reads per sample. The data analysis was performed in collaboration with PhD candidate Amund Holte Berger, Department of Clincal Sciences, Unversity of Bergen. Quality control was performed using the FastQC software, and reads were aligned to the GRCh38.p12 reference transcriptome by the Kallisto pseudoalligner (Bray *et al.*, 2016).

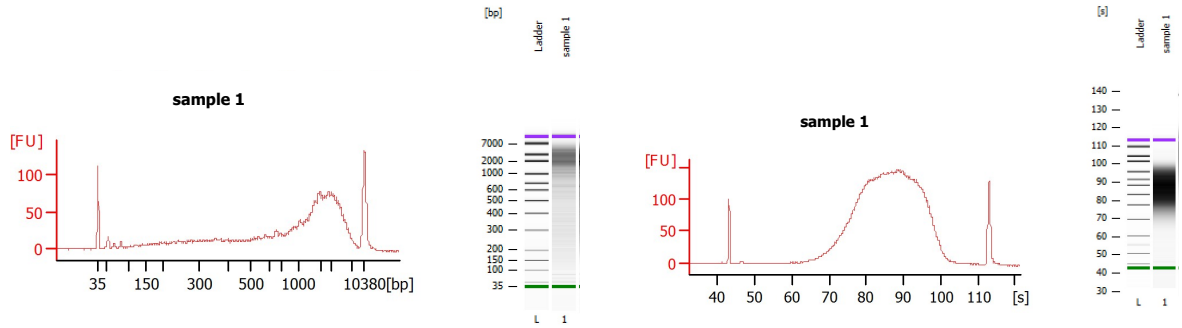

Figure 3.5: An example of Agilent Bioanalyzer output for the amplified cDNA (left) and after library preparation (right) from control 1. *The results for the amplified cDNA indicate the presence of cDNA fragments, with lengths above 1000 bp. The results after library preparation indicate the presence of cDNA fragments of a concentration and size range suitable for sequencing.*

3.14 Statistical analysis

For the qPCR and flow cytometry data, a non-parametric, two-tailed Mann-Whitney test was performed by using Graphpad software. This test considers differences in medians, shape and spread between two groups (Hart, 2001). The use of a non-parametric test was chosen due to the low number of samples, preventing an assumption of a normal distribution. Results were found statistical significant if $P < 0.05$. For the RNA-seq data analysis, P-values were obtained by application of the WALD test. Calculation of FDR (false discovery rate) values was subsequently performed by use of the Bejamini-Hockberg transformation (Benjamini and Hochberg, 1995). This was done to account for the notion that an increase number of tests increases the likelihood of false positives. Results were found statistical significant if FDR < 0.05.

4. Results

4.1 Validation of the T_{reg} isolation protocol

Flow cytometry was used to assess the success of the magnetic bead separation, and to determine whether there was an inverse correlation between the expression of CD127 and FOXP3. PBMC and bead-separated cells from one donor were stained for CD4, CD25 and either CD127 or FOXP3.

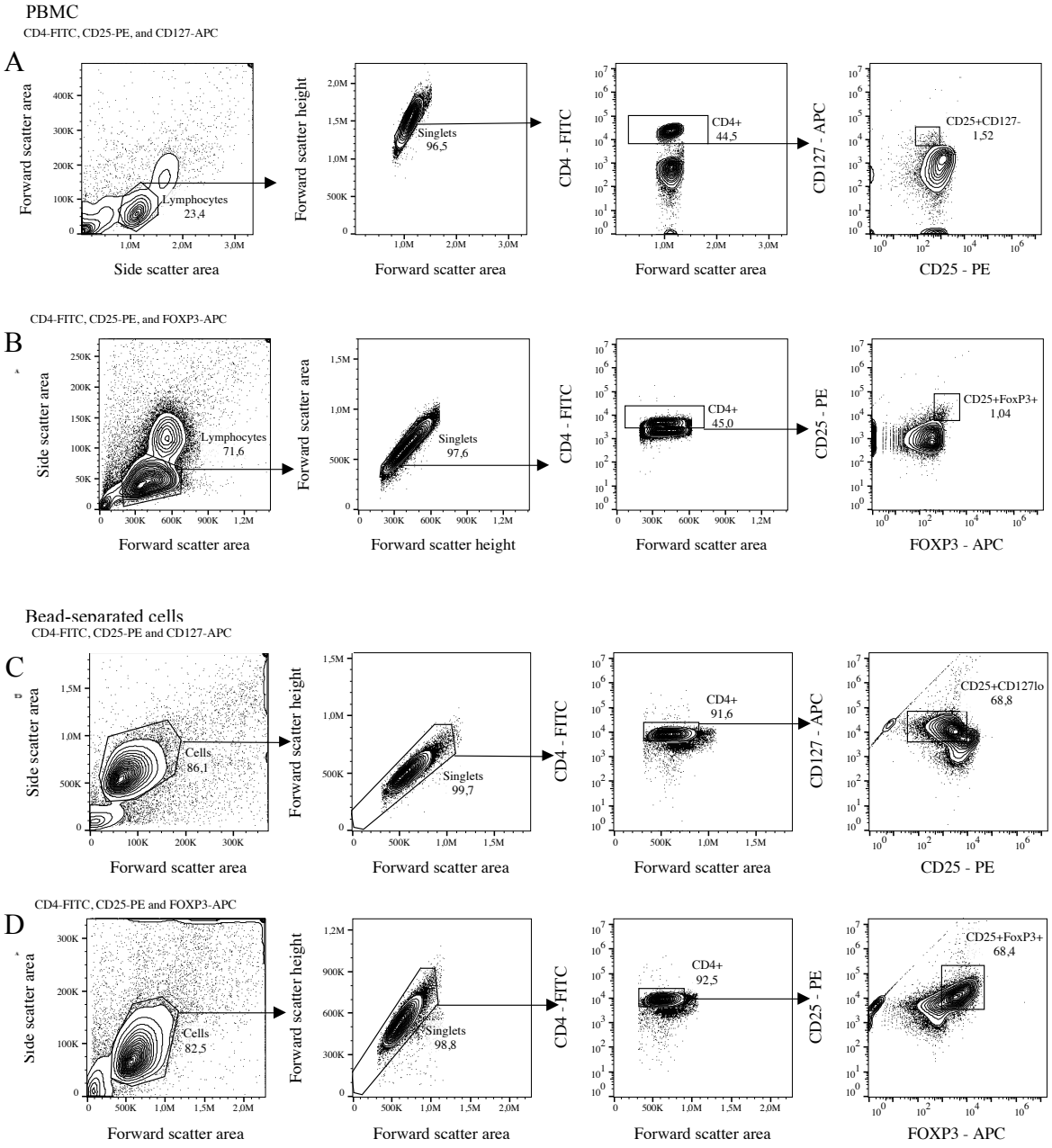

Figure 4.1: Results from flow cytometry assessment of PBMC (A and B) and bead separated cells (C and D) stained with CD4, CD25 and either CD127 or FOXP3. *First, a plot of forward scatter area versus side scatter area is used to gate for lymphocytes, and a plot of forward scatter area versus forward scatter height is used to gate for cells having passed by the lasers as single cells. Then, a plot of forward scatter area versus FITC fluorescence is used to gate for $CD4^+$ cells. Finally, a plot of APC fluorescence versus PE fluorescence is used to gate for the $CD25^+CD127^{lo}$ or $CD25^+FOXP3^+$ population.*

The frequency of T_{regs}, defined either as $CD4^+CD25^+CD127^{lo}$ or $CD4^+CD25^+FOXP3^+$, was found to be markedly increased after the magnetic bead separation. However, there still remained a number of non-T_{regs}. The observed frequency was similar regardless of whether $CD127^{lo}$ or $FOXP3^+$ was used to define the T_{reg} population.

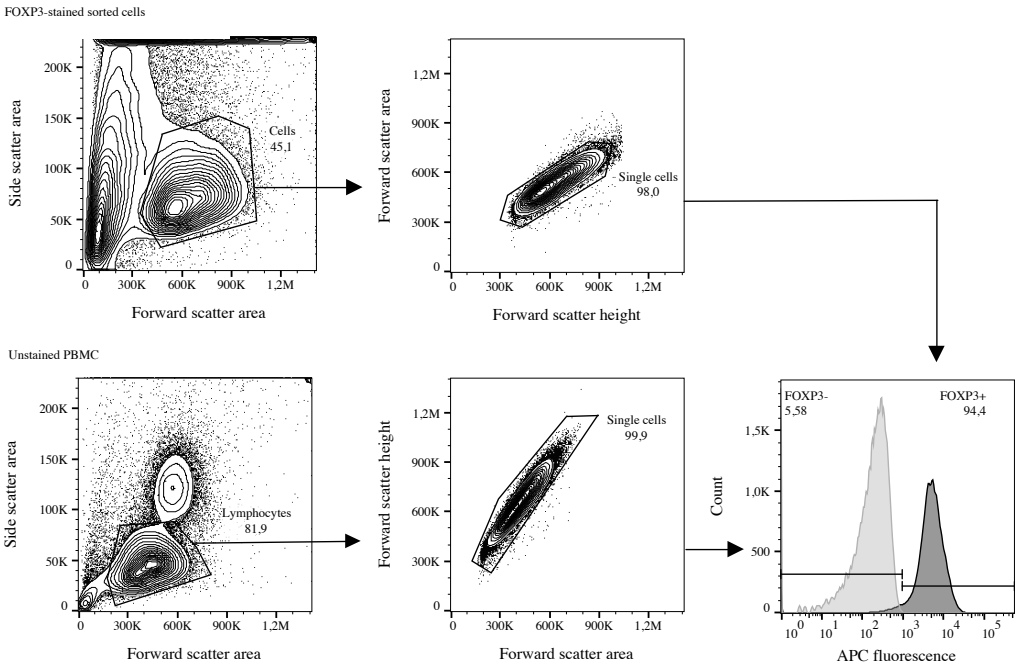

Figure 4.2: FOXP3-staining of $CD4^+CD25^+CD127^{lo}$ cells after FACS. *For the sorted cell sample, a cell gate was set on a forward scatter area versus side scatter area plot, and a single cell gate was set on a forward scatter versus side scatter height plot. Then, an APC fluorescence versus cell count plot was used to gate for $FOXP^+$ and $FOXP3^-$ cells. The negative population was defined based on an unstained PBMC sample. The gating strategy for the PBMC was the same, except for the cell gate being replaced by a lymphocyte gate on the forward scatter area versus side scatter area plot.*

To assess whether the sorted $CD4^+CD25^+CD127^{lo}$ cells were also $FOXP3^+$, FOXP3 staining and flow cytometric assessment was performed on one sample of sorted cells from a representative healthy control. When an unstained PBMC sample was used to define the negative population, approximately 94% of the sorted cells were $FOXP3^+$, after removing cells that had not passed singly by the lasers and debris (figure 4.2).

4.2 Protein profiling study using flow cytometry

The antibody panel (table 3.1) was used for assessment of PBMC samples from 6 APS-1 patients and 7 controls (representative data in figures 4.3 and 4.4). A comparison of the frequency of positive cells for the respective markers for the patients and the controls was performed using Graphpad software (figure 4.5, table 4.1).

Patient 1

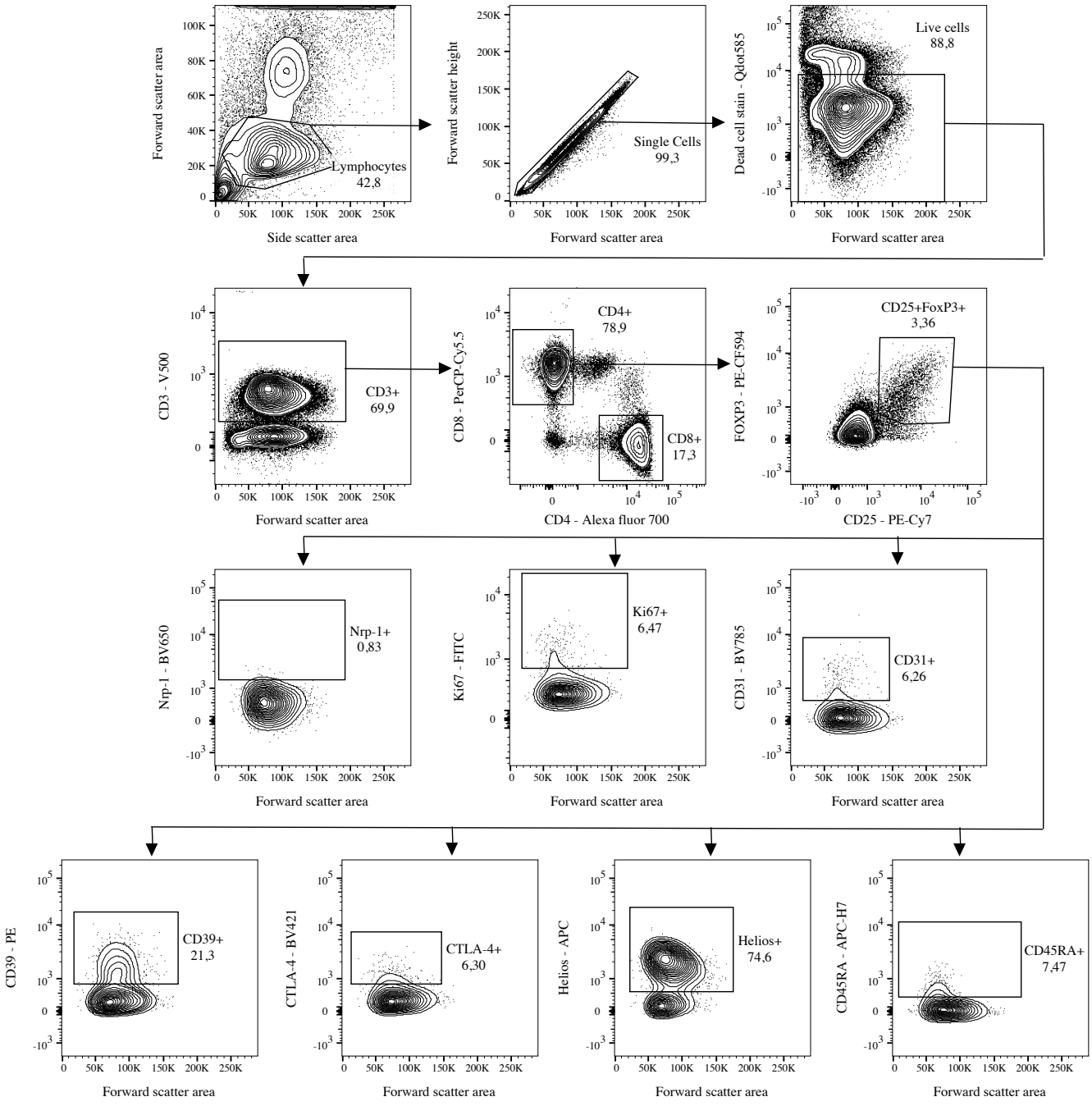

Figure 4.3: The result from assessment of patient 1 PBMC by the flow cytometry antibody panel. *First, a plot of forward scatter area versus side scatter area was used to gate for lymphocytes, followed by a forward scatter area versus forward scatter height plot in order to gate for cells having passed singly by the lasers. Then, a plot of forward scatter area versus QDot 585 fluorescence was used to gate for live cells. A plot of forward scatter area versus V500 fluorescence was used to gate for T cells, defined as $CD3^+$. To gate for single-positive $CD4^+CD8^-$ cells, a plot of PerCy-Cy5.5 fluorescence versus Alexa fluor 700 fluorescence was used. Then, a gate was set for the T_{regs}, defined as $CD25^+FOXP3^+$, on a plot of PE-CF594 fluorescence versus Pe-Cy7 fluorescence. For this population, plots of forward scatter area versus the fluorescence of the relevant fluorochrome was used to define cells positive for Neuropilin-1, Ki-67, CD31/Pecam-1^+, CD39/ENTPD-1^+, CD152/CTLA-4^+ and Helios$^+$, respectively.*

Control 1

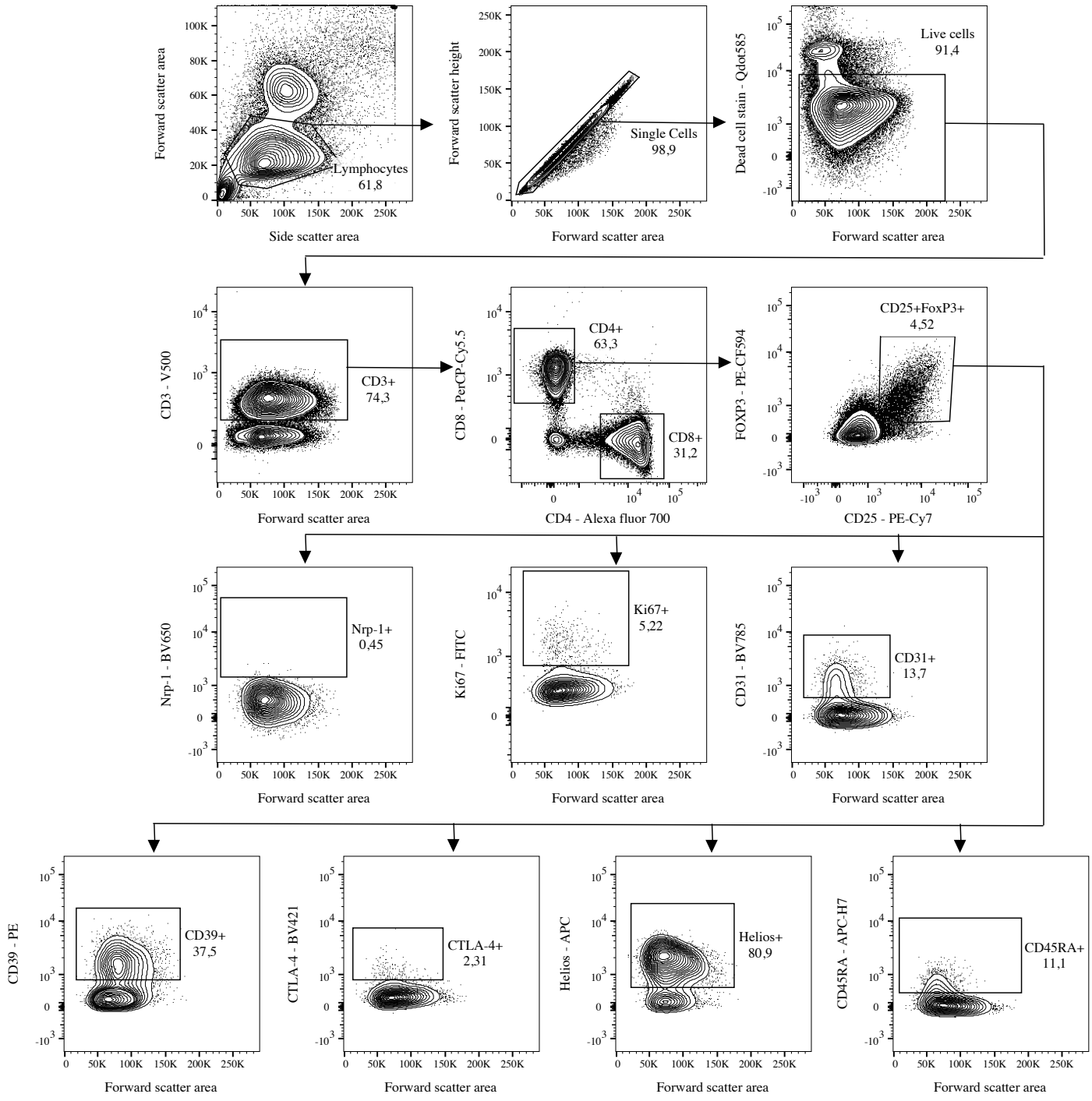

Figure 4.4: The result from assessment of control 1 PBMC by the flow cytometry antibody panel. *First, a plot of forward scatter area versus side scatter area was used to gate for lymphocytes, followed by a forward scatter area versus forward scatter height plot in order to gate for cells having passed singly by the lasers. Then, a plot of forward scatter area versus QDot 585 fluorescence was used to gate for live cells. A plot of forward scatter area versus V500 fluorescence was used to gate for T cells, defined as $CD3^+$. To gate for single-positive $CD4^+CD8^-$ cells, a plot of PerCy-Cy5.5 fluorescence versus Alexa fluor 700 fluorescence was used. Then, a gate was set for the T_{regs}, defined as $CD25^+FOXP3^+$, on a plot of PE-CF594 fluorescence versus Pe-Cy7 fluorescence. For this population, plots of forward scatter area versus the fluorescence of the relevant fluorochrome was used to define cells positive for Neuropilin-1, Ki-67, CD31/Pecam-1^+, CD39/ENTPD-1^+, CD152/CTLA-4^+ and Helios$^+$, respectively.*

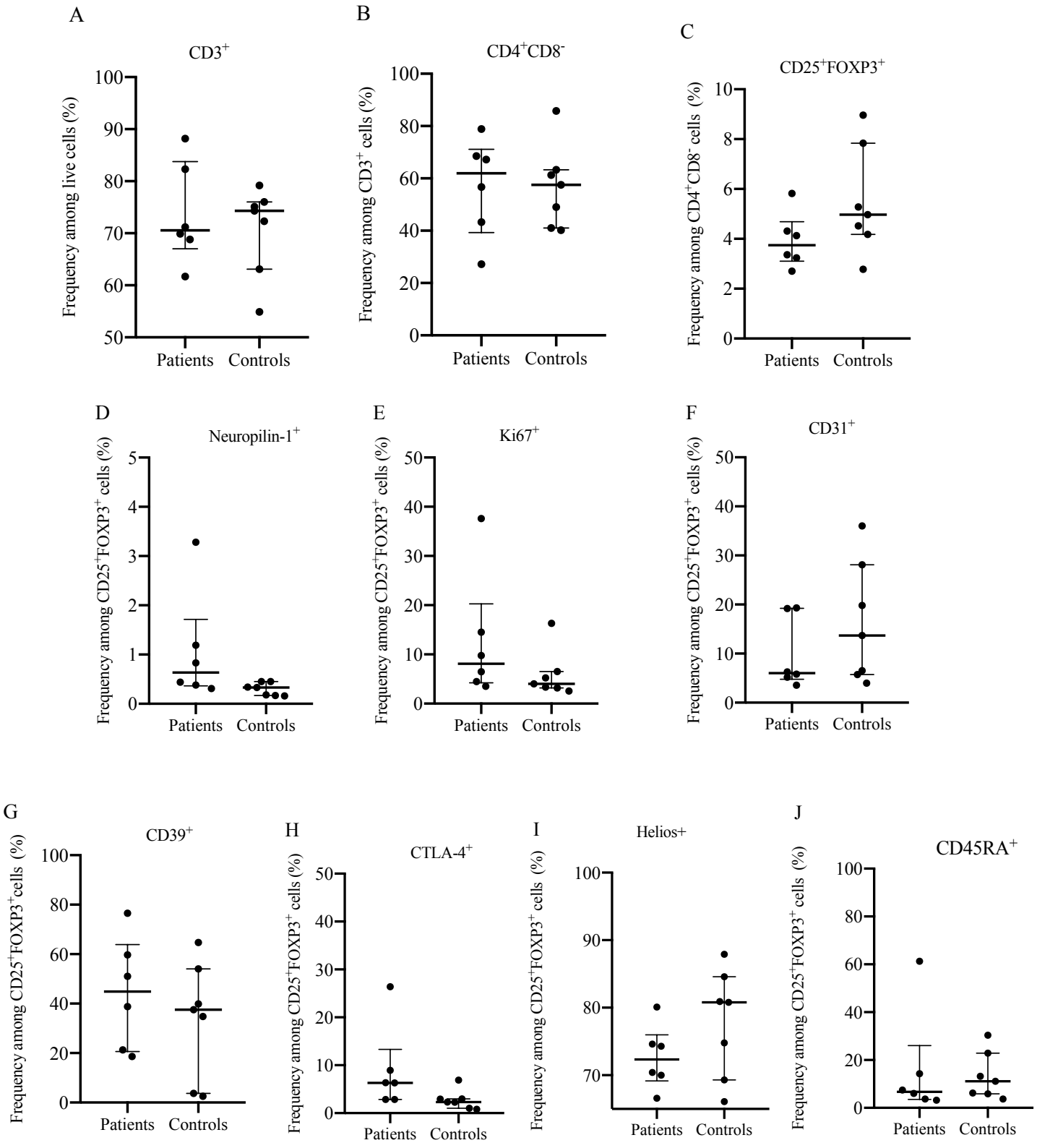

Figure 4.5: A comparison of the frequency of positive cells for the respective markers, within the respective parent gates, in PBMC from APS-1 patients and controls. *The plots are based on the gating levels as shown in figures 4.3 and 4.4. The horizontal lines indicate medians, and the error bars indicate interquartile ranges.*

Based on the median percentage frequency values, the frequency of $CD3^+$ cells and $CD4^+CD8^-$ cells were similar between APS-1 patients and controls. The frequency of $CD25^+FOXP3^+$ cells was also relatively similar between the two groups, although these cells have a slightly reduced frequency in the APS-1 patients compared to the controls. Within the $CD25^+FOXP^+$ population, the frequency of cells positive for CD31, a marker of recent thymic emigrants (Kimmig *et al.*, 2002), CD45RA, a marker of naïve cells (Michie *et al.*, 1992), and Helios was found to be slightly higher in the control group compared to the patient group. For Ki-67, a marker of cellular proliferation (Gerdes *et al.*, 1983), Neuropilin-1, CD39, and CTLA-4, the opposite result was found, with the highest frequency of positive cells being found in the patient group. However, for all the tested markers, the differences between APS-1 patients and controls were small, and the spread between individuals relatively large. Based on a two-tailed Mann-Whitney test, none of the observed differences was found to be significant.

Table 4.1*: Median frequency of cells positive for the respective markers, within the parent gates as indicated by figures 3´4.3 and 4.4. The P-value obtained by a two-tailed Mann-Whitney test is also shown.*

	Median frequency within parent gate (%), patients	**Median frequency within parent gate (%), controls**	**P-value**
$CD3^+$	71.20	73.70	0.7922
$CD4^+CD8^-$	56.70	53.25	>0.9999
$CD25^+FOXP3^-$	3.745	4.970	0.1375
$Nrp\text{-}1^+$	0.6350	0.3300	0.0670
$Ki67^+$	8.120	4.000	0.1807
$CD31^+$	6.035	13.70	0.2949
$CD39^+$	44.90	37.50	0.5338
$CTLA\text{-}4^+$	6.330	2.310	0.0670
$Helios^+$	72.35	80.80	0.2343
$CD45RA^+$	6.735	11.10	0.6282

When performing the flow cytometry staining protocol, the CTLA-4 staining was performed prior to permeabilization, so that the resulting fluorescence would pertain to cell surface-bound CTLA-4 only. To assess the effect of also staining for intracellular CTLA-4, a sample of control 1 PBMC was stained both before and after permeabilization. The result of surface staining alone was compared with the results from the main protocol. When combining intracellular and cell surface staining for CTLA-4, a large increase was observed in the frequency of $CTLA\text{-}4^+$ cells within the $CD3^+CD4^+CD8^-CD25^+$ population (29.1%) compared to the frequency obtained with cell surface staining alone (2.67%) (figure 4.6).

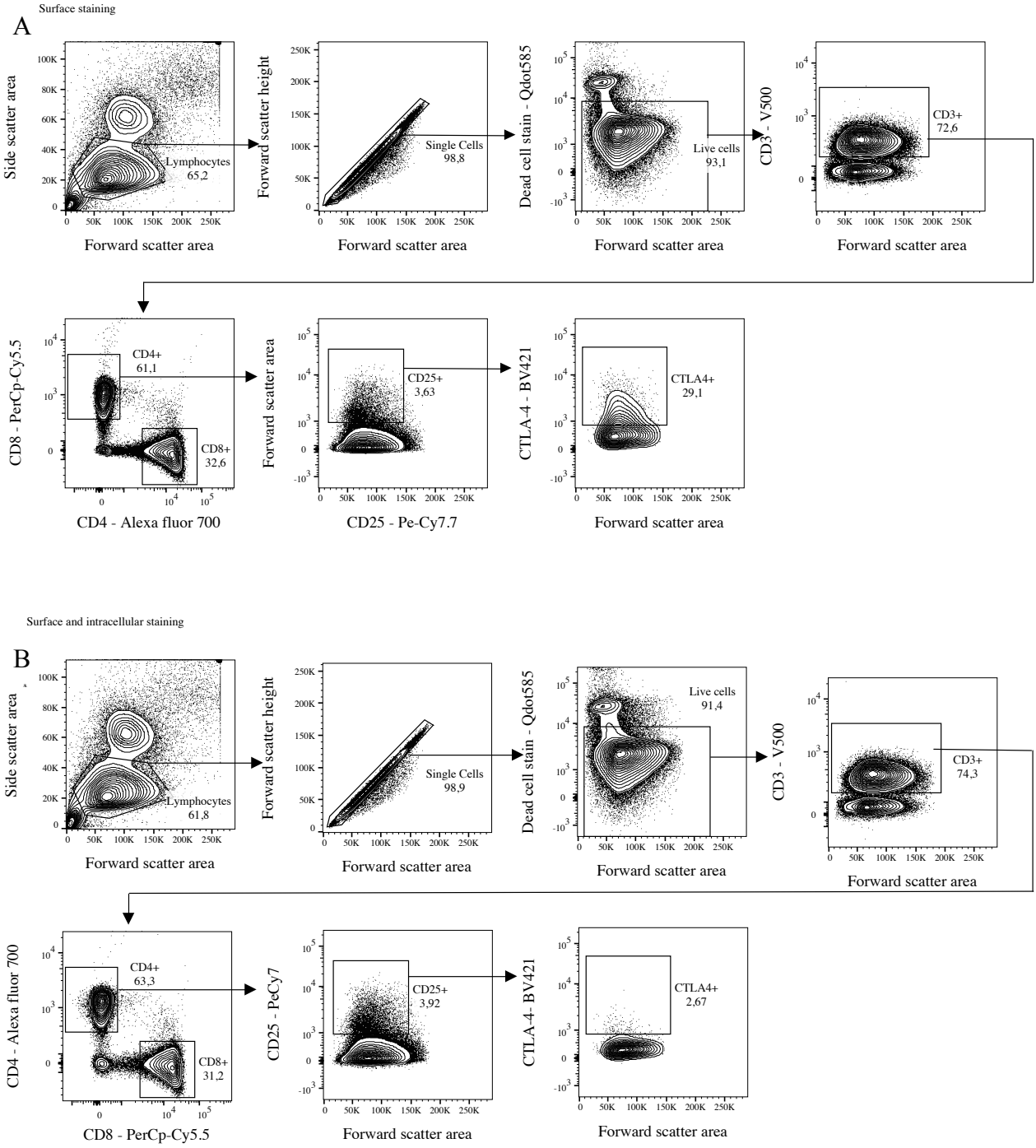

Figure 4.6: The result of performing both cell surface and intracellular staining for CD152/CTLA-4 (A), versus performing cell surface staining only (B). *Gates were set for lymphocytes, singe cells, live cells, $CD3^+$ cells and $CD4^+CD8^-$ cells as before. Then, a forward scatter area versus PE-Cy7 fluorescence were used to gate for cells showing high expression of CD25. Finally, a plot of forward scatter area versus BV412 fluorescence was used to gate for CTLA-4^+ cells within the $CD25^+$ population. When performing both cell surface and intracellular staining, 29.1% of $CD25^+$ cells were also CTLA-4^+, while the corresponding number when performing cell surface staining only was 2,57%.*

Previous reports (Booth *et al.*, 2010) have indicated that the frequency of $CD45RA^+$ T_{regs} decreases with age. To assess whether such an effect was present, a plot was created showing the age of all controls versus the observed $CD45RA^+$ frequency within the $CD3^+CD4^+CD8^-CD25^+FOXP3^+$ population (figure 4.7). With the exception of one control exhibiting a high CD45RA-frequency at age 52, the trend was otherwise a decrease with increasing age.

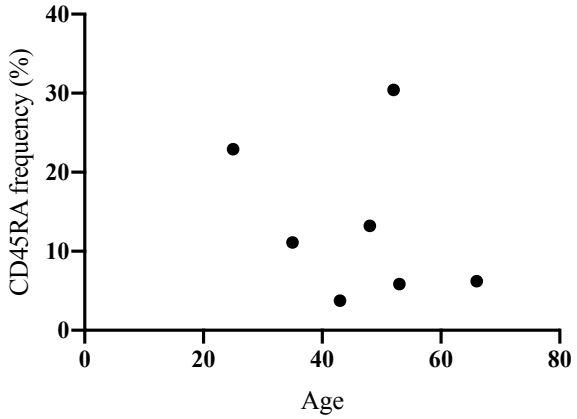

Figure 4.7: A plot of control age versus $CD45RA^+$ frequency in the $CD3^+CD4^+CD8^-CD25^+FOXP3^+$ population. *The general trend is a decreasing frequency with increasing age.*

4.3 Assessment of gene expression at the RNA level

4.3.A Real-time quantitative PCR of candidate genes

PBMC and T_{reg} bulk samples from 4 APS-1 patients and 8 healthy controls were assessed for expression levels of *FOXP3*, *AIRE* and *HELIOS* by the qPCR protocol. The PBMC samples were also assessed for expression levels of *CTLA-4*, *ENTPD-1* and *GITR*, the T_{reg} samples were not assessed for these last three due to limited material availability.

For each individual, fold change values for the expression of the assessed genes in T_{reg} relative to PBMC were calculated (figure 4.8). For *FOXP3*, there was a large increase in expression levels in T_{regs} compared to the PBMC, with median fold change values above 130 both for the patients and controls. *CTLA-4* and *HELIOS* were also indicated to have a substantial increase in expression levels in the T_{regs} compared to the PBMC, with a median fold change value of 36 for *CTLA-4,* and of 22 and 14 for *HELIOS,* for the patient and controls, respectively. For the remaining genes, increases in expressing levels in the T_{regs} compared to the PBMC were also observed, in descending order *GITR*, *AIRE* and *ENTPD-1*. However, these increases were relatively small.

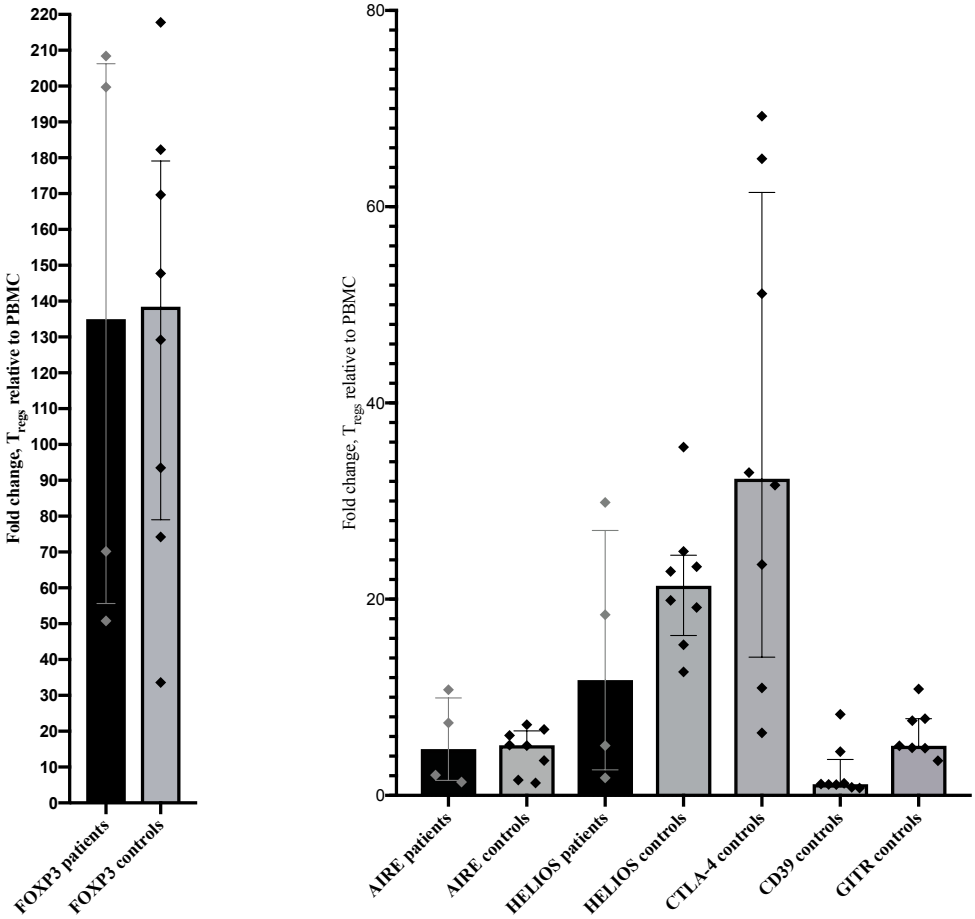

Figure 4.8: Fold change of the expression of each of the assessed genes in T_{regs} compared to PBMC from the same individual. *The bars indicate median fold change values within the patient or control group, and the error bars indicate interquartile ranges. Fold change values were calculated by the formula* $2^{-\Delta\Delta C_T}$, *where* $\Delta\Delta C_T$ *represent the difference between normalized* C_T *values for* T_{regs} *and PBMC from the same individual. A large fold change was observed for* FOXP3*, resulting in the need to place this gene in a separate plot (left) in order to ensure suitable scaling of the Y-axis. For the remaining genes (right), increases were also observed, with the largest fold change values observed for* CTLA-4 *and* HELIOS. *Smaller fold change values for* GITR, AIRE *and* CD39 *indicated that slight increases in expression levels in* T_{regs} *compared to PBMC was present also for these genes.*

Pairwise comparisons of the median ΔC_T values of the patients and the controls were performed for each respective gene (figure 4.9). For *FOXP3*, *AIRE*, and *HELIOS*, this was done both for PBMC and T_{reg} samples. For *CTLA-4*, *ENTPD-1*, and *GITR*, this was done for PBMC samples only. No clear differences were observed in the ΔC_T values between the patient and the control group, for any of the genes, regardless of whether PBMC or T_{reg} samples were assessed.

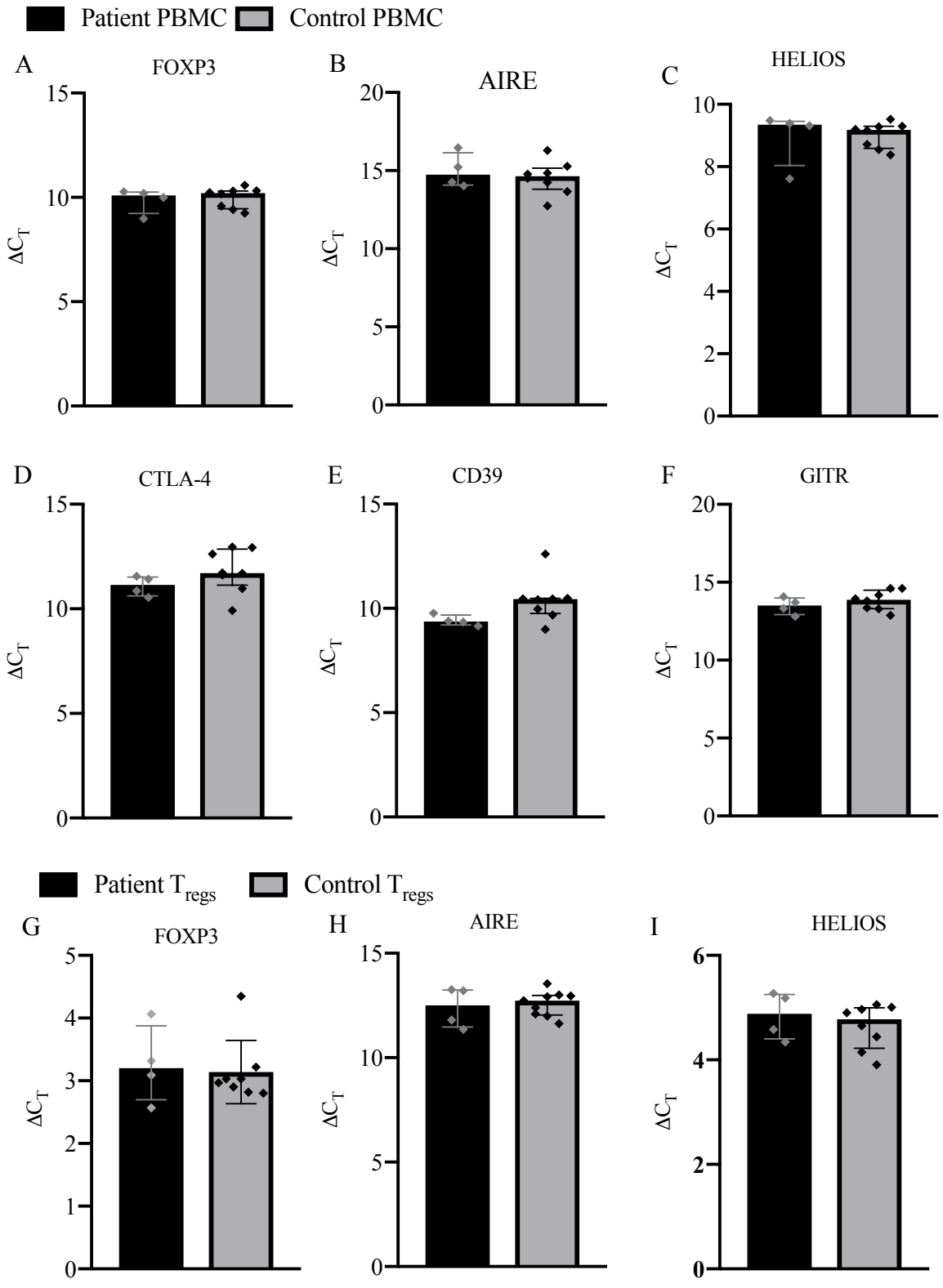

Figure 4.9: Comparative plots of median ΔC_T values for the patients and controls, both for PBMC and Treg samples, for each of the genes assessed by qPCR. *Based on the pairwise comparisons of median ΔC_T values, no large differences appear to exist in the expression levels of* FOXP3, AIRE, HELIOS, CTLA-4, CD39, *or* GITR *between the patients and controls. This holds true both for the PBMC and the T_{reg} samples. The error bars indicate interquartile ranges.*

The qPCR protocol was also tested on single cell samples (data not shown), using the gene expression assays for *B2M* and *FOXP3*. The resulting raw C_T values were relatively high for *B2M*, reflecting the very low initial amount of template, and lacking altogether for *FOXP3*. When assessing a 10 cell-sample, the situation was slightly improved, but still far from the values that would allow reliable assessment. Attempts at optimization of the current qPCR protocol were done, but found insufficient to alleviate the issue.

4.3.B Conventional PCR of candidate genes

A protocol for the assessment of the expression of a number of other candidate genes based on conventional PCR was developed. Based on the obtained results for one representative control (figure 4.10), none of these genes were indicated to have increased levels of expression in T_{reg} compared to PBMC. Thus, they were not considered to be highly T_{reg}-specific. As they could still have important functions in T_{regs}, comparative experiments using T_{reg} samples from APS-1 patients and controls were planned. Unfortunately, the lack of sufficient sample material from the APS-1 patients prevented the execution of such experiments.

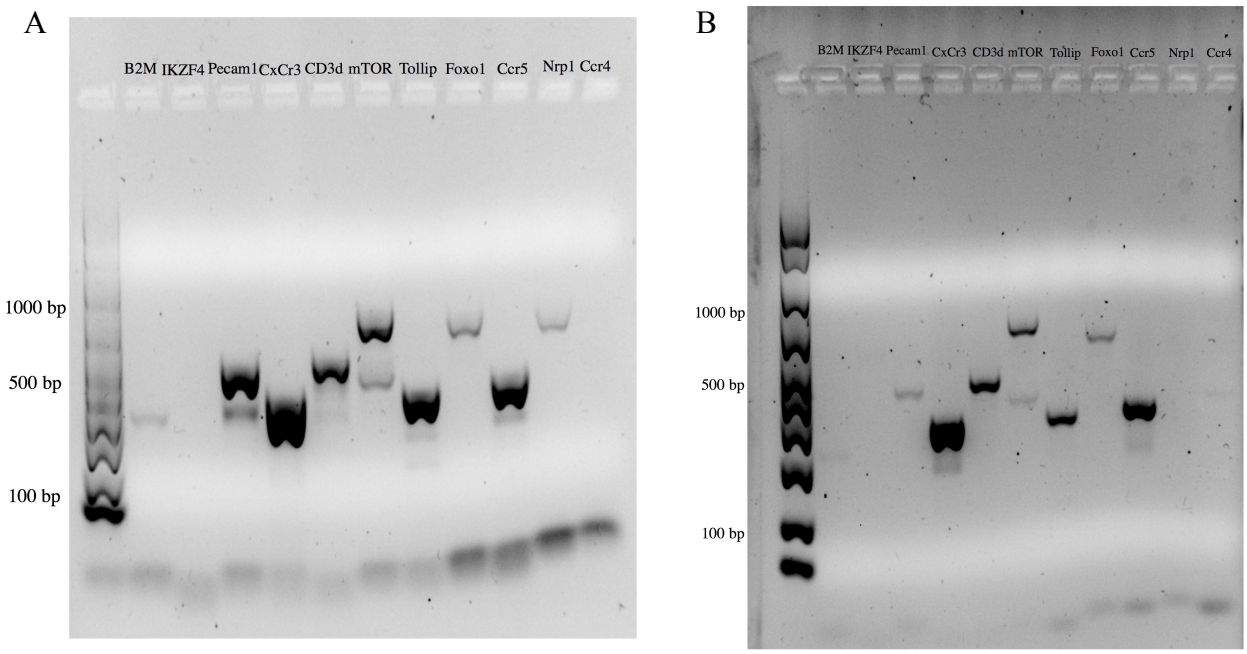

Fgure 4.10: The result of conventional PCR for selected candidate genes using PBMC (A) and T_{reg} (B) samples from control 1, visualized by agarose gel electrophoresis. *None of the assessed genes appeared to be highly increased in expression in the T_{reg} sample compared to the PBMC sample.*

4.3.C RNA sequencing

RNA-sequencing was performed on samples of 5000 $CD4^+CD25^+CD127^-$ T_{regs} from 4 patients and 4 healthy controls, and standard quality controls were executed. Thereafter, an assessment of candidate genes of particular interest (supplementary information table S.4), was performed. For each of these genes, pairwise comparisons of the TPM (transcript per million) values for the APS-1 patients and controls were performed (figure 4.12). As for the qPCR results, most did not exhibit significant changes, however, a significant increase in mTOR expression was observed for the APS-1 patients (figure 4.11). The significance level was set based on FDR (false discovery rate) values.

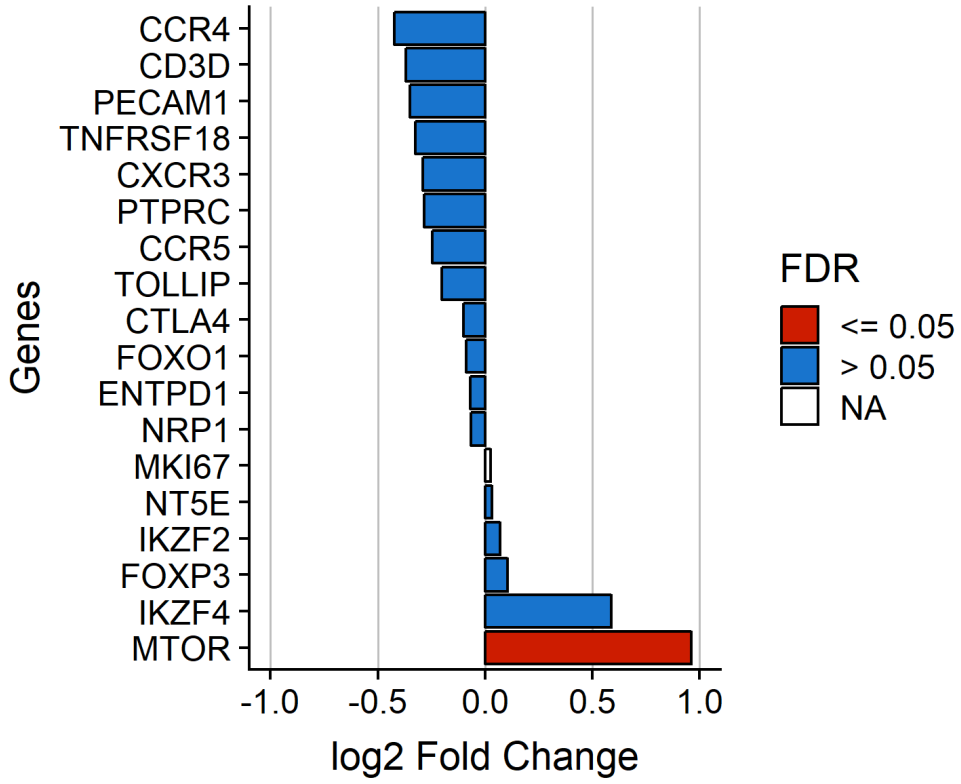

Figure 4.11: Log2 fold change values for the candidate genes in T_{regs} from APS-1 patients relative to controls, as determined by the RNA-seq experiment. *Based on the calculated FDR values, the only gene exhibiting a significant change in expression level in the T_{regs} from the patient group was mTOR.*

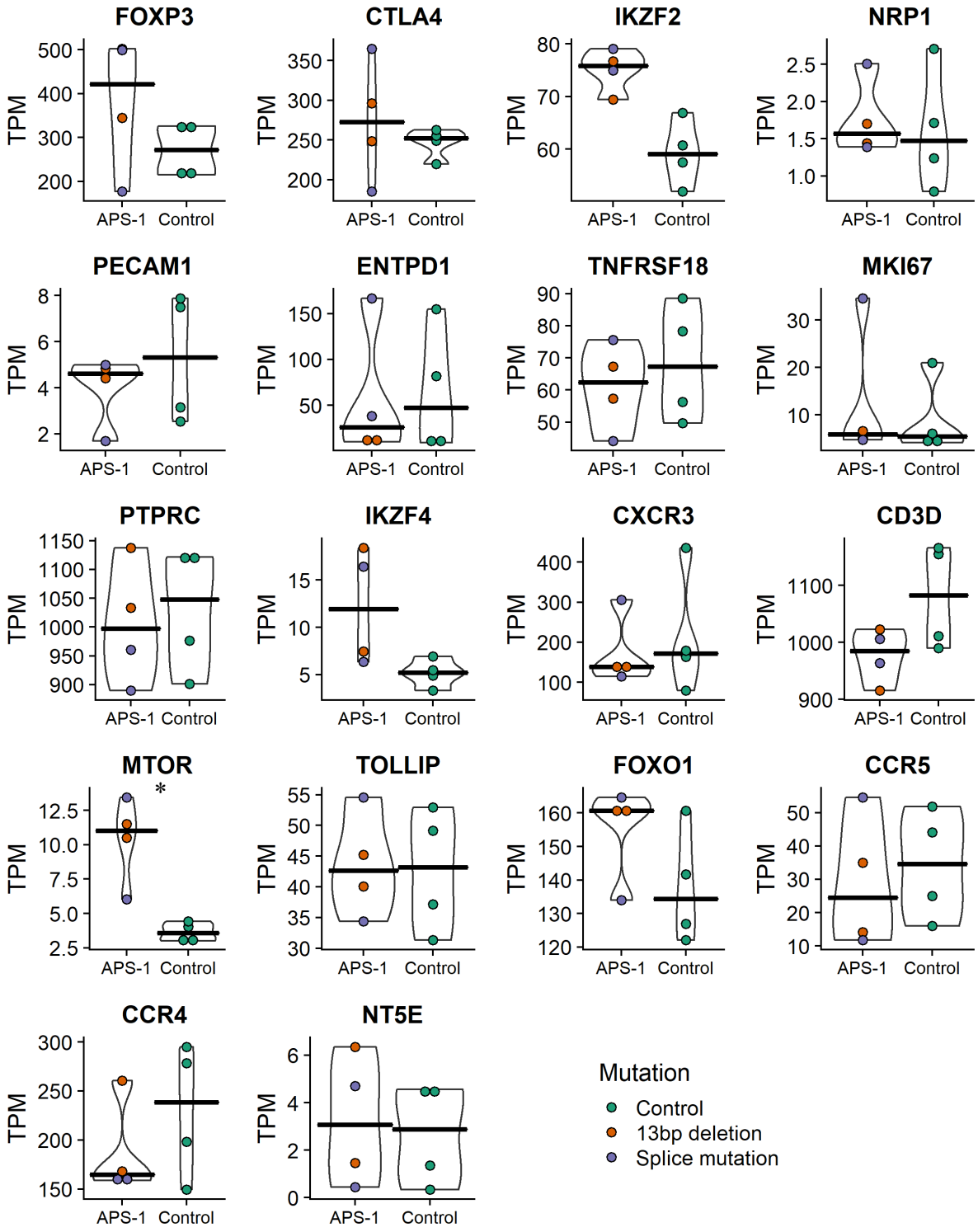

Figure 4.12: Pairwise comparison of the expression levels of selected candidate genes as determined by RNA-seq, indicated by TMP (transcript per million) values, between APS-1 patients and controls. *The assessed genes were* FOXP3, CTLA-4, IKZF2 *(encoding HELIOS)*, Neuropilin-1, PECAM-1, ENTPD-1 (*encoding CD39),* TNFRSF18 *(encoding GITR),* MKI-67, PTPRC *(encoding CD45),* IKZF4, CXCR3, CD3δ, mTOR, TOLLIP, FOXO1, CCR5, CCR4 *a*nd NT5E (*Encoding CD73). The horizontal lines indicate median values. With the exception of mTOR, none of the observed differences were statistically significant.*

Next, a global search for expression level perturbations was performed. A volcano plot was created (figure 4.13), showing the log2 fold change values versus -log10 FDR values. On the volcano plot, the genes found to have the most extensive changes in expression levels in the APS-1 patients compared to the controls were identified. A plot of log2 fold change versus gene count was also created. This plot indicated that, although the majority of the genes exhibited no substantial changes in gene expression levels in the APS-1 patients (indicated by log2 fold change values close to zero), a number exhibited such changes. The presence of genes with increased expression levels for the APS-1 patients compared to controls (indicated by positive log2 fold change values) was especially evident. For the genes exhibiting the highest decrease (figure 4.14) and increase (figure 4.15) in the APS-1 patients compared to the controls, pairwise comparisons were done based on median TPM values.

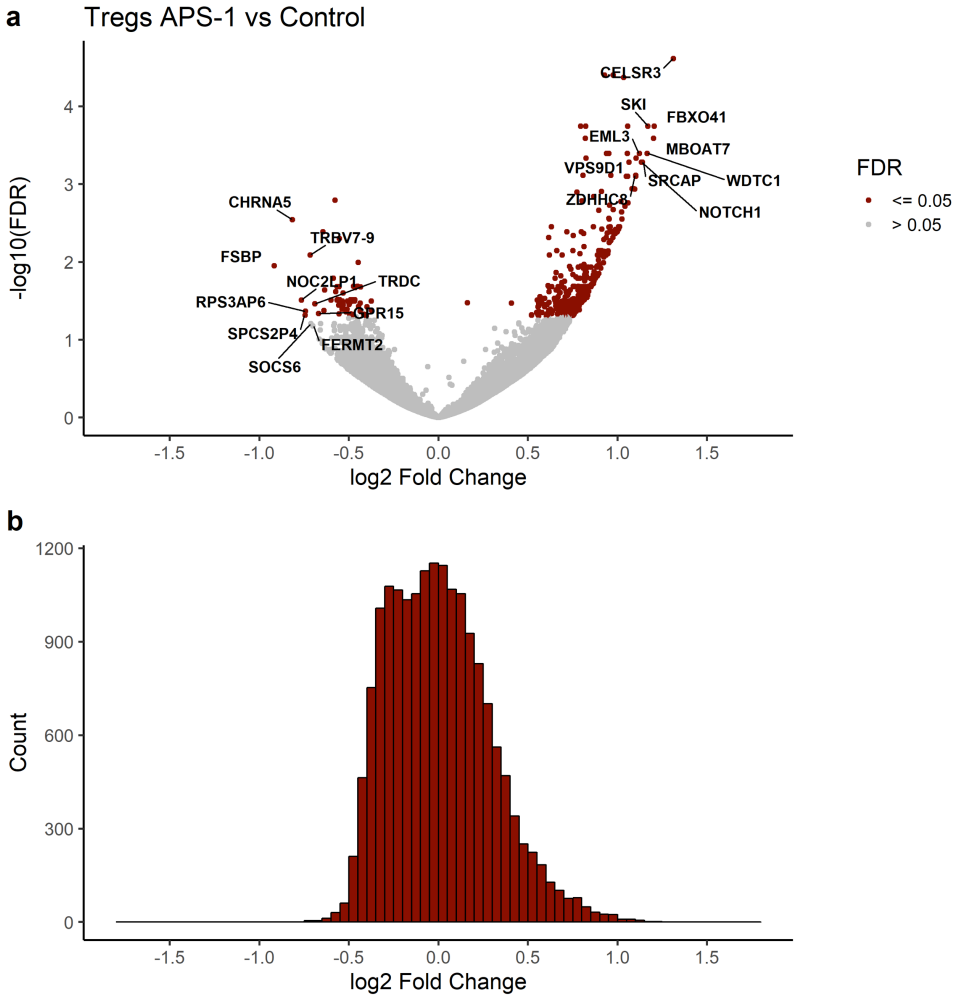

Figure 4.13: Vulcano plot of genes (top) showing log2 fold change for APS-1 patients relative to controls, versus –log10 FDR, and a plot of the log2 fold change versus gene count (bottom). *Genes exhibiting significant changes in expression levels between patients and controls, defined as having FDR values of 0.05 or lower, are indicated in red in the volcano plot.*

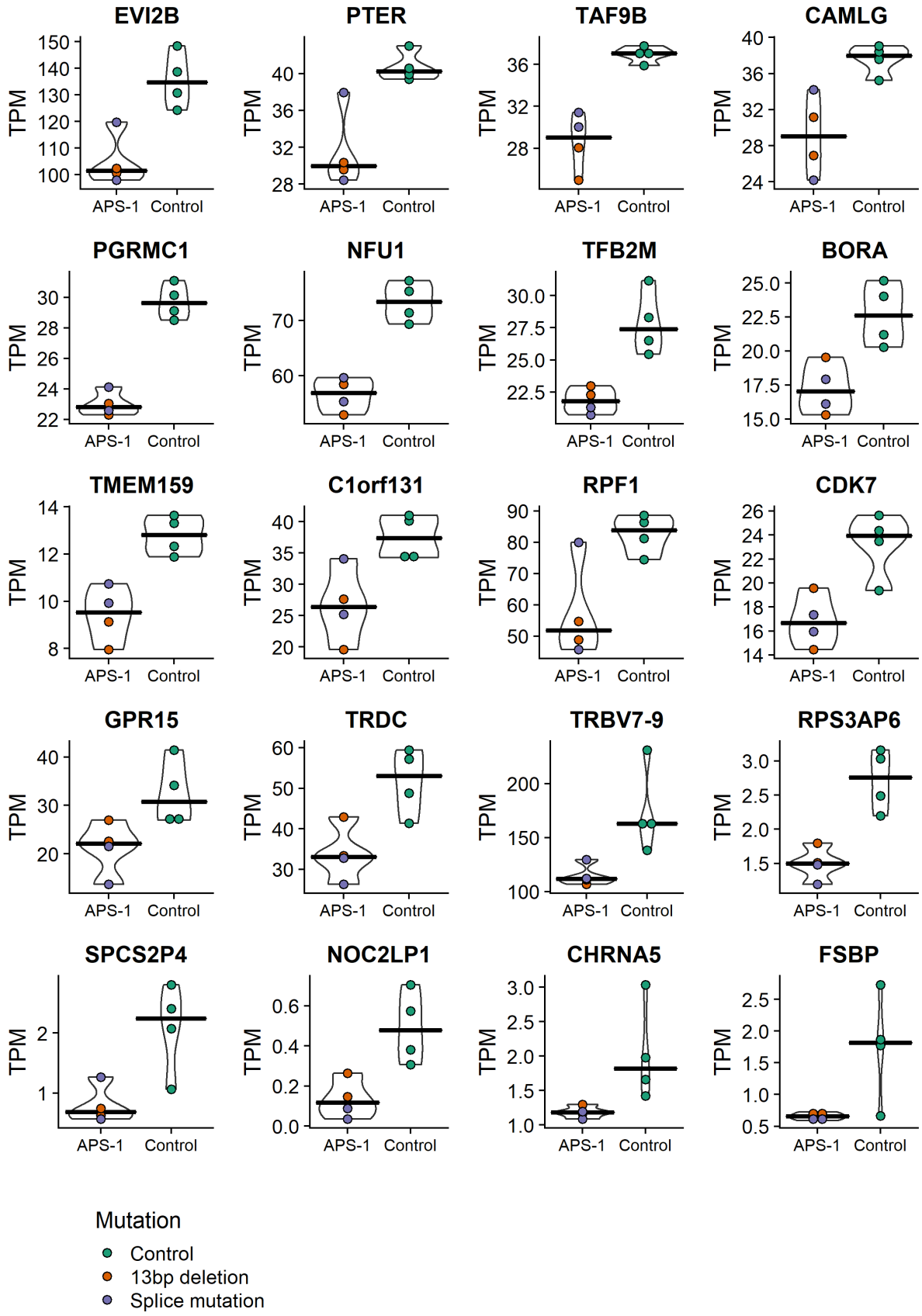

Figure 4.14: Pairwise comparison of the genes found to exhibit the largest decrease in expression levels in the APS-1 patients compared to controls, based on the RNA-se experiment. *The horizontal lines indicate medians among each group, measured as trancripts per million (TPM). All differences were found significant based on the calculated FDR values.*

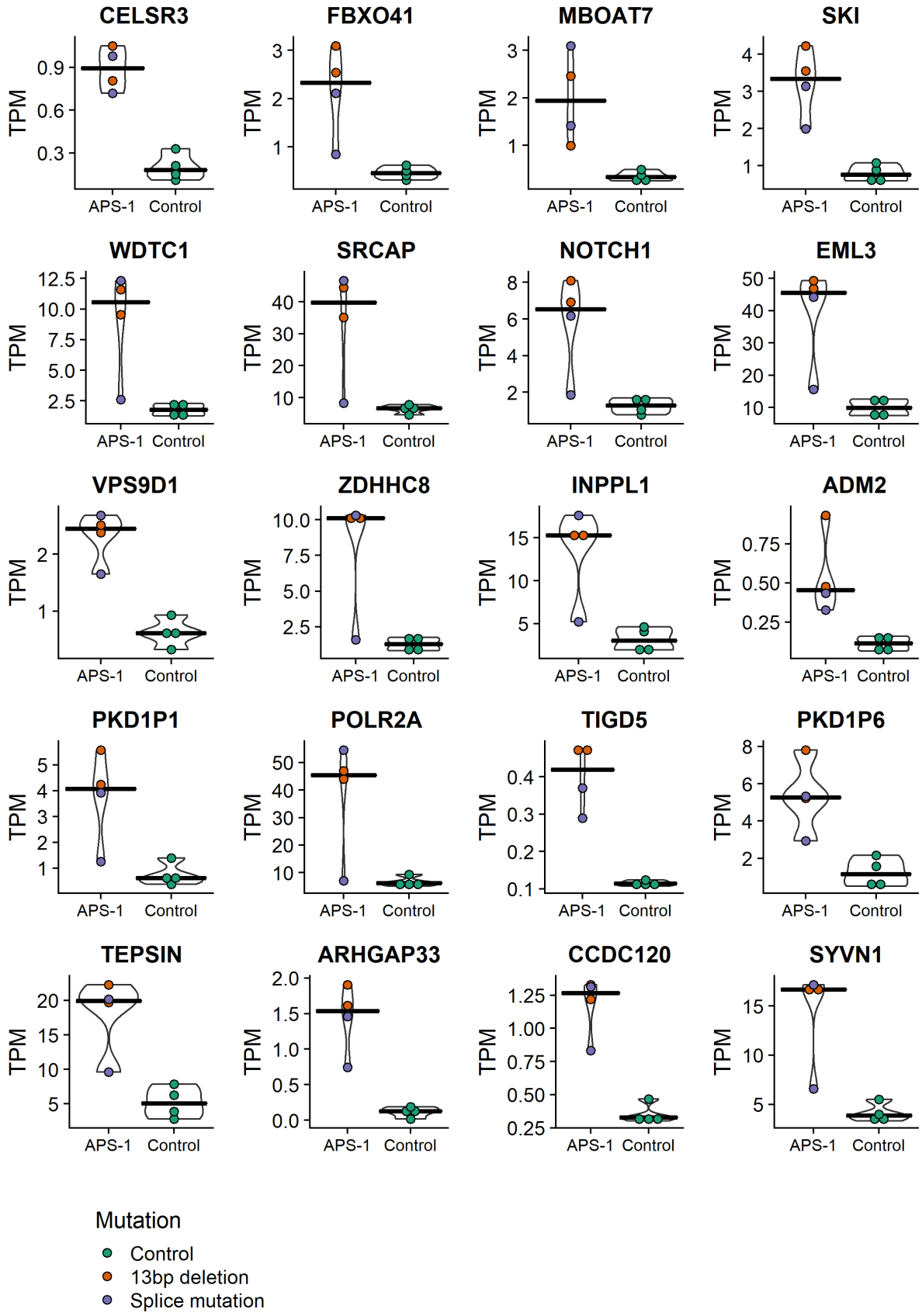

Figure 4.15: Pairwise comparison of the expression levels of the genes found to exhibit the largest increase in expression levels in the APS-1 patients compared to controls, based on the RNA-seq experiment. *The horizontal lines indicate medians among each group, measured as transcripts per million (TPM). All differences were found significant based on the calculated FDR values.*

Due to methodological challenges with the SMART-Seq V.4 kit, the cDNA synthesis and pre-amplification was performed in two separate runs. This could potentially cause batch effects, where the variation in the obtained data is largely explained by variations between the two runs. To assess whether such a batch effect was present in the obtained data set, a PCA plot was created (figure 4.16). On this plot, the x-axis corresponds to the factor explaining the largest amount of variation (PC1), and the y-axis corresponds to the factor explain the second largest amount of variation (PC2). If a major cause of the observed variation was a batch effect, the samples from the two different runs would be seen as two distinct clusters on the PCA plot. Such an effect is not observed. In the same manner, the PCA plot was used to determine whether the AIRE condition, age or sex was a major cause of the observed variation in the data set (figure 4.16). As the data points do not cluster according to any of these parameters, this do not appear to be the case.

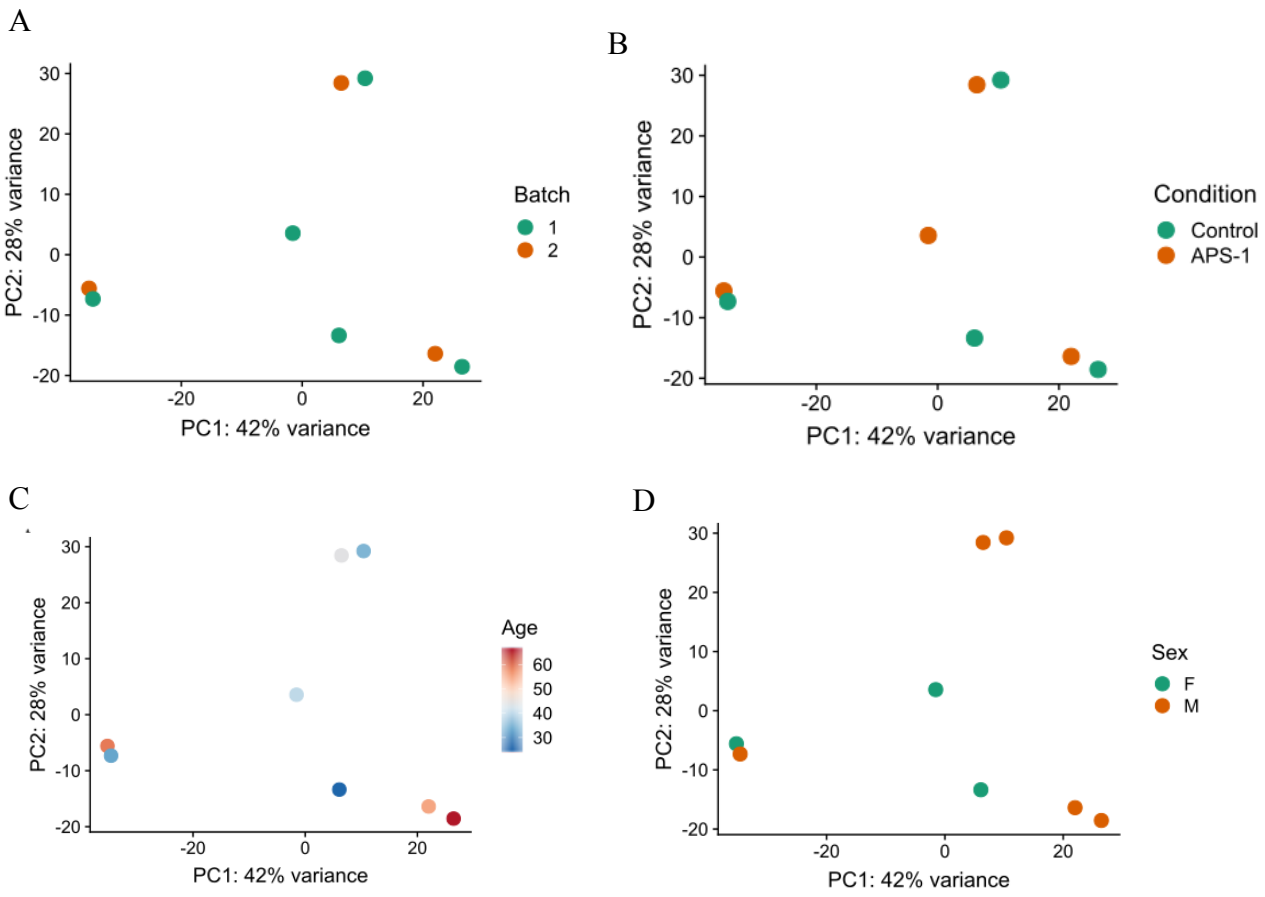

Figure 4.16: PCA plots based on the RNA-seq experiment, where data points are identified according to batch (A), AIRE condition (B), age (C) or sex (D). *The axes represent the factors explaining the largest and second largest amount of the observed variance, termed PC1 and PC2, respectively. The assessed samples do not cluster according to any of the assessed paramteres, indicating that these are not major causes of the observed variation between samples.*

5. Discussion

5.1 T_{regs} can be isolated from peripheral blood samples by bead separation followed by fluorescence-activated cell sorting

We have here developed a protocol for the separation of T_{regs} from peripheral blood, and shown that this protocol yields T_{reg} samples of high purity. To validate the separation protocol, both PBMC and cells separated by the use of magnetic beads were stained by antibodies targeting CD4, CD25 and either CD127 or FOXP3. Based on assessment by flow cytometry (figure 4.1), it was indicated that, after separation using magnetic beads, the frequency of T_{regs} was markedly increased compared to PBMC. This held true whether the T_{regs} were defined as $CD4^+CD25^+CD127^{lo}$ or $CD4^+CD25^+FOXP3^+$. Although these results indicate that a relatively high frequency of T_{regs} could be obtained by the bead separation protocol, the purity was still considered insufficient for downstream applications, calling for the need for complementing isolation procedures. Further, the correlation between $CD127^{lo}$ and $FOXP3^+$ frequency underlines the reported possibility of using CD127 as a surrogate marker for FOXP3 (Liu *et al.*, 2006).

The findings resulted in the development of a protocol for T_{reg} isolation by FACS, based on surface marker staining only (figure 3.2). By this approach, the need for fixation and permeabilization was avoided, a treatment which could restrict the utility of the sorted cells in downstream applications. To assess whether sorted $CD4^+CD25^+CD127^{lo}$ cells also expressed FOXP3, the sorted cells were stained with an antibody targeting FOXP3. By flow cytometric assessment, it was indicated that the frequency of $FOXP3^+$ cells among the sorted $CD4^+CD25^+CD127^-$ population was 94.4% in a representative experiment, after removal of debris and cells not having passed singly by the lasers (figure 4.2). This was taken as an indication that the T_{reg} purity after FACS was sufficiently high to proceed with downstream protocols.

5.2 The expression of selected candidate genes is overall similar in APS-1 patients and controls

To assess for perturbations in the expression of selected candidate genes in APS-1 patients at the protein level, a flow cytometry panel was developed (table 3.1) and used for staining of PBMC samples from APS-1 patients and controls (figures 4.3-4.5, table 4.1). No large differences between the APS-1 patients and controls were found, although some interesting

trends are present. One interesting observation is a subtle decrease in the frequency of $CD3^+CD4^+CD8^-CD25^+CD127^-$ T_{regs} in the samples from the ASP-1 patients compared to the controls, which corresponds well with previous findings (Ryan *et al.*, 2005; Wolff *et al.*, 2010). Also, it is intriguing to observe a small decrease in the frequency of $Helios^+$ and $CD31^+$ cells within the$CD3^+CD4^+CD8^-CD25^+FOXP3^+$ population. These findings could corroborate a previously suggested impairment of thymic generation of T_{regs} in APS-1 (Koivula *et al.*, 2017). It could be that the AIRE-deficiency in APS-1 patients lead to impaired antigen presentation in the thymus, so that potential T_{regs} do not receive TCR signals within the appropriate affinity range for maturation. It is, however, worth noting the discrepancy observed between the result for HELIOS and Neuropilin-1. As both have been suggested to be markers of nT_{regs}, it was surprising to observe that the frequency of Neuropilin-1 $CD3^+CD4^+CD8^-CD25^+FOXP3^+$ cells was reduced for the patients compared to the controls. A potential explanation could lie with the low frequency of cells positive for Neuropilin-1, as this could negatively affect the reliability of the results. In addition, reliability of HELIOS as a marker for nTregs is debated (Verhagen and Wraith, 2010; Himmel *et al.*, 2013).

A reduced frequency of naïve cells in APS-1 was indicated by a reduced frequency of naïve $CD45RA^+$ cells among the $CD3^+CD4^+CD8^-CD25^+FOXP3^+$ population. By contrast, the frequency of cells positive for as Ki67, CTLA-4 and CD39 was reduced, markers indicating cellular proliferation and an active T_{reg} state (Ring *et al.*, 2009). For CTLA-4, intracellular expression has been indicated to be constitutive, while recycling to the plasma membrane is dependent on activation (Mead *et al.*, 2005). It could be envisioned that, in the APS-1 patients, an increased presence of reactive T cells (Liston *et al.*, 2003) causes an increased likelihood of T_{reg} activation, and that this is the explanation for these observations. Based on the results, it is tempting to speculate that T_{regs} in APS-1 maintains the ability to react to encounters with self-reactive T cells by inducing increased proliferation and an active phenotype. The activation status of T_{regs} in APS-1 patients has been discussed by two previous publications, with opposing conclusions (Kekäläinen *et al.*, 2007; Laakso *et al.*, 2010).

It should be clearly stated that great caution is required in the interpretation of the flow cytometry findings. One issue is the low abundancy of the T_{reg} population in PBMC samples. This would be of especial concern with regard to the rarer markers, as exemplified by Neuropilin-1. To alleviate this issue, the ideal solution would be to increase the number of PBMC used. Unfortunately, this was not achievable due to the need to avoid excessive blood

sampling of the patients. Another issue is the large inter-individual variation observed. Such variations could be due to factors such as age or sex, for instance, the frequency of $CD45RA^+$ T_{regs} has been reported to be decreased with increasing age (Booth *et al.*, 2010). This trend was observed within the control group (figure 4.7). Other factors, such as recent infections, would also be a cause of confounding variation. To reduce such factors a larger data set encompassing a higher number of individuals should ideally be in place, in addition to age- and sex- matching between the patient and control group. Unfortunately, such measures were not feasible within the frame of the current project. As it is, none of the observed trends were found to be significant at the 5% level by application of a two-tailed Mann-Whitney test (table 4.1).

To determine whether any changes in expression levels of selected candidate genes between APS-1 patients and controls could be observed at the RNA level, qPCR was used for assessment of both PBMC and T_{reg} samples. By this approach, we have shown a substantial increase in expression of *FOXP3*, and lower increases in the expression of other T_{reg}-associated genes, in T_{regs} relative to PBMC from the same individual (figure 4.8). We have also shown that no large differences were observed in the expression of any of the assessed genes when comparing APS-1 patients and healthy controls, although a minor decrease in *ENTPD-1* expression in the PBMC from the APS-1 patients compared to control PBMC was observed (figure 4.9). This finding is in disagreement with the findings for the corresponding protein product, CD39, in the flow cytometry experiment. The cause could potentially lie in regulatory mechanism at the level of translation, although a likely explanation would be that the experimental set-up yielded an insufficient sensitivity for reliable detection of subtle changes.

The upregulation of a number of T_{reg}-associated genes in T_{regs} compared to PBMC from the same individuals was an expected result, and increased the confidence in the cell sorting approach and the qPCR protocol. A puzzling observation, however, was that of a slight increase in *AIRE* expression in T_{regs} relative to PBMC (figure 4.8). A low level of *AIRE* expression in peripheral cells has been reported by previous studies (Gardner *et al.*, 2008; Suzuki *et al.*, 2008). However, it was surprising to also find *AIRE* expressed the T_{reg} samples, as this has never been shown. A factor reducing the fidelity of this result is the low expression levels of *AIRE,* an issue could have been alleviated by the use of higher input concentrations. On the other hand, this would have reduced the number of genes that could be assessed with the available sample material, and the selected standard input was hence considered a reasonable compromise.

Another confounding factor could be the choice of reference gene, as the expression of the selected gene potentially could vary between PBMC and T_{reg} samples. Reports are in disagreement regarding the fidelity of commonly used reference genes (Thellin *et al.*, 1999; Livak and Schmittgen, 2001; Radonić *et al.*, 2004), and the decision to use *B2M* was based on previous experience within the research group. Limited assessment of *S18* as reference was performed (data not shown), and the result was found to be slightly deviating from those obtained with *B2M.* The use of a mean value based on assessment of several reference genes would have been the method of choice, had sufficient sample material been available.

To enable assessment of gene expression at the RNA level by limited amounts of sample input, a RNA-seq protocol for samples of 5000 cells was developed. This protocol was subsequently employed for T_{regs} from APS-1 patients and controls. Based on the obtained data for a number of pre-selected candidate genes, most did not exhibit significant changes in expression levels in the patients compared to controls. The exception was mTOR, which exhibited a significant increase in expression in the APS-patients versus controls. It could be hypothesized that an increased mTOR level would negatively affect the ability of T_{regs} to maintain lineage identity and mediate suppressive function, as down-modulation of mTOR activity has been linked to the integration of IL-2 signaling and FOXP3 expression (Delgoffe *et al.*, 2009). In support of this view, transient inhibition of mTOR by rapamycin has been indicated to increase T_{reg} cell proliferation (Procaccini *et al.*, 2010). A rapamycin-induced expansion of T_{regs} has been suggested as a contributing cause in the beneficial effects of this compound in treatment of systemic lupus erythematosus (Fernandez *et al.*, 2006; Kato and Perl, 2014).

The candidate genes were selected based on previous knowledge of their roles in T_{regs} and their previously reported utility in describing relevant features of the cells, such as origin and activation status. The decision to use an approach based on candidate genes was based on its potential for yielding a detailed understanding of specific mechanisms hypothesized to be relevant. However, this only gives a limited picture and prevents considerations of the overall situation. If such an overview is the goal, a wider search is necessary.

5.3 The expression levels of a number of genes are perturbed in T_{regs} from APS-1 patients

A global search for gene expression level perturbations was performed based on the RNA-seq data. By this approach, we have shown that a number of genes exhibit significant differences in expression levels between APS-1 patients and controls (figure 4.13).

Among the genes exhibiting the largest decrease in expression levels in APS-1 patients compared to controls (figure 4.14) were *TRBV7-9*, encoding the 7-9 variable domains of the TCR receptor β chain (Hedlund *et al.*, 2013), *CAMLG*, which blocks a calcium-dependent signals from the T-cell receptor that normally leads to T cell activation (Bram and Crabtreet, 1994), *GPR15*, a chemoattractant receptor involved in the homing of T cells to the colon (Kim *et al.*, 2013), and *TRDC*, encoding the βchain of the T cell receptor constant domain (Biondi *et al.*, 1989). Other interesting genes among this group is *CDK7* and *BORA*, involved in cell cycle progression (Rochette-Egly *et al.*, 1997; Seki *et al.*, 2008). If the cell cycle progression of T_{regs} in APS-1 patients is reduced, this could be envisioned to reduce their ability for clonal expansion upon encounter with autoreactive T cells.

Among the group of genes exhibiting the largest increase in expression levels in APS-1 patients compared to controls (figure 4.15) include *SKI* and *NOTCH1*, which both may affect TGF-β signaling (Sun *et al.*, 1999; Blokzijl *et al.*, 2003). As TGF-β has been linked to T_{reg} suppressive function and to the induction of T_{reg} lineage identity in the periphery (Nakamura, Kitani and Strober, 2001; Fantini *et al.*, 2004), this is an intriguing finding. Equally intriguing is the increased expression of *INPPL1*, encoding the SHIP2 protein involved in negative regulation of the PI3K pathway (Clément *et al.*, 2001), especially considering the reported link between PI3K signaling and mTOR (Delgoffe *et al.*, 2009). As an interaction between the CREB-binding protein and *AIRE* has been reported (Pitkänen *et al.*, 2000), it is also interesting to see an increase in the expression of *SCRAP*, an activator of the CREB-binding protein (Johnston *et al.*, 1999). Finally, it is worth mention that an increase was also observed in the expression of *FBOXO41*, which encodes a member of the F box protein family. F box proteins constitute a part of the SCF (Skp, Cullin, F-box containing) complex, which has E3 ubiquitin ligase activity (Zheng *et al.*, 2002). Downstream of this complex are signaling pathways involved in regulation of the cell cycle and in regulation of signaling though MCH class II (Chang *et al.*, 1996; Matsuki *et al.*, 2007) .

It is worth noting that the number of transcripts in the input samples would affect the result. For genes with a low number of transcripts, the reliability of the assessment would be reduced, as failure to detect any one transcript would cause large effects. It could also be envisioned that the pre-amplification step has the potential to cause undesired biases on the obtained results.

Ideally, the number of biological replicates should be increased in order to increase fidelity un in the results.

Finally, it should be pointed out that medications frequently prescribed to APS-1 patients, such as cortisol replacement therapy in the case of adrenal insufficiency, may have impacts on the immune system. This could affect the results of all the applied techniques.

5.4 Conclusions

In summary, some subtle trends could be observed when comparing the expression of selected candidate genes in APS-1 patients and controls at the protein level. The trends would corroborate a view where the thymic development of T_{regs} could be affected, but the T_{regs} that manage to complete maturation and emigrate to the periphery retain their capability for activation upon encounters with self-reactive lymphocytes. However, these observations failed to reach statistical significance, and are not supported by assessment at the RNA level. Hence, if such differences are present, they appear to be subtle and more sensitive approaches would be needed for reliable detection.

An exception to the lack of statistical significance is a detected perturbation of *mTOR* expression by the RNA-seq experiment. As mTOR already is being scrutinized as a potential target for therapy in other autoimmune diseases, this was a highly interesting finding. The RNA-seq experiment also enabled a global search for expression level perturbations, not limited to pre-selected candidate genes. By this approach, significant differences in expression levels of a substantial number of genes was found when comparing APS-1 patients and controls. It thus appears that, even though the candidate gene-based approach yielded few clear perturbations in APS-1, such perturbations do exist. To validate these findings and to explore their functional relevance, further experiments would be required.

5.5 Future perspectives

Current knowledge of T_{reg} biology is rapidly expanding, and substantial efforts are being undertaken in order to implement clinical uses of this cell population. For instance, significant perturbations has been discovered in the T_{reg} gene expression profile in pediatric patients with type 1 diabetes, yielding potential biomarkers for diagnostic use (Pesenacker *et al.*, 2016). Encouragement of the T_{reg}-mediated tolerance mechanism in patients with immune-mediated

diseases, for instance by IL-2 treatment or adoptive T_{reg} transfer, has been studied with promising results (Koreth *et al.*, 2011; Lutterotti *et al.*, 2013; Noyan *et al.*, 2017). However, many questions still remain regarding T_{regs} and their role in autoimmunity. Continued work on human samples would be necessary in order to confirm whether current knowledge from murine models is consistent with the situation in humans, as it has been indicated that inter-species differences in thymic development may exist (Kekäläinen *et al.*, 2007). Expanding the search for perturbations in APS-1 in particular could lead to the discovery of biomarkers with clinical value for patients with this condition. As APS-1 constitute an interesting model disease for autoimmunity, knowledge of basic immunology mechanism can be elucidated by work on this condition, and considerations regarding potential transfer value to other autoimmune diseases would be highly relevant. Finally, expanded knowledge regarding communication across immune cell populations would be a requirement for the safe and successful adoption of T_{reg}-based therapies in clinical practice.

To answer these questions, continued effort into improving methodologies would be necessary. Single-cell based approaches especially could prove highly useful. T_{regs} represent a small cell population, so techniques requiring low input would enable studies into these cells without the need for drawing excessive volumes of peripheral blood. Also, single-cell analysis would facilitate the assessment of subpopulations within the T_{reg} populations, for instance, it would be possible to say that a particular cell appears to be an nT_{reg} or an iT_{reg}, and see whether cells falling into either of these two categories showed any significant differences. Previous reports have indicated qPCR to be achievable, although a pre-amplification step, potentially causing undesired effects, would likely be required (Pop *et al.*, 2005; Flatz *et al.*, 2011; Shalek *et al.*, 2013). A low-input RNA-seq protocol was successfully implemented in this project, and this protocol could likely be optimized for use on single-cell samples. As this experiment identified a number of genes with significant perturbations in the expression levels in APS-1, such as *mTOR, SKI* and *NOTCH1*, further assessment of these genes and the molecular pathways they are involved in would be highly relevant. To assess the capabilities of the T_{regs} to respond to extracellular signals, flow cytometry of cells after stimulation would be interesting. The flow cytometry studies could be complemented by additional protein-level techniques, for instance fluorescence microscopy or CyTOF. Another exciting prospect would be the use of the novel 10X Chromium technology for single-cell analysis both at the protein and the RNA level (Zemmour *et al.*, 2018). With continued methodological advancement, it would seem reasonable to expect highly interesting discoveries regarding T_{reg} biology in the future.

Abbreviations

APC: Antigen-presenting cell
AIRE: Autoimmmune regulator
APECED: Autoimmune polyendocrinopathy-candidasis-ectodermal dystrophy
APS-1: Autoimmune polyendocrine syndrome 1
BSA: Bovine serum albumin
CBP : CREB-binding protein
CCR: Chemokine receptor
CD: Cluster of differentiation
CNS2: Conserved non-coding sequence 2
CREB protein: cAMP response element binding protein
CTL: Cytotoxkic T cell
CTLA-4: Cytotoxic T-lymphocyte-associated antigen 4
CXCR: C-X-C motif chemokine receptor 3
CXL1: C-X-C motif ligand 1
DC: Dendritic cell
DMSO: Dimethyl sulfoxide
DN: Double-negative
DP: Double-positive
EDTA : Ethylenediaminetetraacetic acid
ENTPD-1: Ectonucleosidase triphosphate diphosphohydrolase 1
FACS : Fluorescence-activated cell sorting
FEZF2 : Fez family zinc finger protein 2
FoxO: Forkhead box O
FOXP3: Forkhead box P3
GITR: Glucocorticoid-induced TNFR family related gene
IDO: Indoleamine 2,3-dioxygenase
IKZ: Ikaros family zinc finger proteins
IL: Interleukin
IPEX: Immune dysregulation, polyendocrinopathy, enteropathy, X-linked syndrome
iT_{reg}: Induced regulatory T cell
LFA-1: leukocyte function-associated antigen-1
MHC: Major histocompability complex
mTEC: Medullary thymic epithelial cell
mTOR: Mammalian target of rapamycin
Nrp-1: Neuropilin-1
nT_{reg}: Natural regulatory T cell
NT5E: 5' nucleotidase ecto
PAMP: Pathogen-associated molecular pattern
PBS: Phosphate-buffered saline
PBMC: Peripheral blood mononuclear cell
PECAM: Platelet endothelial cell adhesion molecule
PI3K: Phosphoinositide 3-Kinase
PKB: Protein Kinase B
PTEN: Phosphatase and tensin homolog
SCID mice: Severe combined immunodefiency mice
SP: Single-positive
STAT: signal transducer and activator of transcription
TCR: T cell receptor
T_H cell: Helper T cell
TGF-β: Transforming growth factor β
TMP: Transcript per million
TNFR: Tumor necrosis factor receptor
TOLLIP: Toll-interacting protein
TRA: Tissue-restricted antigen
T_{reg}: Regulatory T cell

References

Abramson, J. *et al.* (2010) 'Aire's partners in the molecular control of immunological tolerance.', *Cell*, 140(1), pp. 123–135. doi: 10.1016/j.cell.2009.12.030.

Agrawal, A., Eastman, Q. M. and Schatz, D. G. (1998) 'Implications of transposition mediated by V (D) J - recombination proteins RAG1 and RAG2 for origins 8 of antigen-specific immunity', *Nature*, 394(6695), pp. 744–751. doi: 10.1007/BF02786485.

Allison, J., Mcintyre, W. and Bloch, D. (1982) 'Tumor-specific antigen of murine T-lymphoma defined with monoclonal antibody', *Journal of immunology*, 129(5), pp. 2293–2300.

Anderson, J. R. *et al.* (1957) 'AUTO-ANTIBODIES IN ADDISON'S DISEASE', *The Lancet*, 269(6979), pp. 1123–1124. doi: 10.1016/S0140-6736(57)92329-2.

Anderson, M. S. *et al.* (2002) 'Projection of an immunological self shadow within the thymus by the aire protein', *Science*, 298(5597), pp. 1395–1401. doi: 10.1126/science.1075958.

Anderson, M. S. *et al.* (2005) 'The cellular mechanism of Aire control of T cell tolerance', *Immunity*, 23(2), pp. 227–239. doi: 10.1016/j.immuni.2005.07.005.

Aschenbrenner, K. *et al.* (2007) 'Selection of Foxp3+regulatory T cells specific for self antigen expressed and presented by Aire+medullary thymic epithelial cells', *Nature Immunology*, 8(4), pp. 351–358. doi: 10.1038/ni1444.

Ashton-Rickardt, P. G. *et al.* (1994) 'Evidence for a differential avidity model of T cell selection in the thymus', *Cell*, 76(4), pp. 651–663. doi: 10.1016/0092-8674(94)90505-3.

Baecher-Allan, C. *et al.* (2001) 'CD4+CD25high Regulatory Cells in Human Peripheral Blood', *Journal of immunology*, 167(3), pp. 1245–1253. doi: 10.4049/jimmunol.167.3.1245.

Baldwin, K. K. *et al.* (1999) 'Negative selection of T cells occurs throughout thymic development', *Journal of Immunology*, 163(2), pp. 689–698.

Benjamini, Y. and Hochberg, Y. (1995) 'Controlling the False Discovery Rate: a Practical and Powerful Approach to Multiple Testing', *Journal of the Royal Statistical Society*, 57(1), pp. 289–300. doi: 10.2307/2346101.

Bennett, C. L. *et al.* (2001) 'The immune dysregulation, polyendocrinopathy, enteropathy, X-linked syndrome (IPEX) is caused by mutations of FOXP3', *Nature Genetics*, 27(1), pp. 20–21. doi: 10.1038/83713.

Bennouna, S. *et al.* (2003) 'Cross-Talk in the Innate Immune System: Neutrophils Instruct Recruitment and Activation of Dendritic Cells during Microbial Infection', *The Journal of Immunology*, 171(11), pp. 6052–6058. doi: 10.4049/jimmunol.171.11.6052.

Bensinger, S. J. *et al.* (2004) 'Distinct IL-2 Receptor Signaling Pattern in CD4+CD25+ Regulatory T Cells', *The Journal of Immunology*, 172(9), pp. 5287–5296. doi: 10.4049/jimmunol.172.9.5287.

Bhela, S. *et al.* (2017) 'The Plasticity and Stability of Regulatory T cells during Viral-Induced Inflammatory Lesions', *J. Immunol*, 199(4), pp. 1342–1351.

Biondi, A. *et al.* (1989) 'T-cell receptor delta gene rearrangement in childhood T-cell acute lymphoblastic leukemia', *Blood journal*, 73(8), pp. 2133–2138.

Blokzijl, A. *et al.* (2003) 'Cross-talk between the Notch and TGF-beta signaling pathways mediated by interaction of the Notch intracellular domain with Smad3', *Journal of Cell Biology*, 163(4), pp. 723–728. doi: 10.1083/jcb.200305112.

Bluestone, J. A. *et al.* (2015) 'Type 1 diabetes immunotherapy using polyclonal regulatory T cells', *Science Translational Medicine*, 7(315), p. 315ra189. doi: 10.1126/scitranslmed.aad4134.

Booth, N. J. *et al.* (2010) 'Different Proliferative Potential and Migratory Characteristics of Human CD4+ Regulatory T Cells That Express either CD45RA or CD45RO', *The Journal of Immunology*, 184(8), pp. 4317–4326. doi: 10.4049/jimmunol.0903781.

Bram, R. J. and Crabtreet, G. R. (1994) 'Calcium signalling in T cells stimulated by a cyclophilin B-binding protein', *Nature*, 371(6495), pp. 355–358. doi: 10.1038/371355a0.

Bray, N. L. *et al.* (2016) 'Near-optimal probabilistic RNA-seq quantification', *Nature Biotechnology*, 34(5), pp. 525–527. doi: 10.1038/nbt.3519.

Brenner, M. B. *et al.* (1986) 'Identification of a putative second T-cell receptor', *Nature*, 322(6075), pp. 145–149. doi: 10.1038/322145a0.

Brocker, T., Riedinger, M. and Karjalainen, K. (1997) 'Targeted Expression of Major Histocompatibility Complex (MHC) Class II Molecules Demonstrates that Dendritic Cells Can Induce Negative but Not Positive Selection of Thymocytes In Vivo', *J. Exp. Med*, 185(3), pp. 541–550. doi: 10.1084/jem.185.3.541.

Call, M. E. *et al.* (2002) 'The organizing principle in the formation of the T cell receptor-CD3 complex', *Cell*, 111(7), pp. 967–979. doi: 10.1016/S0092-8674(02)01194-7.

Cerottini, J.-C., Nordin, A. A. and Brunner, K. T. (1970) 'In vitro cytotoxic activity of thymus cells sensitized to alloantigens', *Nature*, 227(5253), pp. 72–73.

Chang, B. *et al.* (1996) 'SKP1 connects cell cycle regulators to the ubiquitin proteolysis machinery through a novel motif, the F-box', *Cell*, 86(2), pp. 263–274. doi: 10.1016/S0092-8674(00)80098-7.
Chen, W. *et al.* (2003) 'Conversion of Peripheral CD4 + CD25 − Naive T Cells to CD4 + CD25 + Regulatory T Cells by TGF-β Induction of Transcription Factor Foxp3', *The Journal of Experimental Medicine*, 198(12), pp. 1875–1886. doi: 10.1084/jem.20030152.
Clément, S. *et al.* (2001) 'The lipid phosphatase SHIP2 controls insulin sensitivity', *Nature*, 409(6816), pp. 92–97. doi: 10.1038/35051094.
Cooper, M. D., Peterson, R. D. A. and Good, R. A. (1965) 'Delineation of the thymic and bursal lymphoid systems in the chicken', *Nature*, 205(4967), pp. 143–146. doi: 10.1038/205143a0.
Cowan, J. E. *et al.* (2018) 'Aire controls the recirculation of murine Foxp3+regulatory T-cells back to the thymus', *European Journal of Immunology*, 48(5), pp. 844–854. doi: 10.1002/eji.201747375.
Deaglio, S. *et al.* (2007) 'Adenosine generation catalyzed by CD39 and CD73 expressed on regulatory T cells mediates immune suppression', *The Journal of Experimental Medicine*, 204(6), pp. 1257–1265. doi: 10.1084/jem.20062512.
Delgoffe, G. M. *et al.* (2009) 'The mTOR Kinase Differentially Regulates Effector and Regulatory T Cell Lineage Commitment', *Immunity*. doi: 10.1016/j.immuni.2009.04.014.
Delgoffe, G. M. *et al.* (2013) 'Stability and function of regulatory T cells is maintained by a neuropilin-1–semaphorin-4a axis', *Nature*, 501(7466), pp. 252–256. doi: 10.1038/nature12428.
Derbinski, J. *et al.* (2001) 'Promiscuous gene expression in medullary thymic epithelial cells mirrors the peripheral self', *Nature immunology*, 2(711), pp. 1032–1039. doi: 10.1038/ni723.
Derbinski, J. *et al.* (2005) 'Promiscuous gene expression in thymic epithelial cells is regulated at multiple levels', *The Journal of Experimental Medicine*, 202(1), pp. 33–45. doi: 10.1084/jem.20050471.
Derbinski, J. *et al.* (2008) 'Promiscuous gene expression patterns in single medullary thymic epithelial cells argue for a stochastic mechanism', *Proceedings of the National Academy of Sciences*, 105(2), pp. 657–662. doi: 10.1073/pnas.0707486105.
Doyle, C. and Strominger, J. L. (1987) 'Interaction between CD4 and class II MHC molecules mediates cell adhesion', *Nature*, 330(6145), pp. 256–259. doi: 10.1038/330256a0.
Fallarino, F. *et al.* (2006) 'The Combined Effects of Tryptophan Starvation and Tryptophan Catabolites Down-Regulate T Cell Receptor -Chain and Induce a Regulatory Phenotype in Naive T Cells', *The Journal of Immunology*, 176(11), pp. 6752–6761. doi: 10.4049/jimmunol.176.11.6752.
Fantini, M. C. *et al.* (2004) 'Cutting Edge: TGF- Induces a Regulatory Phenotype in CD4+CD25- T Cells through Foxp3 Induction and Down-Regulation of Smad7', *The Journal of Immunology*, 172(9), pp. 5149–5153. doi: 10.4049/jimmunol.172.9.5149.
Feng, Y. *et al.* (2014) 'Control of the inheritance of regulatory T cell identity by a cis element in the foxp3 locus', *Cell*, 158(4), pp. 749–763. doi: 10.1016/j.cell.2014.07.031.
Fernandez, D. *et al.* (2006) 'Rapamycin reduces disease activity and normalizes T cell activation-induced calcium fluxing in patients with systemic lupus erythematosus', *Arthritis and Rheumatism*, 54(9), pp. 2983–2988. doi: 10.1002/art.22085.
Flatz, L. *et al.* (2011) 'Single-cell gene-expression profiling reveals qualitatively distinct CD8 T cells elicited by different gene-based vaccines', *Proceedings of the National Academy of Sciences*, 108(14), pp. 5724–5729. doi: 10.1073/pnas.1013084108.
Fontenot, J. D. *et al.* (2005) 'A function for interleukin 2 in Foxp3-expressing regulatory T cells', *Nature Immunology*, 6(11), pp. 1142–1151. doi: 10.1038/ni1263.
Fontenot, J. D., Gavin, M. A. and Rudensky, A. Y. (2003) 'Foxp3 programs the development and function of CD4+CD25+ regulatory T cells', *Nature Immunology*, 4(4), pp. 330–336. doi: 10.1038/ni904.
Freudenthal, P. S. and Steinman, R. M. (1990) 'The distinct surface of human blood dendritic cells, as observed after an improved isolation method.', *Proceedings of the National Academy of Sciences*, 87(19), pp. 7698–7702. doi: 10.1073/pnas.87.19.7698.
Gallegos, A. M. and Bevan, M. J. (2004) 'Central Tolerance to Tissue-specific Antigens Mediated by Direct and Indirect Antigen Presentation', *The Journal of Experimental Medicine*, 200(8), pp. 1039–1049. doi: 10.1084/jem.20041457.
Garcia, K. C. *et al.* (1996) 'An apha beta T cell receptor structure at 2.5 Å and its orientation in the TCR-MHC complex', *Science*, 274(5285), pp. 209–219. doi: 10.1126/science.274.5285.209.
Gardner, J. M. *et al.* (2008) 'Deletional tolerance mediated by extrathymic aire-expressing cells', *Science*, 321(5890), pp. 843–847. doi: 10.1126/science.1159407.
Gardner, J. M. *et al.* (2013) 'Extrathymic aire-expressing cells are a distinct bone marrow-derived population that induce functional inactivation of CD4+T cells', *Immunity*, 39(3), pp. 560–570. doi: 10.1016/j.immuni.2013.08.005.
Gavin, M. A. *et al.* (2007) 'Foxp3-dependent programme of regulatory T-cell differentiation', *Nature*, 445(7129), pp. 771–775. doi: 10.1038/nature05543.

Gerdes, J. *et al.* (1983) 'Production of a mouse monoclonal antibody reactive with a human nuclear antigen associated with cell proliferation', *International Journal of Cancer*, 31(1), pp. 13–20. doi: 10.1002/ijc.2910310104.
Gregersen, P. K. and Behrens, T. W. (2006) 'Genetics of autoimmune diseases - Disorders of immune homeostasis', *Nature Reviews Genetics*, 7(12), pp. 917–921. doi: 10.1038/nrg1944.
Gregg, R. *et al.* (2005) 'The number of human peripheral blood CD4+CD25highregulatory T cells increases with age', *Clinical and Experimental Immunology*, 140(3), pp. 540–546. doi: 10.1111/j.1365-2249.2005.02798.x.
Guerau-de-Arellano, M. *et al.* (2009) 'Neonatal tolerance revisited: a perinatal window for Aire control of autoimmunity', *The Journal of Experimental Medicine*. doi: 10.1084/jem.20090300.
Hart, A. (2001) 'Mann-Whitney test is not just a test of medians: differences in spread can be important', *BMJ*, 323(7309), pp. 391–393. doi: 10.1136/bmj.323.7309.391.
Hayday, A. C. *et al.* (1985) 'Structure, organization, and somatic rearrangement of T cell gamma genes', *Cell*, 40(2), pp. 259–269. doi: 10.1016/0092-8674(85)90140-0.
Hedlund, G. *et al.* (2013) 'The Tumor Targeted Superantigen ABR-217620 Selectively Engages TRBV7-9 and Exploits TCR-pMHC Affinity Mimicry in Mediating T Cell Cytotoxicity', *PLoS ONE*, 8(10), p. e79082. doi: 10.1371/journal.pone.0079082.
Hedrick, S. M. (2004) 'The acquired immune system: A vantage from beneath', *Immunity*, 21(5), pp. 607–615. doi: 10.1016/j.immuni.2004.08.020.
Hill, J. A. *et al.* (2007) 'Foxp3 Transcription-Factor-Dependent and -Independent Regulation of the Regulatory T Cell Transcriptional Signature', *Immunity*, 27(5), pp. 786–800. doi: 10.1016/j.immuni.2007.09.010.
Himmel, M. E. *et al.* (2013) 'Helios+ and Helios- Cells Coexist within the Natural FOXP3 + T Regulatory Cell Subset in Humans', *The Journal of Immunology*, 190(5), pp. 2001–2008. doi: 10.4049/jimmunol.1201379.
Hinterberger, M. *et al.* (2010) 'Autonomous role of medullary thymic epithelial cells in central CD4+ T cell tolerance', *Nature Immunology*, 11(6), pp. 512–519. doi: 10.1038/ni.1874.
Hori, S., Nomura, T. and Sakaguchi, S. (2003) 'Control of regulatory T cell development by the transcription factor Foxp3.', *Science (New York, N.Y.)*, 299(5609), pp. 1057–61. doi: 10.1126/science.1079490.
Hou, P.-F. *et al.* (2017) 'Age-related changes in CD4+CD25+FOXP3+ regulatory T cells and their relationship with lung cancer', *PLoS ONE*, 12(3), p. e0173048.
Hubert, F. X. *et al.* (2011) 'Aire regulates the transfer of antigen from mTECs to dendritic cells for induction of thymic tolerance', *Blood*, 118(9), pp. 2462–2472. doi: 10.1182/blood-2010-06-286393.
Humblet-Baron, S. *et al.* (2016) 'IL-2 consumption by highly activated CD8 T cells induces regulatory T-cell dysfunction in patients with hemophagocytic lymphohistiocytosis', *Journal of Allergy and Clinical Immunology*, 138(1), pp. 200–209. doi: 10.1016/j.jaci.2015.12.1314.
Huo, F. *et al.* (2018) 'Deficiency of autoimmune regulator impairs the immune tolerance effect of bone marrow-derived dendritic cells in mice', *Autoimmunity*, 51(10), pp. 10–17. doi: 10.1080/08916934.2017.1422124.
Husebye, E. S. *et al.* (2009) 'Clinical manifestations and management of patients with autoimmune polyendocrine syndrome type I', *Journal of Internal Medicine*, 265(5), pp. 514–529. doi: 10.1111/j.1365-2796.2009.02090.x.
Huynh, A. *et al.* (2015) 'Control of PI(3) kinase in Tregcells maintains homeostasis and lineage stability', *Nature Immunology*, 16(2), pp. 188–196. doi: 10.1038/ni.3077.
Janeway, C. A. (1989) 'Approaching the asymptote? Evolution and revolution in immunology', in *Cold Spring Harbor Symposia on Quantitative Biology*, pp. 1–13. doi: 10.1101/SQB.1989.054.01.003.
Jia, L. *et al.* (2018) 'Tolerogenic dendritic cells induced the enrichment of CD4+FoxP3+ regulatory T cells via TGF-beta in mesentheric lymph nodes of murine LPS-induced tolerance model', *Clinical Immunology*, 197, pp. 118–129.
Johnston, H. *et al.* (1999) 'Identification of a novel SNF2/SW12 protein family member, SRCAP, which interacts with CREB-binding protein', *The Journal of Biological Chemistry*, 274(23), pp. 16370–16376.
Kato, H. and Perl, A. (2014) 'Mechanistic Target of Rapamycin Complex 1 Expands Th17 and IL-4+ CD4-CD8- Double-Negative T Cells and Contracts Regulatory T Cells in Systemic Lupus Erythematosus', *The Journal of Immunology*, 129(9), pp. 4134–4144. doi: 10.4049/jimmunol.1301859.
Keene, J.-A.-A. and Forman, J. (1982) 'Helper activity is required for the in vivo generation of cytotoxic T lymphocytes', *The Journal of Experimental Medicine*, 155(3), pp. 768–782. doi: 10.1084/jem.155.3.768.
Kekäläinen, E. *et al.* (2007) 'A defect of regulatory T cells in patients with autoimmune polyendocrinopathy-candidiasis-ectodermal dystrophy.', *Journal of immunology (Baltimore, Md. : 1950)*, 178(2), pp. 1208–1215. doi: 10.4049/jimmunol.178.2.1208.
Kim, H.-J. *et al.* (2015) 'Stable inhibitory activity of regulatory T cells requires the transcription factor Helios', *Science*, 350(6258), pp. 334–339. doi: 10.1126/science.aad0616.
Kim, S. V. *et al.* (2013) 'GPR15-mediated homing controls immune homeostasis in the large intestine mucosa', *Science*, 340(6139), pp. 1456–1459. doi: 10.1126/science.1237013.
Kimmig, S. *et al.* (2002) 'Two Subsets of Naive T Helper Cells with Distinct T Cell Receptor Excision Circle

Content in Human Adult Peripheral Blood', *The Journal of Experimental Medicine*, 195(6), pp. 789–794. doi: 10.1084/jem.20011756.
Kingston, R., Jenkinson, E. J. and Owen, J. J. T. (1985) 'A single stem cell can recolonize an embryonic thymus, producing phenotypically distinct T-cell populations', *Nature*, 317(6040), pp. 811–813. doi: 10.1038/317811a0.
Kisielow, P. *et al.* (1975) 'Ly antigens as markers for functionally distinct subpopulations of thymus-derived lymphocytes of the mouse', *Nature*, 253(5488), pp. 219–220. doi: 10.1038/253219a0.
Kisielow, P. *et al.* (1988) 'Tolerance in T-cell-receptor transgenic mice involves deletion of nonmature CD4+8+thymocytes', *Nature*, 333(6175), pp. 742–746. doi: 10.1038/333742a0.
Knoechel, B. *et al.* (2005) 'Sequential development of interleukin 2–dependent effector and regulatory T cells in response to endogenous systemic antigen', *The Journal of Experimental Medicine*, 202(10), pp. 1375–1386. doi: 10.1084/jem.20050855.
Koble, C. and Kyewski, B. (2009) 'The thymic medulla: a unique microenvironment for intercellular self-antigen transfer', *The Journal of Experimental Medicine*, 206(7), pp. 1505–1513. doi: 10.1084/jem.20082449.
Koivula, T. T. *et al.* (2017) 'Clonal analysis of regulatory t cell defect in patients with autoimmune polyendocrine syndrome type 1 suggests intrathymic impairment', *Scandinavian Journal of Immunology*, 86(4), pp. 221–228. doi: 10.1111/sji.12586.
Koreth, J. *et al.* (2011) 'Interleukin-2 and regulatory T cells in graft-versus-host disease.', *The New England journal of medicine*, 365(22), pp. 2055–2066. doi: 10.1056/NEJMoa1108188.
Kukurba, K. and Motgomery, S. B. (2015) 'RNA Sequencing and Analysis', *Cold Spring Harbor Protocols*, 11, pp. 951–969.
Kuniyasu, Y. *et al.* (2000) 'Naturally anergic and suppressive CD25(+)CD4(+) T cells as a functionally and phenotypically distinct immunoregulatory T cell subpopulation', *International immunology*, 12(8), pp. 1145–1155. doi: 10.1093/intimm/12.8.1145.
Lanzavecchia, A. (1985) 'Antigen-specific interaction between T and B cells', *Nature*, 314(6011), pp. 537–539. doi: 10.1038/314537a0.
Lee, H. M. *et al.* (2012) 'A Broad Range of Self-Reactivity Drives Thymic Regulatory T Cell Selection to Limit Responses to Self', *Immunity*, 37(3), pp. 475–486. doi: 10.1016/j.immuni.2012.07.009.
Lei, Y. *et al.* (2011) 'Aire-dependent production of XCL1 mediates medullary accumulation of thymic dendritic cells and contributes to regulatory T cell development', *The Journal of Experimental Medicine*, 208(2), pp. 383–394. doi: 10.1084/jem.20102327.
Leventhal, D. S. *et al.* (2016) 'Dendritic Cells Coordinate the Development and Homeostasis of Organ-Specific Regulatory T Cells', *Immunity*, 44(4), pp. 847–859. doi: 10.1016/j.immuni.2016.01.025.
Li, X. *et al.* (2014) 'Function of a foxp3 cis-element in protecting regulatory T cell identity', *Cell*, 158(4), pp. 734–748. doi: 10.1016/j.cell.2014.07.030.
Lin, J. *et al.* (2016) 'Increased generation of Foxp3+regulatory T cells by manipulating antigen presentation in the thymus', *Nature Communications*, 7, p. 10562. doi: 10.1038/ncomms10562.
Lio, C. W. J. and Hsieh, C. S. (2008) 'A Two-Step Process for Thymic Regulatory T Cell Development', *Immunity*, 28(1), pp. 100–111. doi: 10.1016/j.immuni.2007.11.021.
Liston, A. *et al.* (2003) 'Aire regulates negative selection of organ-specific T cells', *Nature Immunology*, 4(4), pp. 350–354. doi: 10.1038/ni906.
Liston, A. *et al.* (2004) 'Gene Dosage–limiting Role of Aire in Thymic Expression, Clonal Deletion, and Organ-specific Autoimmunity', *The Journal of Experimental Medicine*, 18(200), pp. 1015–1026. doi: 10.1084/jem.20040581.
Liu, W. *et al.* (2006) 'CD127 expression inversely correlates with FoxP3 and suppressive function of human CD4 $^{+}$ T reg cells', *The Journal of Experimental Medicine*, 203(7), pp. 1701–1711. doi: 10.1084/jem.20060772.
Liu, Z. *et al.* (2015) 'Immune homeostasis enforced by co-localized effector and regulatory T cells', *Nature*, 528(7581), pp. 225–230. doi: 10.1038/nature16169.
Livak, K. J. and Schmittgen, T. D. (2001) 'Analysis of relative gene expression data using real-time quantitative PCR and the 2-ΔΔCT method', *Methods*, 25(4), pp. 402–408. doi: 10.1006/meth.2001.1262.
Lutterotti, A. *et al.* (2013) 'Antigen-specific tolerance by autologous myelin peptide-coupled cells: A phase 1 trial in multiple sclerosis', *Science Translational Medicine*, 5(188), p. 188ra75. doi: 10.1126/scitranslmed.3006168.
Löseke, S. *et al.* (2003) 'Differential expression of IFN-α subtypes in human PBMC: Evaluation of novel real-time PCR assays', *Journal of Immunological Methods*, 276(1–2), pp. 207–222. doi: 10.1016/S0022-1759(03)00072-3.
Laakso, S. M. *et al.* (2010) 'Regulatory T cell defect in APECED patients is associated with loss of naive FOXP3+precursors and impaired activated population', *Journal of Autoimmunity*, 35(4), pp. 351–357. doi: 10.1016/j.jaut.2010.07.008.
Malchow, S. *et al.* (2013) 'Aire-dependent thymic development of tumor-associated regulatory T cells', *Science*, 339(6124), pp. 1219–1224. doi: 10.1126/science.1233913.

Malchow, S. *et al.* (2016) 'Aire Enforces Immune Tolerance by Directing Autoreactive T Cells into the Regulatory T Cell Lineage', *Immunity*, 44(5), pp. 1102–1113. doi: 10.1016/j.immuni.2016.02.009.
Mallick, C. A. *et al.* (1993) 'Rearrangement and diversity of T cell receptor β chain genes in thymocytes: A critical role for the β chain in development', *Cell*, 73(3), pp. 513–519. doi: 10.1016/0092-8674(93)90138-G.
Matsuki, Y. *et al.* (2007) 'Novel regulation of MHC class II function in B cells', *EMBO Journal*, 26(3), pp. 846–854. doi: 10.1038/sj.emboj.7601556.
Matsutani, T. *et al.* (2007) 'Comparison of CDR3 length among thymocyte subpopulations: Impacts of MHC and BV segment on the CDR3 shortening', *Molecular Immunology*, 44(9), pp. 2378–2387. doi: 10.1016/j.molimm.2006.10.026.
Matsutani, T. *et al.* (2011) 'Shortening of complementarity determining region 3 of the T cell receptor α chain during thymocyte development', *Molecular Immunology*, 44(9), pp. 2378–2387. doi: 10.1016/j.molimm.2010.11.003.
Mead, K. I. *et al.* (2005) 'Exocytosis of CTLA-4 Is Dependent on Phospholipase D and ADP Ribosylation Factor-1 and Stimulated during Activation of Regulatory T Cells', *The Journal of Immunology*, 174(8), pp. 4803–4811. doi: 10.4049/jimmunol.174.8.4803.
Mellor, A. L. *et al.* (2002) 'Cells Expressing Indoleamine 2,3-Dioxygenase Inhibit T Cell Responses', *The Journal of Immunology*, 168(8), pp. 3771–3776. doi: 10.4049/jimmunol.168.8.3771.
Meredith, M. *et al.* (2015) 'Aire controls gene expression in the thymic epithelium with ordered stochasticity', *Nature Immunology*, 16(9), pp. 942–949. doi: 10.1038/ni.3247.
Merkenschlager, M. and von Boehmer, H. (2010) 'PI3 kinase signalling blocks Foxp3 expression by sequestering Foxo factors: Figure 1.', *The Journal of Experimental Medicine*. doi: 10.1084/jem.20101156.
Michie, C. A. *et al.* (1992) 'Lifespan of human lymphocyte subsets defined by CD45 isoforms', *Nature*, 360(6401), pp. 264–265. doi: 10.1038/360264a0.
Moore, B. Y. M. A. S. and Owen, J. J. T. (1967) 'Experimental studies on the development of the thymus', *Journal of experimental medicine*, 126(4), pp. 715–726.
Mouri, Y. *et al.* (2017) 'Mode of Tolerance Induction and Requirement for Aire Are Governed by the Cell Types That Express Self-Antigen and Those That Present Antigen', *The Journal of Immunology*, 199(12), pp. 3959–3971. doi: 10.4049/jimmunol.1700892.
Möller, G. (1988) 'Do Suppressor T Cells Exist?', *Scandinavian Journal of Immunology*, 27(3), pp. 247–250. doi: 10.1111/j.1365-3083.1988.tb02344.x.
Nagamine, K. *et al.* (1997) 'Positional cloning of the APECED gene', *Nature Genetics*, 17(4), pp. 393–398. doi: 10.1038/ng1297-393.
Nakamura, K., Kitani, A. and Strober, W. (2001) 'Cell contact-dependent immunosuppression by CD4(+)CD25(+) regulatory T cells is mediated by cell surface-bound transforming growth factor beta.', *The Journal of experimental medicine*, 194(5), pp. 629–644. doi: 10.1084/jem.194.5.629.
Niemi, H. J. *et al.* (2015) 'A normal T cell receptor beta CDR3 length distribution in patients with APECED', *Cellular Immunology*, 295(2), pp. 99–104. doi: 10.1016/j.cellimm.2015.03.005.
Noyan, F. *et al.* (2017) 'Prevention of Allograft Rejection by Use of Regulatory T Cells With an MHC-Specific Chimeric Antigen Receptor', *American Journal of Transplantation*, 17(4), pp. 917–930. doi: 10.1111/ajt.14175.
Oh, J. *et al.* (2017) 'Capacity of tTreg generation is not impaired in the atrophied thymus', *PLoS Biology*, 15(11), p. e2003352. doi: 10.1371/journal.pbio.2003352.
Onishi, Y. *et al.* (2008) 'Foxp3+ natural regulatory T cells preferentially form aggregates on dendritic cells in vitro and actively inhibit their maturation', *Proceedings of the National Academy of Sciences*, 105(29), pp. 10113–10118. doi: 10.1073/pnas.0711106105.
Orabona, C. *et al.* (2004) 'CD28 induces immunostimulatory signals in dendritic cells via CD80 and CD86', *Nature Immunology*, 5(11), pp. 1134–1142. doi: 10.1038/ni1124.
Ota, K. *et al.* (1990) 'T-cell recognition of an immuno-dominant myelin basic protein epitope in multiple sclerosis', *Nature*, 346(6280), pp. 183–187. doi: 10.1038/346183a0.
Owen, J. J. T., Cooper, M. D. and Raff, M. C. (1974) 'In vitro generation of B lymphocytes in mouse foetal liver, a mammalian "bursa equivalent"', *Nature*, 249(5455), pp. 361–363. doi: 10.1038/249361a0.
Paust, S. *et al.* (2004) 'Engagement of B7 on effector T cells by regulatory T cells prevents autoimmune disease.', *Proceedings of the National Academy of Sciences of the United States of America*, 101(28), pp. 10398–10403. doi: 10.1073/pnas.0403342101.
Perheentupa, J. (2006) 'Autoimmune polyendocrinopathy-candidiasis-ectodermal dystrophy.', *The Journal of clinical endocrinology and metabolism*, 91(8), pp. 2843–2850. doi: 10.1210/jc.2005-2611.
Perry, J. S. A. *et al.* (2014) 'Distinct contributions of Aire and antigen-presenting-cell subsets to the generation of self-tolerance in the thymus', *Immunity*, 41(3), pp. 414–426. doi: 10.1016/j.immuni.2014.08.007.
Pesenacker, A. M. *et al.* (2016) 'A Regulatory T-cell gene signature is a specific and sensitive biomarker to identify children with new-onset type 1 diabetes', *Diabetes*, 65(4), pp. 1031–1039. doi: 10.2337/db15-0572.
Piccirillo, C. A. *et al.* (2002) 'CD4+CD25+ Regulatory T Cells Can Mediate Suppressor Function in the

Absence of Transforming Growth Factor β1 Production and Responsiveness', *Journal of Experimental Medicine*, 196(2), pp. 237–246. doi: 10.1084/jem.20020590.
Pinto, S. *et al.* (2013) 'Overlapping gene coexpression patterns in human medullary thymic epithelial cells generate self-antigen diversity', *Proceedings of the National Academy of Sciences*, 110(37), pp. E3491–E3505. doi: 10.1073/pnas.1308311110.
Pitkänen, J. *et al.* (2000) 'The autoimmune regulator protein has transcriptional transactivating properties and interacts with the common coactivator CREB-binding protein', *Journal of Biological Chemistry*, 275(22), pp. 16802–16809. doi: 10.1074/jbc.M908944199.
Poliani, P. L. *et al.* (2010) 'Human peripheral lymphoid tissues contain autoimmune regulator-expressing dendritic cells', *American Journal of Pathology*, 176(3), pp. 1104–1112. doi: 10.2353/ajpath.2010.090956.
Pop, S. M. *et al.* (2005) 'Single cell analysis shows decreasing FoxP3 and TGFβ1 coexpressing CD4 + CD25 + regulatory T cells during autoimmune diabetes', *The Journal of Experimental Medicine*, 201(8), pp. 1333–1346. doi: 10.1084/jem.20042398.
Procaccini, C. *et al.* (2010) 'An Oscillatory Switch in mTOR Kinase Activity Sets Regulatory T Cell Responsiveness', *Immunity*, 33(6), pp. 929–941. doi: 10.1016/j.immuni.2010.11.024.
Radonić, A. *et al.* (2004) 'Guideline to reference gene selection for quantitative real-time PCR', *Biochemical and Biophysical Research Communications*, 313(4), pp. 856–862. doi: 10.1016/j.bbrc.2003.11.177.
Ring, S. *et al.* (2009) 'CD4+CD25+regulatory T cells suppress contact hypersensitivity reactions through a CD39, adenosine-dependent mechanism', *Journal of Allergy and Clinical Immunology*, 123(6), pp. 1287–1296. doi: 10.1016/j.jaci.2009.03.022.
Robb, R. J., Munck, A. and Smith, K. A. (1981) 'T cell growth factor receptors. Quantitation, specificity, and biological relevance.', *The Journal of experimental medicine*, 154(5), pp. 1455–1474. doi: 10.1084/jem.154.5.1455.
Rochette-Egly, C. *et al.* (1997) 'Stimulation of RARα activation function AF-1 through binding to the general transcription factor TFIIH and phosphorylation by CDK7', *Cell*, 90(1), pp. 97–107. doi: 10.1016/S0092-8674(00)80317-7.
Rosenblum, M. D. *et al.* (2011) 'Response to self antigen imprints regulatory memory in tissues', *Nature*, 480(7378), pp. 538–542. doi: 10.1038/nature10664.
Rosenstein, Y. *et al.* (1989) 'Direct evidence for binding of CD8 to HLA class I antigens.', *The Journal of experimental medicine*, 169(1), pp. 149–160. doi: 10.1084/JEM.169.1.149.
Rosenthal, A. S. and Shevach, E. M. (1973) 'Function of macrophages in antigen recognition by guinea pig T lymphocytes: I. Requirement for histocompatible macrophages and lymphocytes', *Journal of Experimental Medicine*, 138(5), pp. 1194–1212. doi: 10.1084/jem.138.5.1194.
Ryan, K. R. *et al.* (2005) 'CD4+CD25+T-regulatory cells are decreased in patients with autoimmune polyendocrinopathy candidiasis ectodermal dystrophy [1]', *Journal of Allergy and Clinical Immunology*, 116(5), pp. 1158–1159. doi: 10.1016/j.jaci.2005.08.036.
Sakaguchi, S. (1982) 'Study on cellular events in post-thymectomy autoimmune oophoritis in mice. II. Requirement of Lyt-1 cells in normal female mice for the prevention of oophoritis', *Journal of Experimental Medicine*, 156(6), pp. 1577–1586. doi: 10.1084/jem.156.6.1577.
Sakaguchi, S. *et al.* (1995) 'Immunologic Self-Tolerance Maintained by Activated T Cells Expressing 11-2 Receptor a-Chains (CD25). Breakdown of a single mechanism of self-tolerance causes various autoimmune diseases..', *J. Immunol*, 155(3), pp. 1152–1164. doi: 10.4049/jimmunol.171.1.417.
Salomon, B. *et al.* (2000) 'B7/CD28 Costimulation Is Essential for the Homeostasis of the CD4+CD25+ Immunoregulatory T Cells that Control Autoimmune Diabetes', *Immunity*, 12(4), pp. 431–440. doi: 10.1016/S1074-7613(00)80195-8.
Santegoets, S. J. A. M. *et al.* (2015) 'Monitoring regulatory T cells in clinical samples: consensus on an essential marker set and gating strategy for regulatory T cell analysis by flow cytometry', *Cancer Immunology, Immunotherapy*. doi: 10.1007/s00262-015-1729-x.
Sauer, S. *et al.* (2008) 'T cell receptor signaling controls Foxp3 expression via PI3K, Akt, and mTOR', *Proceedings of the National Academy of Sciences*. doi: 10.1073/pnas.0800928105.
Schneider, H. *et al.* (2005) 'CTLA-4 up-regulation of lymphocyte function-associated antigen 1 adhesion and clustering as an alternate basis for coreceptor function.', *Proceedings of the National Academy of Sciences of the United States of America*, 102(36), pp. 12861–12866. doi: 10.1073/pnas.0505802102.
Seki, A. *et al.* (2008) 'Bora and the kinase Aurora A cooperatively activate the kinase Plk1 and control mitotic entry', *Science*, 320(5883), pp. 1655–1658. doi: 10.1126/science.1157425.
Setoguchi, R. *et al.* (2005) 'Homeostatic maintenance of natural *Foxp3* $^{+}$ CD25 $^{+}$ CD4 $^{+}$ regulatory T cells by interleukin (IL)-2 and induction of autoimmune disease by IL-2 neutralization', *The Journal of Experimental Medicine*, 201(5), pp. 723–735. doi: 10.1084/jem.20041982.
Shalek, A. K. *et al.* (2013) 'Single-cell transcriptomics reveals bimodality in expression and splicing in immune cells', *Nature*, 498(7453), pp. 236–240. doi: 10.1038/nature12172.

Shan, J. *et al.* (2015) 'Interplay between mTOR and STAT5 signaling modulates the balance between regulatory and effective T cells', *Immunobiology*, 220(4), pp. 510–517. doi: 10.1016/j.imbio.2014.10.020.
Shimizu, J. *et al.* (2002) 'Stimulation of CD25+CD4+regulatory T cells through GITR breaks immunological self-tolerance', *Nature Immunology*, 3(2), pp. 135–142. doi: 10.1038/ni759.
Shrestha, S. *et al.* (2015) 'Tregcells require the phosphatase PTEN to restrain TH1 and TFHcell responses', *Nature Immunology*, 16(2), pp. 178–187. doi: 10.1038/ni.3076.
Simpson, J. G., Gray, E. S. and Beck, J. S. (1975) 'Age involution in the normal human adult thymus', *Clinical and experimental immunology*.
Sun, Y. *et al.* (1999) 'Interaction of the Ski oncoprotein with Smad3 regulates TGF-b signaling', *Mol Cell*, 4(4), pp. 449–509. doi: 10.1016/S1097-2765(00)80201-4.
Suzuki, E. *et al.* (2008) 'Expression of AIRE in thymocytes and peripheral lymphocytes', *Autoimmunity*, 41(2), pp. 133–139. doi: 10.1080/08916930701773941.
Tada, T. O. M. I. O., Okumura, K. O. and Tokuhisa, T. (1978) 'Two distinct types of helper t cells involved in the secondary antibody response : independent and synergistic effects of Ia- and Ia+ helper t cells.', *In Vitro*, 147(2), pp. 446–458. doi: 10.1084/jem.147.2.446.
Takaba, H. *et al.* (2015) 'Fezf2 Orchestrates a Thymic Program of Self-Antigen Expression for Immune Tolerance', *Cell*, 163(4), pp. 975–987. doi: 10.1016/j.cell.2015.10.013.
Taniguchi, R. T. *et al.* (2012) 'Detection of an autoreactive T-cell population within the polyclonal repertoire that undergoes distinct autoimmune regulator (Aire)-mediated selection', *Proceedings of the National Academy of Sciences*, 109(20), pp. 7847–7852. doi: 10.1073/pnas.1120607109.
Taniguchi, T. *et al.* (1983) 'Structure and expression of a cloned cDNA for human interleukin-2', *Nature*, 302(5906), pp. 305–310. doi: 10.1038/302305a0.
Teh, H. S. *et al.* (1988) 'Thymic major histocompatibility complex antigens and the αβ T-cell receptor determine the CD4/CD8 phenotype of T cells', *Nature*, 335(6187), pp. 229–233. doi: 10.1038/335229a0.
Thellin, O. *et al.* (1999) 'Housekeeping genes as internal standards: Use and limits', *Journal of Biotechnology*, 75(2), pp. 291–295. doi: 10.1016/S0168-1656(99)00163-7.
Thiault, N. *et al.* (2015) 'Peripheral regulatory T lymphocytes recirculating to the thymus suppress the development of their precursors', *Nature Immunology*, 16(6), pp. 628–634. doi: 10.1038/ni.3150.
Thornton, A. M., Korty, P. E., Tran, D. Q., Wohlfert, E. A. , Murray, P. E. , Belkaid, Y., S. E. M. (2010) 'Expression of Helios, an Ikaros Transcription Factor Family Member, Differentiates Thymic-Derived from Peripherally Induced FoxP3+ T Regulatory Cells', *The Journal of Immunology*, 184(7), pp. 3433–3441.
Thornton, A. M. and Shevach, E. M. (1998) 'CD4+CD25+ immunoregulatory T cells suppress polyclonal T cell activation in vitro by inhibiting interleukin 2 production.', *The Journal of experimental medicine*, 188(2), pp. 287–296. doi: 10.1084/jem.188.2.287.
Vahl, J. C. *et al.* (2014) 'Continuous T Cell Receptor Signals Maintain a Functional Regulatory T Cell Pool', *Immunity*, 41(5), pp. 722–736. doi: 10.1016/j.immuni.2014.10.012.
Verhagen, J. and Wraith, D. (2010) 'Comment on "Expression of Helios, an Ikaros Transcription Factor Familiy Member, Differentiates Thymic-Derived from Peripherally Induced FoxP3+ T Regulatory Cells', *Journal of immunology*, 185(12), pp. 7129–7129.
Vose, B. M. and Bonnard, G. D. (1982) 'Human tumour antigens defined by cytotoxicity and proliferative responses of cultured lymphoid cells', *Nature*, 296(5855), pp. 359–361.
Watanabe, N. *et al.* (2005) 'Hassall's corpuscles instruct dendritic cells to induce CD4+CD25+ regulatory T cells in human thymus', *Nature*, 436(7054), pp. 1181–1185. doi: 10.1038/nature03886.
Wing, K. *et al.* (2008a) 'CTLA-4 control over Foxp3+ regulatory T cell function.', *Science*, 322(5899), pp. 271–275. doi: 10.1126/science.1160062.
Wing, K. *et al.* (2008b) 'CTLA-4 control over Foxp3+ regulatory T cell function.', *Science (New York, N.Y.)*, 322(5899), pp. 271–275. doi: 10.1126/science.1160062.
Wojciech, L. *et al.* (2014) 'The same self-peptide selects conventional and regulatory CD4+T cells with identical antigen receptors', *Nature Communications*, 5(5061). doi: 10.1038/ncomms6061.
Wolff, A. S. B. *et al.* (2007) 'Autoimmune polyendocrine syndrome type 1 in Norway: Phenotypic variation, autoantibodies, and novel mutations in the autoimmune regulator gene', *Journal of Clinical Endocrinology and Metabolism*, 92(2), pp. 595–603. doi: 10.1210/jc.2006-1873.
Wolff, A. S. B. *et al.* (2010) 'Flow cytometry study of blood cell subtypes reflects autoimmune and inflammatory processes in autoimmune polyendocrine syndrome type i', *Scandinavian Journal of Immunology*, 71(6), pp. 459–467. doi: 10.1111/j.1365-3083.2010.02397.x.
Yadav, M. *et al.* (2012) 'Neuropilin-1 distinguishes natural and inducible regulatory T cells among regulatory T cell subsets in vivo', *The Journal of Experimental Medicine*, 209(10), pp. 1713–1722. doi: 10.1084/jem.20120822.
Yamano, T. *et al.* (2015) 'Thymic B Cells Are Licensed to Present Self Antigens for Central T Cell Tolerance Induction', *Immunity*, 42(6), pp. 1048–1061. doi: 10.1016/j.immuni.2015.05.013.

Yang, S. *et al.* (2015) 'Regulatory T cells generated early in life play a distinct role in maintaining self-tolerance', *Science*. doi: 10.1126/science.aaa7017.
Yano, M. *et al.* (2008) 'Aire controls the differentiation program of thymic epithelial cells in the medulla for the establishment of self-tolerance', *The Journal of Experimental Medicine*, 205(12), pp. 2827–2838. doi: 10.1084/jem.20080046.
Zabransky, D. J. *et al.* (2012) 'Phenotypic and functional properties of Helios + regulatory T cells', *PLoS ONE*, 7(3), p. e34547. doi: 10.1371/journal.pone.0034547.
Zemmour, D. *et al.* (2018) 'Single-cell gene expression reveals a landscape of regulatory T cell phenotypes shaped by the TCR article', *Nature Immunology*, 19(3), pp. 291–301. doi: 10.1038/s41590-018-0051-0.
Zheng, N. *et al.* (2002) 'Structure of the Cul1-Rbx1-Skp1-F boxSkp2 SCF ubiquitin ligase complex', *Nature*, 416(6882), pp. 703–709. doi: 10.1038/416703a.
Zhou, X. *et al.* (2009) 'Instability of the transcription factor Foxp3 leads to the generation of pathogenic memory T cells in vivo', *Nature Immunology*, 10(9), pp. 1000–1007. doi: 10.1038/ni.1774.
Zinkernagel, R. M. *et al.* (1978) 'On the thymus in the differentiation of "H-2 self-recognition" by T cells: evidence for dual recognition?', *The Journal of experimental medicine*, 147(3), pp. 882–96. doi: 10.1084/jem.147.3.882.
Zinkernagel, R. M. and Doherty, P. C. (1973) 'Cytotoxic thymus-derived lymphocytes in cerebrospinal fluid of mice with lymphocytic choriomeningitis', *Journal of experimental medicine*, 138(5), pp. 1266–1269.
Aaltonen, J. *et al.* (1997) 'An autoimmune disease, APECED, caused by mutations in a novel gene featuring two PHD-type zinc-finger domains', *Nature Genetics*, 17(4), pp. 399–403. doi: 10.1038/ng1297-399.

Supplementary information

Table S.1: *List of the included patients with information about sex, age, AIRE-mutation, auto-antibodies, diagnosis and age of disease debut. Among the recruited patients, two different* AIRE *mutations were represented, designated "30 bp deletion" and "splice mutation"*

No.	Sex	Age	Age of debut	Manifestations	*AIRE* mutation	Auto-antibodies
1	Female	59	10	Adrenal insufficiency Hypoparathyroidism Candidiasis Gastritis Enamel dysplasia Asplenia Ovarian failure Nephritis	c.967-979del13/ large del (13bp)	21-hydroxylase Side chain cleavage enzyme Tryptophan hydroxylase NOD-liker receptor phyrin domain containing 5 17-hydroprogesterone Interleukin-22 Interferon-ω
2	Female	40	21	Adrenal insufficiency Candidiasis	c.879+1G>A/ c.879+1G>A (Splice)	21-hydroxylase NOD-liker receptor phyrin domain containing 5 17-hydroprogesterone Interferon-ω
3	Male	55	43	Hypoparathyroidism Type 1 diabetes Vitiligo Autoimmune thyroiditis Enamel dysplasia Candidiasis	c.879+1G>A/ c.879+1G>A	Aromatic I-amino acid decarboxylase Glutamic acid decarboxylase Tryptophan hydroxylase NOD-liker receptor phyrin domain containing 5 17-hydroprogesterone 21-hydroxylase Tyrosine hydroxylase Interferon-ω
4	Male	44	12	Adrenal insufficiency Candidiasis	c.967-979del13/ c.967-979del13	21-hydroxylase Side chain cleavage enzyme Glutamic acid decarboxylase Interleukin-22 Interferon-ω
5	Female	42	Un-known	Hypoparathyroidism Primary ovarian failure Enamel dysplasia Autoimmune thyroiditis Vit B12 deficiency	c.934G>A	NOD-liker receptor phyrin domain containing 5 Interferon-ω
6	Female	64	23	Hypoparathyroidism Autoimmune thyroiditis	c.879+1G>A/ c.967_979del	NOD-liker receptor phyrin domain containing 5 Interferon-ω

Table S.2: *List of the controls included in the specific studies with information about sex and age*

No.	Sex	Age	Included in
1	Male	35	Protein profiling and RNA study (qPCR, PCR and RNA-seq)
2	Male	53	Protein profiling and RNA study (qPCR)
3	Male	43	Protein profiling study
4	Male	48	Protein profiling study
5	Male	52	Protein profiling study
6	Male	66	Protein profiling study and RNA study (qPCR and RNA-seq)
7	Female	25	Protein profiling study and RNA study (qPCR and RNA-seq)
8	Male	33	RNA study (RNA-seq)
9	Male	60	RNA study (qPCR)
10	Male	30	RNA study (qCR)
11	Male	43	RNA study (qPCR)
12	Male	27	RNA study (qPCR)

Table S.3: *List of the genes assessed in the conventional PCR protocol, with the sequences of forward and reverse primers for each gene.*

Gene	Forward primer	Reverse primer
B2M	ATGTCTCGCTCCGTGGCCT	TCCACTTTTTCAATTCTC
IKZF4	CAGCGTGATTGTGGAAGA	GACTCTGTAGGTAGTTAT
PECAM-1	ACCAGGTGTTGGTGGAAGGAGTG	AACTTGGGTGTAGAGAAG
CXCR3	CTACACCGAGGAAATGGG	TGCAACTGCCCAGAAGGGA
CD3δ	ATGGAACATAGCACGTTT	AAAGCAAGGAGCAGAGTGGC
mTOR	TGGAACTCCGAGAGATGAGTCA	AGGCTTCTGCATCTCCTT
TOLLIP	ATGGCGACCACCGTCAGCA	TCGTACACCGCGTAGCCCAG
FOXO1	TCAACATCAGGCACTTCTCAGAGTA	TACTTGGAAAGTTCTGCTTTGACA
CCR5	AGTGTGATCACTTGGGTGGTG	TGGTGAAGATAAGCCTCACAGC
Neuropilin-1	CTTGGATTTCGCTCAGTTTCCAAA	TCGTGCTGTACTGTGCCTGTTG
CCR4	CTGTATTCCTTGGTTTTTGT	AGGTCCTTGCCCTCAAGGA

Table S.4: *List of the selected candiate genes*

	Flow cyt.	qPCR	RNA-seq	Function
FOXP3	X	X	X	Trancription factor for genes involved in T_{reg} function and lineage stability
AIRE		X		Transcription factor, TRA expression
CD152/CTLA-4	X	X	X	Mediates suppressive function of T_{egs}
HELIOS/IKZF2	X		X	Trancripton factor
Neuropilin-1	X	X	X	Co-receptor for semaphorin and vascular endothelial grown factor
CD39/ENTPD-1	X		X	Hydrolysis of ATP and ADP
CD31/PECAM-1	X	X	X	Cellular migration
GITR/TNFRSF18		X	X	Cell surface receptor on T lymphocytes
Ki-67/MKI67	X		X	Involved in cell cycle progression
CD45RA/PTPRC	X		X	Protein tyrosine kinase
Eos/IKZF4			X	Transcription factor
CXCR3			X	Chemokine receptor
CD3δ			X	Part of the TCR constant domain
mTOR			X	Cell signalling
TOLLIP			X	Adaptor protein of the toll-like receptor
FOXO1			X	Transcription factor, induces expression of FOXP3
CCR5			X	Chemokine receptor
CCR4			X	Chemokine receptor
CD73/NT5E			X	Hydrolysis of AMP